Development of Optimal Biopreservation Methods and Technology for Cellular Therapy and Clinical Diagnosis

Zhiquan Shu

A dissertation

submitted in partial fulfillment of the

requirements for the degree of

Doctor of Philosophy

University of Washington

2013

Reading Committee:

Dayong Gao, Chair

Jae-Hyun Chung

Amy Shen Fried

Program Authorized to Offer Degree:

Mechanical Engineering

University of Washington

Abstract

Development of Optimal Biopreservation Methods and Technology
for Cellular Therapy and Clinical Diagnosis

Zhiquan Shu

Chair of the Supervisory Committee:

Professor Dayong Gao

Department of Mechanical Engineering

Successful biopreservation of bio-samples, including DNA/RNA, proteins, bio-fluids, cells, tissues and organs, is vital for researches and clinical trials, enabling the diagnosis of disease, drug development and cellular therapy. Challenges in biopreservation (particularly cryopreservation) include selection of the optimal cryoprotective agent (CPA), successful addition of CPA, optimization of the cooling protocol, thawing of the frozen samples, removal of CPA after thawing, and others. In this dissertation, a few novel techniques are developed to determine the fundamental cryobiological properties of cells, optimize cryopreservation protocols and the applications of biopreservation in cellular therapy and disease diagnosis.

The optimal cryopreservation protocol for a cell type is determined by the inherent cryobiological characteristics of the cells, including the cell membrane permeabilities to water and the CPA at different temperatures, the osmotically inactive cell volume fraction, the activation energy of water transport across cell membranes, the osmotically inactive cell volume fraction, osmotic tolerance limit, sensitivity to the CPA toxicity, intracellular ice formation (IIF) temperature, and others. To determine these cryobiological properties, two methods are proposed and applied: microfluidic perfusion channel and differential scanning calorimetry (DSC) measurements.

For the microfluidic perfusion channel method, human vaginal mucosal immune cells (T cells and macrophages) were chosen because of their importance in HIV vaccine research and poor long-term preservation with current protocols. Using the micro-fabricated channel, cells can be trapped in the channel and observed under microscopy. Different solutions (2xPhosphate-buffered saline [PBS], 3xPBS, and CPA solutions) were fed into the channel. In response to the perfusion solutions, the cell volume changed (shrank or shrank then expanded). The volume excursion history of individual cells was recorded. After image analysis, the data were simulated to evaluate the cell membrane properties. The results showed that T cells and macrophages had relatively low membrane permeabilities, implying a low optimal cooling rate for these cells. Comparing four different CPAs (Dimethyl sulfoxide (DMSO), glycerol, propylene glycol and ethylene glycol), showed that glycerol crossed the cell membranes very slowly; therefore, it cannot be used for the cryopreservation of these cells. DMSO and propylene glycol could be good CPA options. Tests of CPA cytotoxicity demonstrated similar results. The results also showed that T cells were more susceptible to stresses than macrophages.

While it is technically challenging to use the micro-perfusion channel method at temperatures below the freezing point, DSC can be used to evaluate the cell membrane properties at any sub-zero temperatures. Based on the fundamental theory developed by Devireddy et al., a "slow-fast-fast-slow" cooling program is used for cell suspensions. In the first slow cooling process, the measured heat release of ice crystallization includes the crystallization of extracellular water and the water that is transported from inside of the cells due to extracellular ice formation and consequently the osmolality gradient occurrence across the cell membranes. During the repeated fast cooling processes, cells are assumed to be killed and lysed. Some water will be bound to the proteins and cell debris of the lysed cells. Therefore, in the last slow cooling step, the heat release of ice crystallization will be lower than that of the first slow cooling step. The thermogram difference between the first and the last slow cooling steps can be analyzed to obtain the water transport history across cell membranes in the suspension during freezing; therefore, cell membrane properties at any temperature during cooling can be predicted. This approach was optimized and applied to measure the membrane properties of PBMC lymphocytes (including T cells and monocytes). The results were then applied in theoretical simulation to predict the optimal cooling rate for the cells. The prediction was consistent with the standard operating procedure (SOP) for PBMC cryopreservation.

Another challenge in cryopreservation and cellular therapy is the addition and removal of CPA with minimal injury to the cells. In order to overcome this problem, a multi-functional cell processor based on semi-permeable hollow fibers and "dilution-filtration" working principle was developed. A novel approach of electrical conductivity measurement was also proposed for real-time, online monitoring of the residual CPA

concentration in the cell suspension. The results showed that this system can be applied for successful cell concentration (control of the cell suspension volume) and removal of CPA with much lower cell loss. Furthermore, this automatic device with closed fluid loop can save labor significantly, reduce risk of contamination and decrease cell damage.

Cryopreservation of bacteria and freeze-drying of proteins were also studied in this dissertation. *Mycobacterium tuberculosis* (MTB) was studied due to the challenges in tuberculosis diagnosis. Tuberculosis is the second leading infectious disease (only after HIV) causing death in the world. Fast and accurate diagnosis of MTB is still challenging. Cryopreservation of MTB cells is very important for pathological research, diagnosis and drug development. Due to the small size of MTB cells and the complex cell wall/membrane configuration, it is challenging to study their fundamental cryobiological properties. So, MTB cells were cryopreserved under systematically varied conditions and the effects on recovery were measured. The results showed that among all the parameters, slow cooling rate is the most important for successful MTB cryopreservation. Inconsistencies were found between the results of microbiological culturing and BacLight Live/Dead staining, implying that suboptimal cryopreservation might not cause severe damage to cell wall and/or membrane, but instead cause intracellular injury, which leads to the loss of cell viability. For long-term preservation of the MTB IgY antibodies, freeze-drying was applied. The results showed that the lyophilized IgY antibodies can be well preserved for up to 13 months at either room temperature or 4 ℃.

Plans for further experiments are also presented in this dissertation, including cryopreservation and vitrification of mucosal immune cells and tissues based on

fundamental researches and predicted protocol, multi-center evaluation of the developed techniques and protocols, and further optimization of the multi-functional cell processor.

Table of Contents

Figures

Tables

Acknowledgements

I am deeply indebted to my supervisors Prof. Dr. Dayong Gao and Prof. Dr. Jae-Hyun Chung, whose support, inspiration, suggestions and encouragement helped me all the time not only in my research, but also in my daily life. I would also like to thank my committee members, Prof. Dr. Amy Shen Fried, Prof. Dr. Gerard A. Cangelosi, Prof. Dr. Kyong-Hoon Lee, Prof. Dr. Thomas Furness and Prof. Dr. Shaoyi Jiang for their input to this work.

My colleagues and collaborators supported me much in my research work. I want to thank them for all their help, support, and valuable suggestions. These kind people include but are not limited to: Simon Chen, Weiping Ding, Cifeng Fang, Baiwen Fu, George Zhiyuan Hou, Jinghua Huang, Xianjiang Kang, Xin Liang, Jiaji Pan, Sijie Sun, Ruoxin Wang, Jinyuan Zhang, Xiaoming Zhou and so on in Dr. Gao's Lab, Kieseok Oh, Woonhong Yeo, Jonghoon Kim, Shinnosuke Inoue, etc. in Dr. Chung's Lab, Kris M. Weigel and A.L. Becker in Dr. Cangelosi's Lab, Mr. Scott D. Soelberg in Genome Science Department, Dr. Lei Zhang in Bioengineering, Dr. Florian Hladik, Dr. Jason Carstens, Dr. Shelly Heimfeld and Mr. Sean M. Hughes from Fred Hutchinson Cancer Research Center.

I want to thank all the staff in the Department of Mechanical Engineering for their long-term support.

Especially, I give my special thanks to my family. This dissertation would never have been completed without their encouragement and devotion.

Nomenclature

A	area, μm^2
B	cooling rate, K/min
C	concentration or osmolality (Osm/kg water)
CPA	cryoprotective agent
Ea	activation energy, kcal/mole
EC	electrical conductivity (mS/cm)
h_1	height of slit, μm
h_2	height of microchannel, μm
L_p	membrane permeability to water, μm/(atm·min)
L_{pg}	membrane permeability of water at reference temperature Tr, μm/(atm·min)
N	number of osmoles
P_s	membrane permeability of CPA, cm/min
r	radius (μm), or normalized concentration of NaCl with respective to that in isotonic NaCl solution
R	universal gas constant, 0.08207 atm L/(mole·K)
T	absolute temperature, K
Tr	reference temperature (=273.15K)
V	volume, μm^3
$\overline{V}$	partial volume, μm^3
V_b	osmotically-inactive volume or volume fraction, μm^3 or %

v_w the specific molar volume of water,

Φ diameter, μm

ϕ_s the dissociation constant (=2 for NaCl)

σ reflection coefficients of cell membrane to CPA

v_0 molar volume, μm^3/mole

n_s osmoles of solute, moles

q heat release of DSC data, J/g

α cytocrit, %

ΔH_f latent fusion heat of water, J/g

Subscripts

c total cellular

n non-permeating solute

o initial state

s solutes (CPA or salt)

Superscripts

e extracellular

i intracellular

Chapter 1 Introduction

1.1 Background

Over the last decade the field of regenerative medicine has transited from basic research/pre-clinical animal model testing into actual clinical evaluation for numerous therapeutic disease areas including cancer, heart disease, bone/cartilage, neuro-degenerative, diabetes, gastrointestinal, and autoimmunity (1) (2). Cell-based therapy to modulate immune responses is another active area of clinical investigation, ranging from the treatment of autoimmune diseases such as diabetes to the prevention of solid organ graft rejections following kidney and liver transplantation to boosting immune responses to cancer. Nine cellular therapy products having a $600-$700 million market size (2011) have been approved for use in USA or EU. With the anticipated approval of additional products the cellular therapy market is expected to grow at an annualized rate of greater than 40% through the remainder of the decade, reaching an amount greater than $5 billion between 2015 and 2020 (Figure 1-1). (3-5)

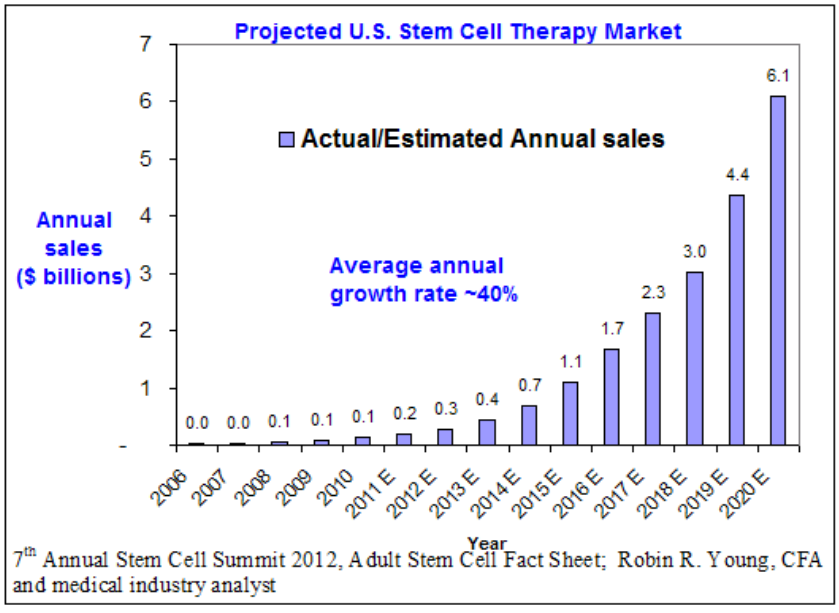

Figure 1-1 Cellular therapy market in USA

A general cellular therapy process is shown in Figure 1-2 using T cell as an example. The process consists of the steps as follows:

1) Collection of cells or tissues from donor
2) T cell selection, stimulation and transduction
3) Expansion of therapeutic polyclonal T cells by feeder cells
4) Harvest of expanded T cells
5) Concentration of harvested T cells to desired cell concentration and volume
6) Cryopreservation of T cells
7) Preparation of cryopreserved and thawed T cells for infusion

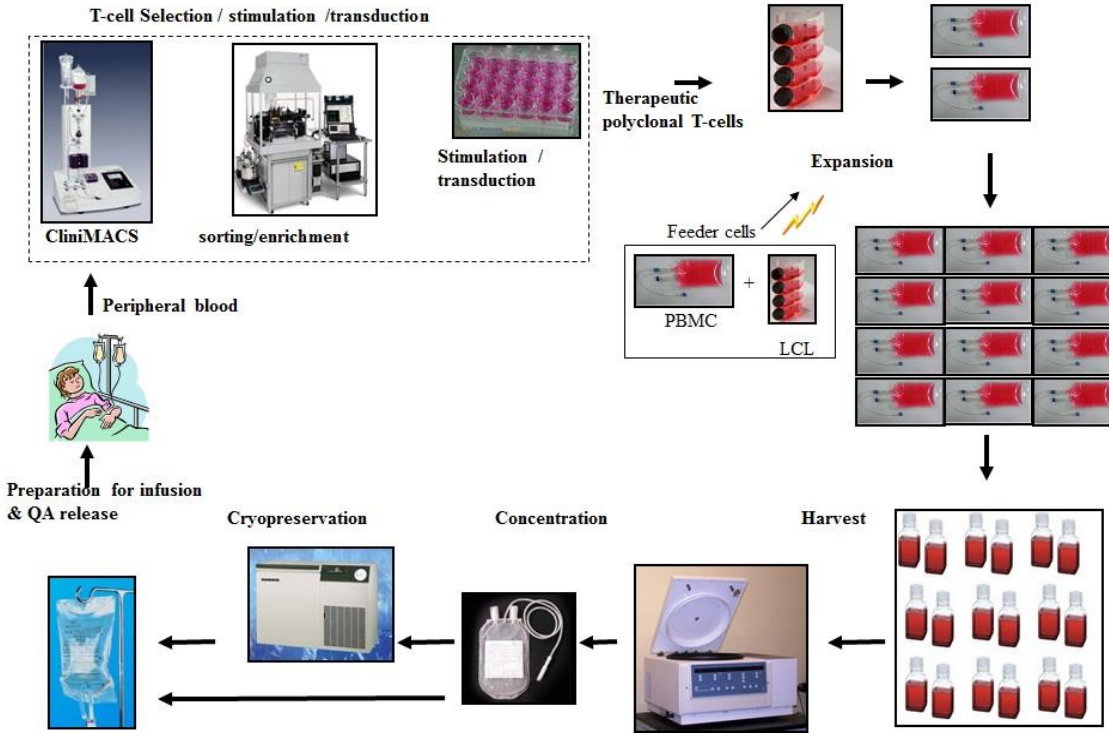

Figure 1-2 Cellular therapy process (T-cell as an example)

All these steps are crucial for the success of cellular therapy. In the last few decades, scientists and engineers have improved the protocols and techniques in each step. Some dedicated instruments are commercially available. However, the current status is still far from optimal.

In this dissertation, we will mainly focus on the challenges in steps 5-7, including cell concentration, cell cryopreservation and post-thawing processing.

1.2 Challenges in cellular therapy

One key to the development and successful application of cell-based therapeutic products is the ex-vivo expansion and recovery of primary cells, which highlights a growing need for more efficient, cost-effective, and safe manufacturing methods (6). One of the major challenges faced by cellular therapy industry is that processing equipment specifically designed for the Good Manufacturing Practice (GMP) manufacture of cellular therapy products is usually not commercially available. So far cell culture processing equipment has been designed for protein production and was never designed with the intention of recovering cells as the final sterile therapeutic product. As a result, "off-the-shelf" equipment solutions are not readily available for cellular therapy GMP manufacturing, and are not designed to maintain an entirely closed system at a suitable scale of operation (e.g. cell culture in < 20L bioreactors). Furthermore, the equipment design is not suitable for scale-up or scale-out and thus impractical for widespread commercialization.

One particularly challenging operation involves cell harvest, concentration and diafiltration out of cell culture media and into a buffer for further processing. This step is very time consuming and labor intensive and commonly performed in open processing steps using centrifugation. The methods can result in low cell product yields (<50%) due to mechanical injury, cell clumping and even activation of stem cells. This open system significantly increases the risk of contamination and threatens patient safety. Therefore, there is an urgent need for a method/device for cell concentration for safe, fast, and easy operation in a reliable and cost-effective manner.

Another big challenge is cell cryopreservation, including optimal freezing and thawing protocols for the specific cell types, pre-freezing preparation and post-thawing processing of the cell products, such as addition and removal of cryoprotective agents. Novel methods, techniques to determine optimal cryopreservation protocols and reliable, easy-to-use devices still remain unfilled urgent needs in this field.

1.3 Cryobiology and cryopreservation

The basic mechanism of preservation of live materials is that any chemical reactions and metabolism will be slowed down or even paused at low temperatures. The "life clock" of these materials (RNA, DNA, cells, tissues, etc.) will be slowed or halted during cryo-

storage, and then resumed after thawing to normal temperatures. Human beings applied low temperature to stop bleeding and swelling even in 2500B.C. in Egypt. But mammalian cells could not be well cryopreserved until 1949, when Polge et al. succeeded in cryopreserving bull sperm with glycerol in liquid nitrogen (7). Since then, cryopreservation has been widely explored and applied for long-term storage of DNA/RNA, proteins, bio-fluids, cells, tissues and organs. It has filled needs in many fields from fundamental research to clinical practice. For example, human sperm can be cryopreserved for years until being used for fertilization. Stem cells (from bone marrow, cord blood or peripheral blood) have been cryopreserved, transported and then transplanted to patients to treat many kinds of diseases since the 1950s (8), such as Hodgkin's and non-Hodgkin's lymphoma (9-17), chemo-sensitive/ lymphoid/ myeloid/ hematological malignancies (9-13, 15, 18-21), osteogenic/fibro-/Ewing sarcoma(10)(22), myeloid or lymphoblastic leukemia (12-15, 21, 23-27), solid tumors (testis, breast) (10, 12, 13, 19-21, 28), amyloidosis (9, 15, 29), medulloblastoma(22), Epstein-Barr virus infection(24), Fanconi anemia(27), myelodysplastic syndrome(14, 24), and so on.

The advantages or applications of cryopreservation include, but are not limited to:

⑴ Allowing the establishment of banks of both healthy and diseased cells (such as sperm, oocyte, stem cells, lymphocyte) or tissues (skin, bone, kidney, cornea, or engineered tissue banking) for clinical applications and scientific studies. Banks of large amounts of cells and tissues allow study and use of materials at times distant from their initial collection in clinical practice and large quantities of samples for testing. Biorepository of diseased cells and tissues (e.g. cancers) is very important for research, vaccine development and drug tests.

⑵ to make it possible for donor-recipient screening and matching. Without large quantities and varieties of cells/tissues from different donors, it is impossible to find matching samples for recipients.

⑶ to provide sufficient time and feasibility for disease screening of donated cells and tissues. For example, in sperm bank, sperm donors should be tested at least

twice for HIV/AIDS with six months apart. The donations can only be accepted if both tests are negative.

(4) transportation between different medical centers or institutes. It usually happens that a matching donation is collected in location A and has to be transported to recipient in location B. Cryopreservation is often the best way to preserve the functions and capabilities of these donations. Additionally, comparative experiments are often implemented by multiple centers. Successful transportation of bio-samples with cryopreservation among multiple sites is thus necessary.

(5) to conduct the gene therapy in the near future, such as study of effects of altering genes. Cryopreserved samples with stable unchanging genes are usually needed as control.

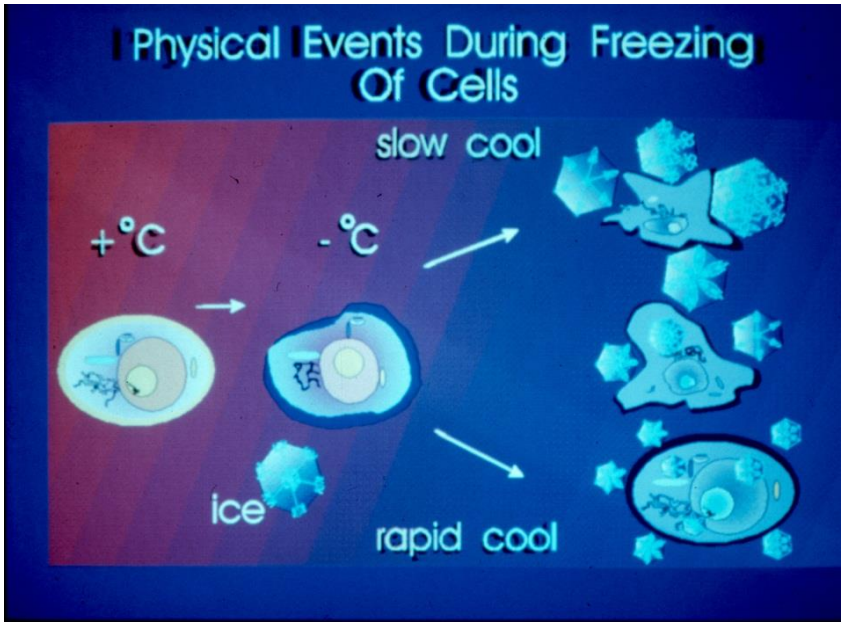

Figure 1-3 “Two-Factor Hypothesis” of cryoinjury

However, currently, many kinds of cells cannot be well cryopreserved. This is because “cryo-injuries” happen during freezing and thawing processes if sub-optimal protocols are applied. In 1970s, Mazur proposed a “two-factor hypothesis” of cryoinjuries (30), as shown in Figure 1-3. When a cell is cooled to subzero temperatures (e.g., -10 ^{o}C),

extracellular ice forms, which causes the extracellular osmolality to increase. The difference of osmolality, and therefore chemical potential of water, between intra- and extracellular environments drives the efflux of water across cell membranes. If the cooling rate is too high, there is not enough time for the efflux of water before intracellular ice formation (IIF). IIF may be fatal to cells, which is called “ice injury”. On the other hand, if cooling rate is too low, water can keep leaving the cells to reach balance of osmolality/water chemical potential, causing the intracellular electrolyte concentration to become very high. High concentration of intracellular electrolytes can be toxic to cells, which is called “solution injury”. Meanwhile, slow cooling may cause severe cell dehydration and shrinkage, exceeding the cell volume excursion tolerance limit. According to this “two-factor hypothesis” (ice injury with high cooling rate and solution injury with low cooling rate), there is an inverted “U” shape of the relationship between cell survival rate and the cooling rate (31), as shown in Figure 1-4. Hence, there is an optimal cooling rate for a specific type of cells, which is determined by the properties of the cell membranes.

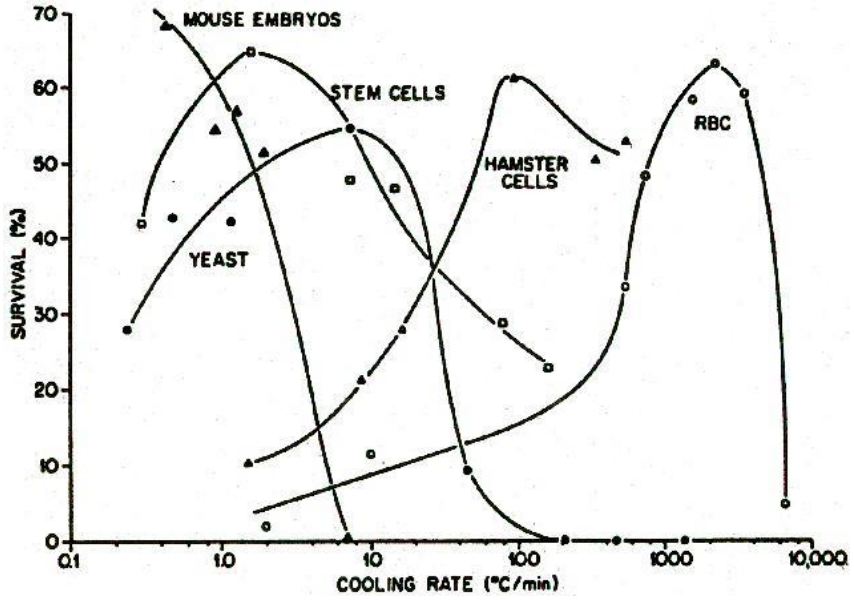

Figure 1-4 Optimal cooling rates of some types of cells (P Mazur, Science 168 (1970))

1.4 General process of cryopreservation

The general process of cell cryopreservation includes:

⑴ Adding cryoprotective agent (CPA) to the cell suspension;

⑵ Freezing the cell suspension with specific protocol;

⑶ Storing the samples at low temperatures;

⑷ Thawing the frozen samples;

⑸ Removing CPA.

The success of cryopreservation depends on many factors. For example, firstly, a specific CPA should be chosen for the cell type according to the cell membrane properties and the CPA toxicity. Secondly, the CPA addition may cause osmotic injury to cells if sub-optimal protocols are applied. Thirdly, ice injury and solution injury may occur to cells during freezing. An optimal cooling rate in a temperature range should be applied. Finally, recrystallization may happen during thawing, which is also fatal to cells. So, generally ultra-fast thawing is applied. Finally, during removal of CPA, osmotic injury, cell clumping or other damage may also happen to the cells. In order to cryopreserve the cells successfully, one should determine the cell type-specific optimal protocol to prevent all these possible injuries.

1.5 Cryoprotective agent (CPA)

In order to decrease cryo-injuries to cells during cryopreservation, some chemical agents, named cryoprotectants, or cryoprotective agents (CPA) are added to cell suspension before freezing. In fact, it was the observation of glycerol's protective function in sperm cryopreservation in 1949 that started the new era of modern cryobiology. After that, more than 100 types of CPAs have been used, such as glycerol, dimethyl sulfoxide (DMSO), ethylene glycol (EG), propylene glycol (PG), trehalose, sucrose, dextran, hydroxyethyl starch (HES), Polyvinylpyrrolidone (PVP), and so on. They can be classified into three types:

⑴ Permeable CPAs, such as glycerol, DMSO, EG, and PG. The mechanism of permeable CPAs is to penetrate into cells, decrease the freezing temperature of the intracellular environment, and fill in the intracellular volume to compensate for the

volume reduction due to water loss and prevent severe cell volume excursion during cooling.

⑵ Non-permeable CPAs, such as sucrose, trehalose, dextran, HES, and PVP. These CPAs cannot penetrate into cells. Their main function is to increase the glass transition temperature (T_g) and glass transition tendency of the extracellular environment dramatically.

⑶ Anti-freezing proteins (AFP). AFPs function with non-colligative property, which means they do not lower the freezing temperature proportional to the AFP concentration. Since the discovery of the existence of AFP in the blood of arctic fish by Canadian scientist Scholander in 1950s (32), and isolation of AFP by DeVries in 1960s (33), AFPs have been studied and applied in many fields including cryopreservation and food industry (e.g., additives in ice cream). As the name implies, AFP can delay or prevent ice crystallization during cooling. AFPs bind to small ice crystals to inhibit the growth and recrystallization of ice. AFPs may also interact with mammalian cell membranes to protect them from cold damage.

To select an optimal CPA for a specific type of cells, one should consider: ⑴ the permeability of the cell membrane to the CPA; ⑵ the toxicity of the CPA to the cells, and ⑶ the availability and cost of the CPA.

1.6 The importance of CPA removal: DMSO as the example

Although the fields of cryopreservation and cellular therapy have benefited from the discovery of CPAs to prevent cryo-injury to cells during freezing, CPAs may also cause severe side-effects to patients if transplanted along with cells.

For example, as the most widely used CPA, dimethyl sulfoxide (DMSO) has been found to cause many side effects after transfusion of hematopoietic stem cells, from mild to severe, even life-threatening. The side effects include gastrointestinal, allergic, cardiovascular and neurological responses, and renal and hepatic dysfunctions. The common clinical symptoms are nausea, vomiting, headache, hypo/hyper-tension, hypo/hyper-thermia, bradycardia/tachycardia, amnesia, heart block, seizure, and so on.

Table 1-1 lists the adverse events after transplantation of cryopreserved hematopoietic stem cells reported mainly in the last decade.

Role of DMSO in the side effects

DMSO [$(CH3)_2SO$] is an amphipathic molecule with a highly polar domain and two apolar groups, making it soluble in both aqueous and organic media, and used for diverse laboratory and clinical purposes as a very efficient solvent for water-insoluble compounds, a hydrogen-bound disrupter, cell-differentiating agent, hydroxyl radical scavenger, intracellular low-density lipoprotein-derived cholesterol mobilizing agent, antidote to the extravasation of vesicant anticancer agents, topical analgesic, and so on. After its commercial availability as solvent in 1950s and studies of clinical uses from 1960s (34-37), it was approved by the United States Food and Drug Administration for the treatment of interstitial cystitis first in 1978, and is also used in the treatments of brain edema, amyloidosis, schizophrenia, urinary musculoskeletal and gastrointestinal disorders, pulmonary adenocarcinoma, rheumatologic and dermatologic diseases, chronic prostatitis, Alzheimer's disease, and as topical analgesic (27, 38-40). Since the first trial of DMSO in prevention of freezing damage to living cells by Lovelock and Bishop in 1959 (41), it has become the most widely used cryoprotective agent in cryopreservation of cells and tissues due to the high cell membrane permeability to DMSO. During freezing, DMSO can permeate across cell membranes easily to inhibit intracellular ice formation and prevent injury of extreme cell volume excursion caused by severe dehydration (31, 42, 43).

However, toxicity and side effects related to DMSO in clinical practice and biological research have been widely reported from mild discomfort to fatality, in a dose-dependent manner. It was reported that DMSO plays multiple roles on cellular functions and cell growth by affecting metabolism, enzymatic activity, cell cycle and apoptosis (44, 45). Lin et al. found that DMSO with concentration higher than 1-2% could induce apoptosis in lymphoma cells (46). DMSO may also lead to uncontrolled differentiation of stem cells (47, 48). Zyuz'kov et al. reported that DMSO could inhibit proliferation, stimulate maturation or change biological properties of the transplanted bone marrow stem cells even when DMSO concentration was low (0.02-0.25%) (49). Pal et al. studied the

exposure of embryos to DMSO and found that DMSO not only affected phenotypic characteristics but also induced alteration in gene expression, differential trajectory and functionality of hepatic cells (45). DMSO was also found to interfere with intracellular calcium concentration (39). All these findings imply that DMSO transfused together with cellular therapy products may affect the function of stem cells and influence the engraftment ability.

Lots of adverse events have been reported to be related to DMSO in stem cell transplantations. A significant uncomfortable response of injected DMSO is the garlic-like odor and taste due to excretion of its metabolite—dimethyl sulfide (DMS). About 45% of infused DMSO is excreted in urine, whereas a small percentage of DMSO is reduced to DMS and secreted through the skin, breath, feces, and urine for up to 2 days after infusion, causing a "noxious, garlic-odor" malodor. DMSO can also induce histamine release. All these factors may affect the central limbic-hypothalamic pathways, leading to nausea, vomiting, diarrhea, headache, flushing, fever, chills, dyspnea, anaphylaxis, vasodilatation and hypotension, pulmonary or abdominal complaints and complex reactions of cognition and emotion (10, 11, 20, 50-53). Premedication with antihistaminics may neutralize DMSO-induced histamine release, whereas it may cause some other more serious complications, such as bradycardia (20).

DMSO has also been reported to be related to neurotoxicity with dose-dependence (11, 17, 19, 54-58). DMSO seems to affect the vascular system including vasoconstriction which then may lead to altered neuronal function (19). Hanslick et al. found that DMSO produced widespread apoptosis in the developing central nervous system (55). Cavaletti et al. found that DMSO administration induced a reduction in nerve conduction velocity and structure changes in sciatic nerve in rats (57). Toxicity analysis of DMSO in rodents indicated a dose-dependent increase in neurotoxicity (22, 57). Animal studies also showed that DMSO affected the sleep structure in rats by increasing light slow wave sleep and reducing deep slow wave sleep (39). Hence, the DMSO-related neurotoxicity must be thoroughly investigated in stem cell transplantation, especially in pediatric use.

Table 1-1 Side effects of hematopoietic stem cell transplantation

Side effect categories	Symptoms	References	Side effect incidence
Allergy	Flushing, rash, pruritus, erythema	(50-52)	In 144 patients, 67.36% patients developed adverse events. Specifically, 43.75% allergic reactions, 25% gastrointestinal symptoms, 20.83% respiratory symptoms, 11.81% cardiovascular and 3.47% neurological symptoms (11). Nephropathy incidence in adults varies between 0 and 29% (23). 26.4% patients with acute renal insufficiency within the first 100 days after transplantation. In retrospective studies, the incidence of renal insufficiency in the early phases following transplantation in pediatric patients was 34-50%. Renal inefficiency rates were 41%, 31%, and 11% of children at 1, 3 and 7 years after transplantation, respectively (53). 25.25% side-effect events in the autologous group during infusion period. 7.73% cardiac side effects, 1.54% sinus bradycardia, and 15.97% non-cardiac side effects (15). 8% of non-cardiac complications and 57.33% for cardiac side effects, where hypertension incidence rate of 36% in patients treated with PBPCs (54). 50% of patients suffered side effects, wherein hypotension (22%), hypertension (4.54%), and bradycardia (4.5%) (55). 0.4% severe adverse reactions and 50% non-cardiac side effects in 1400 infusion studies (56). 65% sinus bradycardia, 29.41% heart block and 41% hypertension, 82% arrhythmias (57). 41% non-cardiac side effects, no bradycardia and arrhythmias (58). 58% systolic hypertension and 64% diastolic hypertension, 32% bradycardia (24).
	Edema, anasarca	(15, 27)	
	Bronchospasm	(59)	
Gastrointestinal complaints	Headache	(12, 14-16, 24, 27, 60)	
	Chest tightness, dyspnea	(12, 16, 24, 61, 62)	
	Abdominal cramping/pain, gastrointestinal distress, diarrhea	(12, 15, 23, 25, 27, 51, 59-62)	
	Nausea, emesis, vomiting	(15, 19, 63)	
Renal dysfunctions	Hemoglobinuria, proteinuria, mild azotemia	(51, 60, 64)	
	Hemolytic-uremic syndrome (HUS)	(64)	
	Urine incontinence	(18, 65)	
	Thrombocytopenia, hemolytic anemia	(23, 64)	
	Renal insufficiency, nephropathy, acute renal failure	(23, 52, 53, 64, 66, 67)	
Cardiovascular complaints	Hypotension, hypertension	(50, 54, 57)	
	Arrhythmias/bradycardia, tachycardia	(13, 26, 29, 67)	
	Hypothermia, hyperthermia	(12, 15, 25, 26, 64, 67)	
	Rigor, tremor	(15, 64, 68)	
	Ischemia, hypoxia, stroke	(50, 63, 68-70)	
	Syncope, coma, somnolence, shock, loss of consciousness, trismus	(17, 18, 22, 50, 63, 71-73)	
	Respiratory arrest, shortness of breath, cardiac arrest, coronary artery spasm	(17, 22, 52, 63, 68, 74, 75)	
	Seizure	(12, 17, 19, 22, 23, 67, 71)	
	Heart block	(27, 61)	
Neurological complaints	Mydriasis, miosis, Dysarthria, bilateral thalamic infarction, ophthalmic deviation, blurred vision	(16-19, 22, 65, 76)	
	Dysgeusia	(51)	
	Reversible leukoencephalopathy (RPL), severe encephalopathy,	(50, 65, 67-69, 71)	
	Central nervous system affected	(17, 52)	
	Transient global amnesia	(16, 22, 63, 65, 77)	
	Cerebral infarction	(63, 77)	
	Cognition problem	(16, 63, 65, 68)	
	Numbness, muscle weakness	(15, 16, 50, 63, 65)	
	Mental acuity, anxiety	(65, 68)	
Hepatic dysfunctions	Progressive jaundice	(52, 64)	

It was also reported that DMSO may be related to renal, hepatic dysfunctions and cardiovascular complications after transplantation (38). The side effects also depend on the dose of DMSO. Ruiz-Delgado et al. found that cryopreserving hematopoietic stem cells with 5% rather than 10% DMSO could result in less toxic reactions of cardiac dysfunction and acute renal failure (27). Donmez et al. found that DMSO content was significantly higher in patients with side effects than those without side effects and higher in patients with cardiac side effects compared to non-cardiac side effects (15). Infusion of DMSO can cause acute vasospasm in swine, suggestive of angiotoxicity (59). Pal et al. suggested the potential DMSO-induced hepatotoxicity by severely affecting the endodermal and hepatic lineage in a concentration-dependent manner (45).

There is another factor that transfusion of stem cells together with DMSO might influence the stem cell functionality and engraftment rate, but has never been mentioned in the literature yet. When cellular therapy products together with 10% DMSO are transfused through veins, the infusion rate usually should be as low as about 10mL/min in order to reduce infusion-induced reactions, which is much lower than the blood flow rate in veins, indicating that stem cells in hypertonic solution are exposed to osmotic environment suddenly with very small volume ratio. This process is similar to one-step fast washing of highly concentrated CPA from cryopreserved cells. Studies have proved that this process could cause extreme cell volume expansion and osmotic injury to cells (60, 61). Thus, cell viability loss due to osmotic injury may happen right after transfusion of stem cell-DMSO suspension and affect engraftment.

It is worth emphasizing that adverse effects related to DMSO are dose-dependent and can even be cumulative when multi-dose cell therapies are implemented (45, 57, 62). Junior et al. recommended that the maximal dose of DMSO to be infused was 1g/kg of bodyweight (17). This implies that special treatments should be taken in pediatric patients because of their light bodyweight. Studies of hematopoietic stem cell transplants in children showed that side effects in this patient group were more severe (63, 64), which confirms the concern mentioned above.

It must be emphasized that adverse events after hematopoietic stem cell transfusion may be multifactorial apart from DMSO toxicity. Often it’s hard to confirm whether the

pathogenesis of the complications is due to DMSO or other factors. Actually there is still debate on the role of DMSO depletion before transfusion. Cordoba et al. found that despite of DMSO depletion and adequate histamine blockage, side effects continued to appear, suggested that these side effects might be related to the number of granulocytes more than DMSO, and removal of DMSO was not needed (11). However, DMSO toxicity may be idiosyncratic, thus be unpredictable and unavoidable (17). Therefore, most researchers recommended removing DMSO before infusion. The washing procedure not only depletes DMSO, but also removes cell debris, reduces the neutrophil number and levels of platelet and while blood cell-derived soluble mediators, and thus decreases the adverse event incidence (9). Some studies already showed that DMSO depletion could reduce adverse effects with minimal effects or even improvements on engraftment (9, 12, 14, 20, 28, 65-67).

How to decrease the side effects

Many approaches have been applied in clinical practice to reduce the adverse effects of hematopoietic stem cell transplantation (9, 17, 27, 68-70), such as: (1) premedication before reinfusion; (2) post-reinfusion hydration and allopurinol administration; (3) slow down the infusion speed and prolong the transfusion time; (4) divide the infusion into two or three aliquots giving several hours or a day apart to reduce infused DMSO amount at a given time; (5) concentrate the infused stem cell concentration to reduce the engraftment volume and infused DMSO content; (6) reduce DMSO concentration for cryopreservation lower than 10%, or use alternative CPA to mix with or replace DMSO; (7) select the specific stem cells after thawing for infusion; and (8) remove DMSO before infusion. Since the side effects are idiosyncratic thus unpredictable so far to our knowledge, all these approaches are suggested to be combined to reduce the reaction incidence as low as possible. Most importantly, DMSO is suggested to be removed before transplantation.

1.7 Challenges in cryopreservation

As mentioned above, choosing the best CPA for a cell type is the first step to successful cryopreservation. It depends on the cell membrane properties, such as the cell membrane permeability to the CPA and the CPA toxicity to the cells. So far the general methods to

measure the cell membrane permeability are based on the measurements of the cell volume excursion history when the cell is suddenly exposed to the CPA solution. The difficulties of the experiments include the design of the micro-perfusion environment, video capturing, and data analysis.

Optimal cooling rate for a cell type is the core problem of cell cryopreservation. It depends on the cell properties, such as osmotically inactive cell volume, the cell membrane permeabilities to water and CPA at different temperatures, the activation energy of water transport across cell membranes, and so on. For a non-empirical scientific study, all these properties should be measured, and subsequently be combined with the theoretical analysis of mass transfer across cell membranes to predict the optimal cooling rate. An easy-to-operate, precise and cost-effective system to determine all these properties is highly needed.

Another challenge in cryopreservation is the addition and removal of CPAs. Currently CPAs are commonly added dropwise to the concentrated cell suspension in an open processing system while an operator provides manual continuous agitation. This method is largely uncontrolled and can easily result in cell damage if the CPA is added too rapidly or too slowly by the operator, exposing the cells to lethal osmotic injury (60) and toxic effects of CPA (42). CPA removal is usually performed via several repeated centrifugation steps, an open processing method that is susceptible to product contamination and further reduces the product yield (<70%). Recently, some methods of CPA removal based on diffusion across hollow fibers or in microfluidic channels have been proposed (71-74). However, these methods are far from practice because of low throughput, low efficiency, high cell loss and operation complexity. Cells transplanted to patients along with CPA can result in significant patient discomfort and severe side-effects. Thus, it would be highly desirable to develop a simple closed system permitting CPA removal after cryopreservation.

1.8 Outline of this dissertation

The dissertation is organized as follows.

Firstly, a microfluidic channel is employed to measure the cell membrane permeabilities to water and different CPAs at room temperature. The results can be used to choose the optimal CPA, design the optimal CPA addition and removal protocols, and predict desired cooling rate roughly. Human vaginal mucosal immune lymphocytes (CD3+ T cells and CD14+ macrophages) are adopted as model cells to demonstrate the feasibility of the microfluidic testing system because of their importance in vaccine development and microbicide tests in HIV.

However, when this system is applied to measure the cell properties at subzero temperatures, a temperature control chamber (such as Instec temperature-controlled chamber) is required, which may cause many technical difficulties. For example, the spacing between microscopic lens and the sample gets much larger, so special lenses with extremely long working distance are required. Another big challenge is the defrosting at sub-zero temperatures. A few glass windows are needed in the cryo-chamber system for sealing and defrosting, such that the quality of captured videos/images decreases dramatically because the working light has to transmit through the chamber windows, glass slide, and/or the PDMS layer of the microfluidic device. Therefore, in this dissertation, secondly, a DSC measurement approach is proposed to assess the cell membrane properties at sub-zero temperatures.

Thirdly, an automatic multifunctional cell processor based on semi-permeable hollow fibers is proposed for CPA addition and removal. This device is also applicable for cell concentration/volume control of the cell suspension. In order to achieve online, real-time monitoring of the residual content of CPA in the cell suspension during CPA removal, an easy method of electrical conductivity measurement is applied.

Fourthly, cryopreservation of bacteria and freeze-drying of proteins are also studied. *Mycobacterium tuberculosis* was chosen to be studied due to the fact that tuberculosis is the 2nd leading infectious disease (only after HIV) causing death in the world and the big challenges in tuberculosis diagnosis. In this part, the studies include optimization of MTB cell cryopreservation and long-term freeze-drying preservation of the MTB-IgY antibody.

In the last chapter, a brief conclusion of the work in this dissertation is given. Future work is also discussed.

Chapter 2 Determination of cell membrane properties at room temperature with a microfluidic perfusion channel and cytotoxicity of cryoprotective agents

2.1 Introduction

HIV is the leading infectious disease causing death in the world (75). It is generally accepted that for an HIV vaccine to be effective it must induce humoral and cellular immune responses at the portals of viral entry, e.g., the genital and rectal mucosa (76). Yet in the clinical vaccine trials conducted so far mucosal immune responses have not been evaluated. In light of the absent or marginal efficacies reported for the HIV vaccines clinically tested to date (77-79), the lack of information on mucosal immunity has been a sore spot. A thorough analysis of the mucosal immune system could have uncovered specific weaknesses or risks of these vaccines, helping to improve the design of the current pipeline of vaccination strategies. Because mucosal tissue sampling is critical for assessing HIV vaccine efficacy, mucosal specimen collection and preservation methods should be studied and optimized. A critical problem we are facing now is our current inability for cryopreserving the collected mucosal specimens without loss of viable immune cells and their functionality.

Similar to those mentioned in Chapter 1, cryopreservation of mucosal specimens is vital to the successful analysis of mucosal immunity in vaccine trials:

(1) Pooling of mucosal specimens: Cryopreservation of mucosal samples affords the flexibility to pool samples obtained at different time points from the same individual. Sometimes one mucosal sample, for example a cervical cytobrush, fails to yield enough cells for a particular assay but several samples pooled together allow the desired analysis.

(2) Banking of mucosal specimens: In many instances, it is desirable to store all or part of a mucosal specimen for analysis at a later time point, often months or years after a sample has been obtained. The reasons for this delayed assaying can be manifold, ranging from practical considerations, for example performing assays in batches rather than with each individual sample as it is obtained, to the

needs to keep samples available for confirmatory assays or to perform more detailed analysis as more sophisticated technologies become available over time.

(3) Shipment of mucosal specimens: Not all sites participating in a clinical trial have the equipment and knowledge to perform the sophisticated phenotypic and functional immune assays required to analyze vaccine- and infection-induced immune responses. Therefore shipment of samples to central laboratories is required where these assays can be performed in optimal manners.

Unfortunately, cryopreservation of mucosal immune cells and tissues has not been successful. So far, the trial protocols are based on the knowledge of cryopreservation of progenitor blood mononuclear cells (PBMC). The recovery rates of mucosal immune cells and tissues are very low. This fact severely hampers our ability to perform mucosal cell-based immune assays on a scale desired for multi-site clinical vaccine trials. It's highly possible that this failure was due to the lack of understanding of the cryobiological characteristics of the mucosal cells and tissues.

The cryobiological characteristics include (a) the lethal intracellular ice formation (IIF) during the freezing process, (b) the ice re-crystallization injury to cells during the thawing process, (c) the cell volume osmotic-excursion tolerance limits, (d) the cell osmotically-inactive volume fraction, (e) the cell membrane permeability coefficients and their activation energies to water and cryoprotective agents (CPAs), and (f) the potential toxicity and osmotic injury caused by the CPAs to cells during adding the CPAs into the cells before freezing and removing the CPAs from cells after thawing. All of these properties are critical determinants for cell death or survival during the cryopreservation process. In this chapter, we will develop an approach to determine the cryobiological characteristics.

Since the majority of HIV infections occur heterosexually across the genital mucosa, and women are more vulnerable to HIV transmission than men (80), we will focus on the female genital mucosa. For practical reasons, we focused on the two cell populations that are central to adaptive cellular immunity, T lymphocytes and APCs (macrophages).

Future studies could evaluate mucosal B cells (humoral immunity) and natural killer (NK) cells (innate immunity).

In this chapter, a microfluidic perfusion channel will be applied to measure the membrane properties of human vaginal mucosal immune cells at room temperature. The results can be used to choose the optimal CPA for cryopreservation and roughly predict the optimal cooling rates for these cell types. CPA toxicity will be also studied.

2.2 Materials and methods

2.2.1 Tissue digestion and cell isolation

- **Human mucosal specimens**

Vaginal biopsies were taken from surgical tissues donated by healthy women undergoing vaginal repair surgeries at Fred Hutchinson Cancer Research Center (FHCRC) in Seattle and in the Department of Gynecology at the University of Washington.

- **Isolation and purification of mucosal immune cells**

Immediately after surgical removal, the vaginal tissues were transported in saline solution on ice to Dr. Hladik's laboratory at FHCRC and twenty 5-mm punch biopsies were taken. Cells were isolated from the biopsies using a two-enzyme digestion protocol developed by Hladik et al. The cell suspension was filtered through filters with pore-size of 70 μm and 20 μm respectively. Cells were then stained for CD45, CD3, CD14, CD19, and viability tests (Table 2-1).

Table 2-1 Multi-color FACS staining panel (provided by Dr. Hladik from FHCRC)

Marker	Color	Clone	Catalogue #	Manufacturer
Viability	Aqua	n. a.	L34957	Invitrogen
CD45	APC	HI30	555485	BD
CD3	PacBlue	UCHT1	558117	BD
CD4	ECD	SFCI12T4D11	6604727	Coulter
CD8	PE	SK1	340046	BD
CD19	APC-H7	SJ25C1	560177	BD
CD14	PE-Cy7	M5E2	557742	BD
HLA-DQ	FITC	TU169	555563	BD

- **Flow cytometric sorting of cell sub-populations**

Cells isolated from human vaginal biopsies were purified by flow cytometric sorting using the antibody panel listed in Table 2-1. Cell sorting was performed on a BD FACSAria machine in the laboratory of the Shared Resources facility of FHCRC. The BD FACSAria machine allows simultaneous sorting of four cell populations, thus giving us the opportunity to sort viable CD45+ mucosal leukocytes into CD3+ T cells, CD14+ macrophages, and CD19+ B cells. T cells and macrophages were then subjected to cryobiological analysis. B cell population was usually not enough for the tests. The representing FACS sorting results are shown in Figure 2-1.

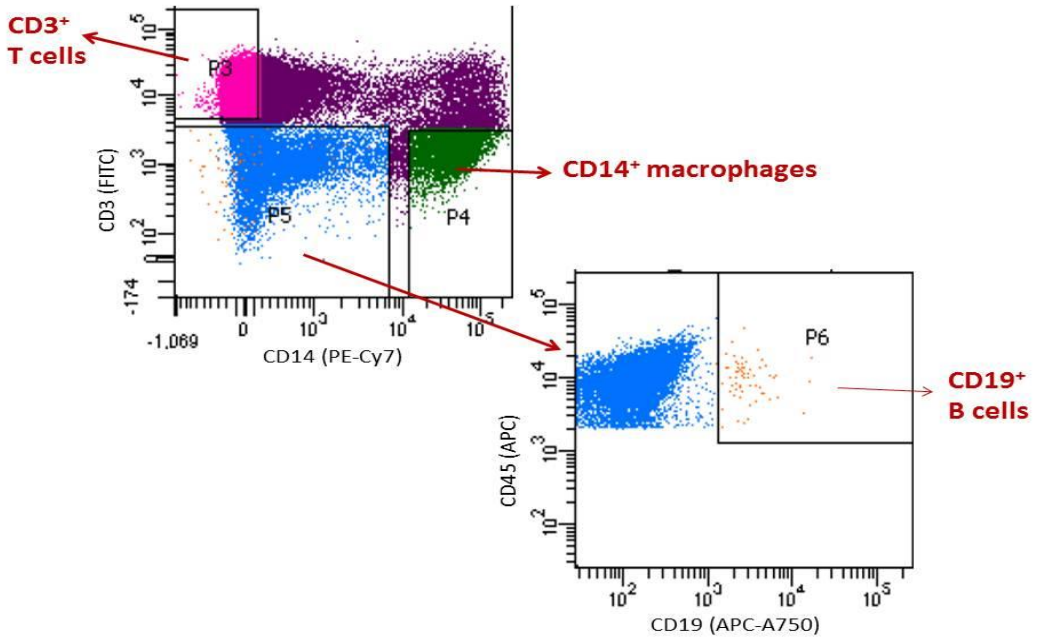

Figure 2-1 FACS sorting of human vaginal immune cells

After the procurement and assessment of the mucosal immune cells as above, the cells were transferred on ice to the Gao Lab at University of Washington, and then stored in the incubator with environment of 37 ℃, 5% CO_2 and 100% humidity for the subsequent tests. The tests were finished as soon as possible (generally within 3-8 hours) because the cells may lose their viability and function after storage.

2.2.2 Microfluidic channel

The sketch of the microfluidic perfusion channel is shown in Figure 2-2. The general idea was originally proposed by Chen in the Gao Lab at University of Washington. Briefly

speaking, the cell suspension is fed at the inlet reservoir, sucked by the syringe pump (Harvard Apparatus) to pass through the micro-channel. Cells are blocked by the PDMS blocker. The channel inner scale is designed specifically for the cell type. For example, the spacing between the glass slide substrate and the PDMS blocker (h1) is smaller than half of the cell diameter such that the cells can be trapped there, even when the cells are exposed to hyperosmotic solutions and shrink significantly. The inner height of the channel (h2) is about 1.5x of the cell diameter such that the cells can pass through the channel without constraint and at the same time monolayer of cells are aligned besides the blocker. The micro-channel modes were fabricated in the Washington Technology Center (WTC) at University of Washington. More details can be found in the references (81, 82).

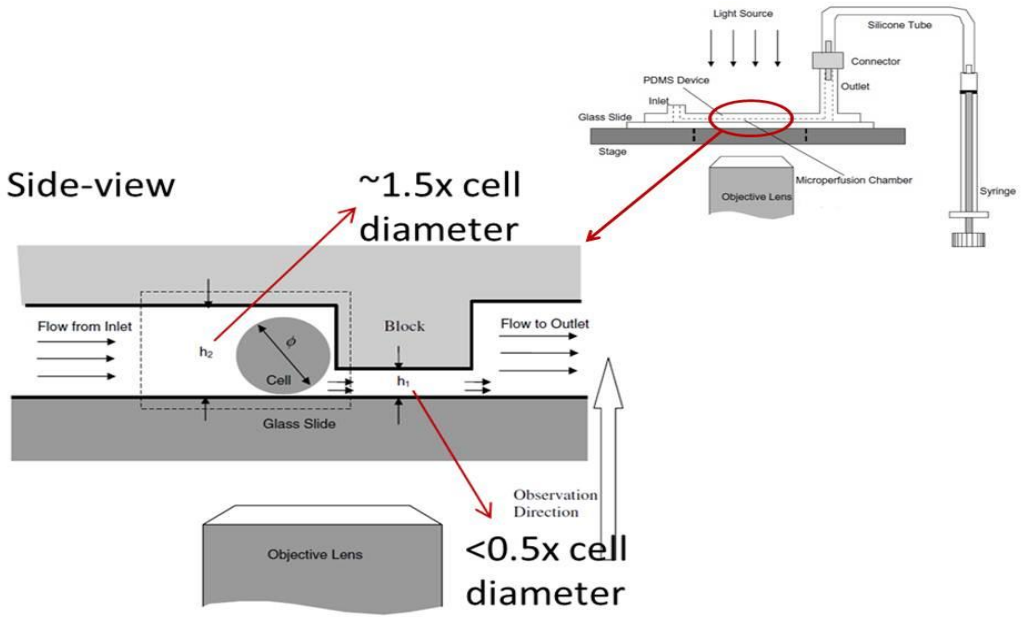

Figure 2-2 Microfluidic perfusion channel

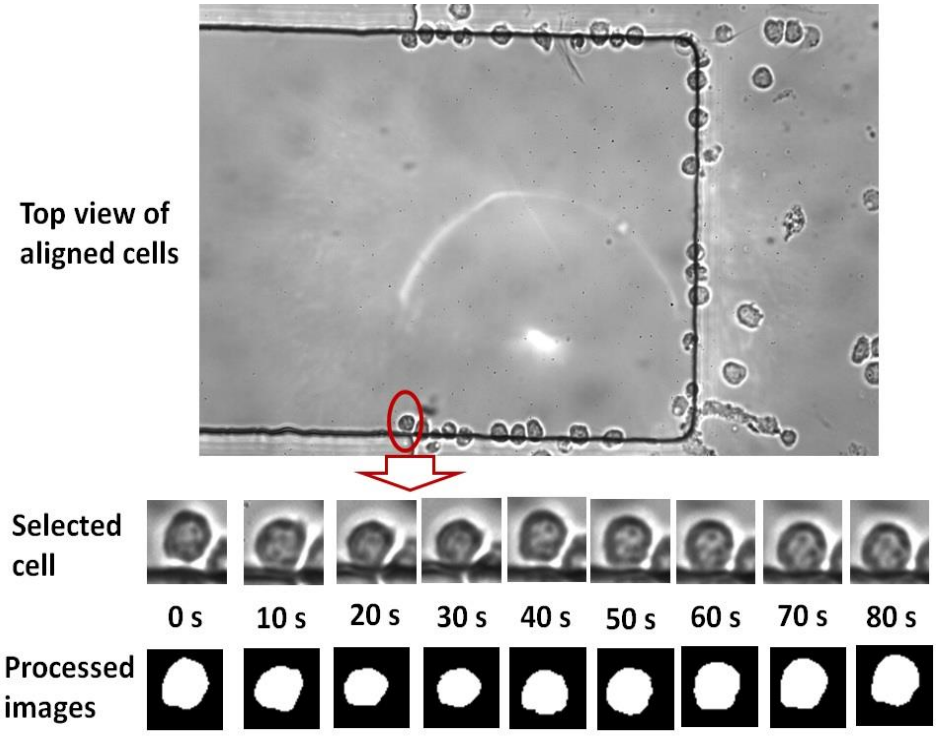

Figure 2-3 Cell volume excursion during perfusion and the image processing

2.2.3 Perfusion solutions

In this experiment, cell membrane permeabilities to water (Lp) and four different kinds of CPAs (DMSO, glycerol, ethylene glycol and propylene glycol) will be tested. In order to get the osmotically inactive cell volume, the cells should be perfused by hypertonic saline solutions with different osmolalities. Two hypertonic PBS saline solutions (2x and 3xPBS) were prepared. The perfusion solutions, composition and osmolalities are listed in Table 2-2. The osmolalities were measured by a vapor pressure osmometer (Wescor Inc., Logan, UT).

Table 2-2 Perfusion solutions and the osmolalities

Perfusion solution	Osmolality (mOsm/kg H_2O)
1x PBS	297
2x PBS	605
3x PBS	881
10% (v/v) DMSO in 0.9% NaCl	1823
1.5M glycerol in 0.9% NaCl	1956
1.5M ethylene glycol in 0.9% NaCl	1761
1.5M propylene glycol in 0.9% NaCl	1575

2.2.4 Experimental procedures

The procedure of cell membrane property measurement with microfluidic perfusion channel is as follows:

(1) A few microfluidic perfusion channels were freshly prepared based on the manufactured mode. 1x PBS solution was pumped into the channels immediately in order to check the availability of the devices and also to keep the channels hydrophilic. The PDMS micro-perfusion device was then fixed on the microscope (Leica) stage for stability during experiments.

(2) Human vaginal mucosal immune cells in 1xPBS (T cells and macrophages) were received from Fred Hutchinson Cancer Research Center. The cell concentration was adjusted to about 5000 cells/mL. The cells were stored in the incubator if more than 2 hours were needed for the experiments; otherwise they were stored on ice.

(3) 10uL cell suspension was fed to the inlet reservoir with pipette. Micro-syringe pump was run to suck cells to the channel with a flux of about 10uL/hour. After about 10min, a few cells were trapped and aligned steadily besides the blocker inside the channel.

(4) After the cells were trapped in the channel, >100uL perfusion solutions was fed at the inlet and pumped into the microchannel. The cells were perfused by the solutions. The cell volume changed. The cell volume excursion was recorded by a high speed camera with high resolution (Phantom v310, Vision Research) with capturing rate of 24 frames per second.

(5) After perfusion for about 2min, the experiment was stopped. The microchannel was flushed with 1xPBS twice to clear the solutions and debris inside the channel. Then the perfusion experiment was repeated.

(6) The above experiments were performed for different cell types (T cells, macrophages) and different perfusion solutions (2xPBS, 3xPBS, DMSO-NaCl, glycerol-NaCl, ethylene glycol-NaCl, and propylene glycol-NaCl).

In order to get more reliable experimental results, a few points in the experiments were optimized and improved.

(1) The inlet reservoir was made large. It can contain at least 500uL liquid. This design is to increase the volume ratio of hyperosmotic perfusion solution and isotonic cell suspension and to decrease the error introduced by the solution mixing.

(2) The distance between inlet reservoir and the cell trapping line was shortened to less than 5mm such that cells could be driven to the trapping line in short time.

(3) When the cell suspension was pumped through the microchannel, the flow rate was set as about 10uL/hour. This flow rate was chosen because it was low enough such that the cells could be trapped in the channel steadily and not flushed away, and at the same time the flow rate was high enough such that after a short period cells or perfusion solutions could reach the blocking line. The inner size of the microchannel is 20um in height and 150um in width. So for a flux of 10uL, the average flow velocity is about $\frac{10uL/hour}{20um\times150um} \approx 0.93mm/sec$. For a distance of 5mm, it will take ~5.4sec for the cells to travel, which is acceptable. However, in the experiments, the situation was more complex. Firstly, it took some time for the syringe pump to reach the steady low flow rate. Air bubbles in the channel and any disturbance of the tubing could make the flow rate unstable. Secondly, it was found that cells were preferred to be concentrated and trapped at the channel entrance until lots of cells aggregated there. This interesting phenomenon is shown in Figure 2-4. As a result, 15~20 minutes were needed to achieve the ideal situation with enough cells trapped in the channel.

(4) The image analysis to assess the 2-D cell area change history, therefore the 3-D cell volume excursion history, was challenging because the quality of the images was restricted by the experiment setup. Regardless of upright microscope or inverted microscopy, the light source should transmit through the PDMS layer or the glass slide, which could make the images foggy, especially for the cell boundary. In order to improve the image quality, phase contrast was applied. At the same time, the image analysis algorithm was also improved (see details as below).

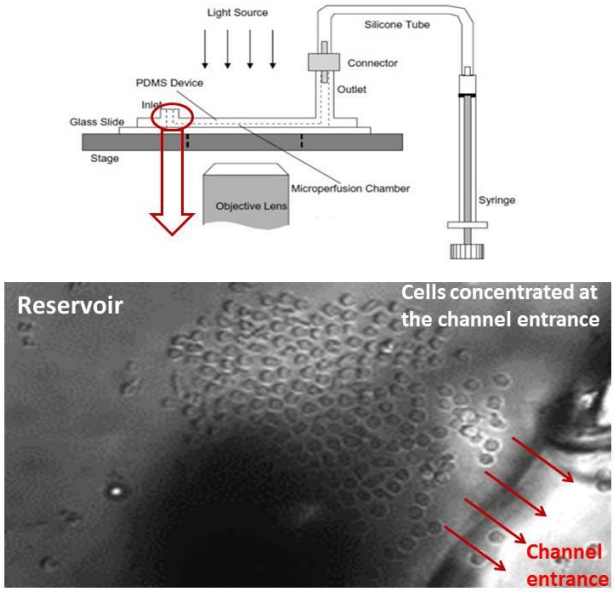

Figure 2-4 Cells are concentrated at the entrance of the microchannel

2.2.5 Image analysis

After video capturing, the videos were converted to images frame by frame by the software of Cine Viewer (Vision Research). For a selected cell, the image spot was cropped from each frame of the image. The cropped images were enhanced and then processed to find the cell boundary (see Figure 2-3). In order to detect the cell boundary precisely, the algorithm of "Active Contour (dual-snake)" was applied. Briefly speaking, initially two rectangles (or circles) outside and inside the cell, respectively, were drawn. The outer rectangle squeezes towards the cell boundary with increasing image intensity and the inner rectangle expands towards to the cell boundary too with decreasing image intensity. Once they meet, the cell boundary was determined. Thereafter, the 2-D cell area is assessed by pixel counting and then converted to 3-D cell volume based of the assuomtion of spherical cell shape. All the image processinges were performed with MatLab software.

2.2.6 Determination of the cryobiological characteristics of the cells

2.2.6.1 Determination of osmotically inactive cell volume fraction (V_b)

Vb is the osmotically inactive volume fraction of the cell. Assuming the cells act as ideal osmometer, it can be determined by Boyle-van't Hoff plot. Briefly, the final steady cell

volumes in isotonic and hypertonic saline solutions (2x and 3x PBS) are plotted in the format of normalized cell volume *Vs* reciprocol of osmolality of the solution (see Figure 2-6). The y-intercept is the Vb, which shows the cell volume fraction when the solution osmolality approaches ∞.

2.2.6.2 Determination of cell membrane permeability to water (L_p)

Values of Lp of the human vaginal mucosal immune cells (T cells and macrophages) were determined by measuring changes in cell volume while cells were perfused by 2x and 3x PBS solutions, where only a non-permeable solute was present. Cell volume was measured from captured cell images by counting the number of pixels using Matlab (The Mathworks, Inc., Natick, MA) (see Figure 2-3). The data were fitted to the differential Equation (2-1) to determine Lp using MLAB curve fitting software (Civilized Software Inc., Silver Spring, MD), which describes the rate of water transport across the cell membrane (60, 83-87):

$$\frac{dV_c(t)}{dt} = L_p \cdot A \cdot (C_n^i - C_n^e) \cdot R \cdot T \qquad (2\text{-}1)$$

Where $V_c(t)$ is the cell volume at time t, Lp is the cell membrane permeability to water (um/atm/min), A is the cell membrane area ($= \boldsymbol{4\pi r^2}$ for a spherical cell shape), $\boldsymbol{C_n^i}$, $\boldsymbol{C_n^e}$ are the intracellular and extracellular osmolalities, respectively, R is the universal gas constant, and T is temperature (K).

Assuming that the cell acts as an ideal osmometer to hypertonic solutions, the intracellular osmolality during cell shrinkage can be determined using the Boyle van't-Hoff relationship applied to the osmotic responses of cells (88):

$$C_n^i = C_0 \cdot \left(\frac{V_0 - V_b}{V - V_b} \right) \qquad (2\text{-}2)$$

Where, C_0 is the initial intracellular osmolality (isotonic, =288mOsm/kg H_2O), V_0 is the isotonic cell volume, and V is the cell volume at C_n^i. The V_b value has already been determined by the Boyle van't-Hoff plot (see above) of cells that were perfused by 2x and 3x PBS solutions.

2.2.6.3 Determination of cell membrane permeability to CPA: Two-parameter transport formalism

When both permeable CPA (e.g., DMSO and glycerol) and non-permeable solute (e.g., salts) co-exist in a solution, the two-parameter transport model can be used to determine the cell membrane permeability to water (L_p) and to the CPA (P_s) (87, 89, 90). Compared with Equation (2-1), the cell volume change is governed not only by non-permeable solute, but also by the concentration of permeable solutes,

$$\frac{dV_c(t)}{dt} = \frac{dV_s(t)}{dt} + L_p \cdot A \cdot (C^i - C^e) \cdot R \cdot T \quad (2\text{-}3)$$

Where, $V_c(t), V_s(t)$ are cell volume and intracellular CPA volume at time t, respectively. C^i, C^e are intra- and extracellular osmolalities (including salts and CPA).

The CPA flux is given by

$$\frac{dN_s(t)}{dt} = P_s A(C_s^e - C_s^i) \quad (2\text{-}4)$$

Where, Ps is the cell membrane permeability to the CPA (cm/min), C_s^e, C_s^i are the extracellular and intracellular CPA osmolalities, respectively. $N_s(t)$ is the mole of intracellular CPA at time t.

$N_s(t)$ and $V_s(t)$ are interchangeable by

$$N_s(t) = V_s(t)/\overline{V}_s \quad (2\text{-}5)$$

Here, $\overline{V}_s$ is the partial volume of the CPA.

The simulation of Lp and Ps was done by least-square curve fitting using software of MLAB (Civilized Software Inc., Silver Spring, MD).

2.2.7 Osmotic tolerance limit tests of the T cells and macrophages

The osmotic tolerance limits of T cells and macrophages were tested as follows:

(1) As described above, the human vaginal mucosal tissues were received from Fred Hutchinson Cancer Research Center, digested and then filtered to achieve immune cells.
(2) In order to test the osmotic tolerance limits of T cells and macrophages, two kinds of CPAs, DMSO and propylene glycol (PG), were selected since the preliminary cell membrane property results showed that they were better options than others (see the results below). CPA Solutions in PBS with different concentrations were prepared as 12%, 16%, 20%, 24% and 28% (v/v)) for DMSO, and 2M, 2.5M, 3M, 3.5M and 4M for PG.
(3) Addition of CPA (DMSO, or propylene glycol): 100uL CPA solution (precooled to 4^{o}C) was added to 100uL cell suspension slowly drop by drop. The tube was agitated during addition. This process was done at 4^{o}C and took about 5min. After addition, the CPA concentration was diluted two-folds to 6%, 8%, 10%, 12%, and 14% for DMSO, and 1M, 1.25M, 1.5M, 1.75M, and 2 M for PG.
(4) The cell suspensions were equilibrated for 10min at 4 ℃.
(5) Removal of CPA: 4mL PBS was added to each tube slowly, drop by drop. The tube was agitated during addition. This process was done at 4^{o}C and took about 5min. Thereafter, the cell suspensions were centrifuged at 450g for 10min. The supernatant was removed and the sedimented cells were resuspended in PBS.
(6) The cells were sorted and the viability assessment was performed by flow cytometry.

This experiment was repeated twice, and in each experiment 2-3 replicates were done for each situation (cell type, CPA type and CPA concentration).

2.2.8 Cytotoxicity of CPAs to the T cells and macrophages

In order to test cytotoxicity of different CPAs to the immune cells, cells were suspended in FBS medium and then CPA solutions were added dropwise to final concentrations of 10% DMSO, 1.5M PG and 1.5M Glycerol. The cells in CPA or FBS alone were incubated for 2h at room temperature (22 ℃), then washed to remove the CPAs by adding large volume of PBS dropwise and slowly, centrifuged, and finally assessed for viability.

For control group, cells were in FBS medium alone without any CPA addition and removal. The control sample was kept in the refrigerator (4 ℃) for the same period of time and also was assessed for viability by flow cytometry.

2.2.9 Preliminary trial of cryopreservation of human vaginal mucosal T cells and macrophages with slow cooling rate

In order to select the optimal CPA for the mucosal immune cell cryopreservation, cryopreservation of T cells and macrophages were also tested. In this trail, DMSO, propylene glycol (PG) and glycerol were compared. Their final concentrations after mixing with cell suspensions were 10% (v/v), 1.5M and 1.5M, respectively. In the experiments, 200 uL precooled CPA solutions with 2x concentration in FBS were added to 200 uL cell suspensions (~500,000 cells were used) in FBS on ice dropwise over ~3-4 minutes. The cells were then equilibrated for 10 minutes in the precooled cooling rate controlled freezing device (box-in-box, see the design below) at 4 ℃ and then placed into the -80 ℃ freezer. About storage overnight , the sample vials were thawed quickly in the 37 ℃ water bath until barely any ice was left, and then 1.8 mL precooled PBS solution was added dropwise over about 4 minutes (slower at first, then speeding up). The cells were then stained for viability and phenotype assessment with flow cytometry.

At the same time, the unfrozen cell samples as control were stored on ice in FBS medium for about 2h before staining for practical reasons.

This experiment was repeated twice.

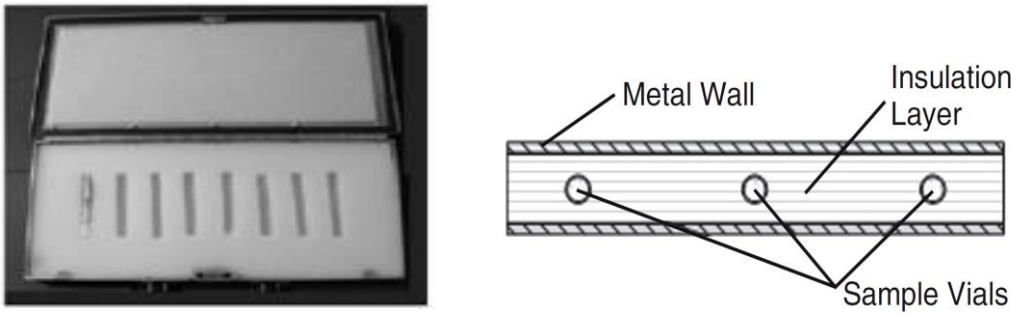

Figure 2-5 Box-in-Box (BIB) system for slow cooling. (A) An opened BIB, in which sample vials are placed in one slot. (B) Cross-section of the BIB system.

For the freezing with a specific cooing rate, a passive cooling rate controlled device—Box-in-Box (BIB)—was developed in our lab and was applied in this experiment. In the BIB system (Figure 2-5), two thermal insulation sheets made of polyethylene foam fill inside the aluminum enclosure. The thickness of the polyethylene foam layer was designed for a low cooling rate and then demonstrated empirically (91). For cryopreservation in BIB, vials were placed in the slots cut into the polyethylene foam. The system was then closed and placed into a -80 ℃ freezer overnight. Dummy samples with only cryoprotective medium were treated the same way. T-type thermocouples (SA-1T; Omega, Stamford, CT) were inserted inside the dummy samples to record temperature history during cooling.

2.3 Results

2.3.1 Determination of osmotically inactive cell volume fraction V_b

The Boyle van't Hoff plots of human vaginal mucosal T cells and macrophages are shown in Figure 2-6 (PBS solutions were prepared at different times for the two cell tests, so the osmolalities were different.). The inactive volume V_b of T cells and macrophages were determined to be 55.0% and 43.8%, respectively according to the y-intercepts.

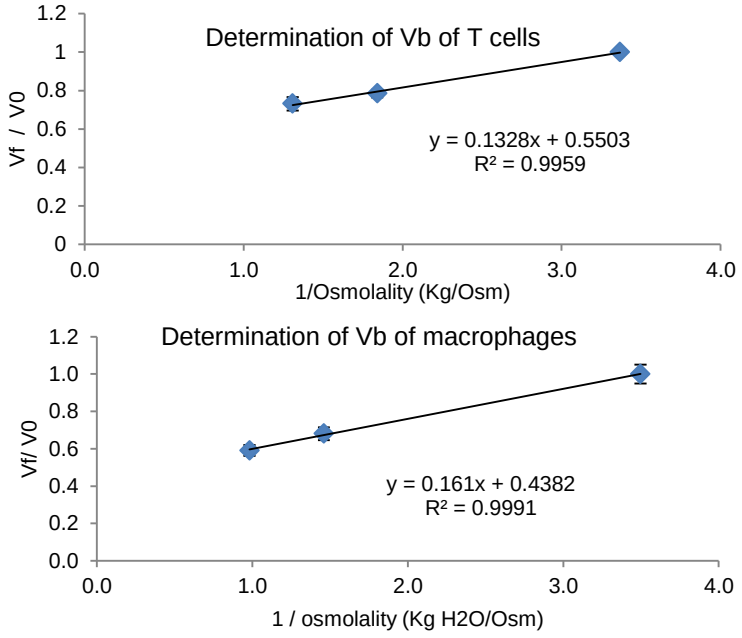

Figure 2-6 Determination of osmotically inactive cell volume fraction

2.3.2 Determination of cell membrane permeabilities to water (Lp) and CPAs (Ps)

An example of the cell volume excursion history when perfused by hypertonic saline solutions (2x, 3xPBS) is shown in Figure 2-7. While perfused by permeable CPA solutions, such as DMSO, the cell volume change is shown in Figure 2-8.

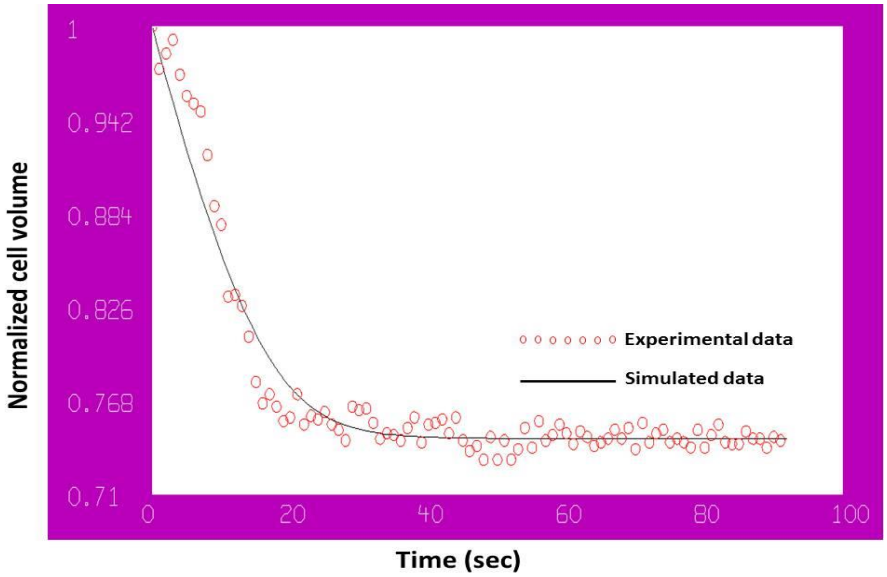

Figure 2-7 Cell volume excursion when perfused by hypertonic saline solution (3xPBS)

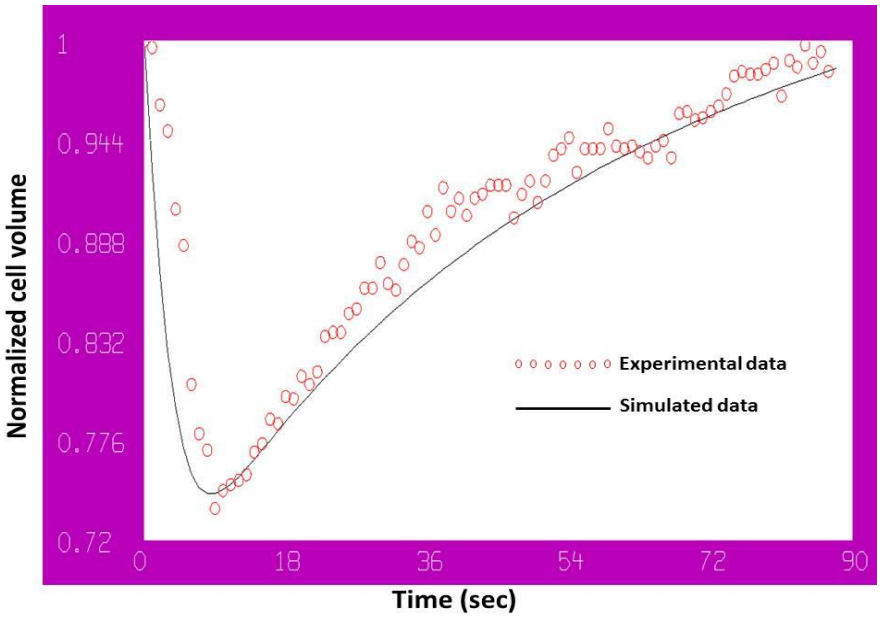

Figure 2-8 Cell volume excursion when perfused by hypertonic CPA solution (DMSO)

Table 2-3 Membrane permeabilities of T cells to water and CPAs

CPA	Lp (um/min/atm)	Ps(xe-3 cm/min)
PBS(n=14)	0.21±0.057	
DMSO(n=8)	0.088±0.049	0.47±0.23
Propylene Glycol (n=8)	0.075±0.053	0.63±0.34
Ethylene Glycol (n=7)	0.097±0.051	0.46±0.17
Glycerol (n=8)	0.054±0.003	0.0050±0.0040

Table 2-4 Membrane permeabilities of macrophage cells to water and CPAs

CPA	Lp (um/min/atm)	Ps(xe-3 cm/min)
PBS (n=15)	0.29±0.064	
DMSO (n=8)	0.24±0.047	0.99±0.37
Propylene Glycol (n=9)	0.23±0.17	1.18±0.49
Ethylene Glycol (n=7)	0.25±0.096	0.42±0.089
Glycerol (n=7)	0.20±0.077	0.0080+0.0030

Figure 2-7 shows volume excursion (shrinkage) of macrophage cells perfused with hypertonic 3X PBS. The results of other situations (T cells or macrophages perfused by 2x or 3xPBS) were similar to this figure. The figure shows that when the cell is exposed to the hypertonic saline solution, its volume decreases and then reaches the final equilibrium value. The volume is monotonically decreasing because there is only water transport across the cell membrane in this situation. Extracellular hypertonic saline solution drives the water efflux from inside to the outside of the cell. Therefore, the intracellular osmolality increases, and finally reaches the balance between intra- and extracellular environments. From Figure 2-7, especially the segment of volume changing period (0~25sec), the water transport ability, i.e., cell membrane permeability to water Lp, can be calculated. At the same time, we can also obtain the final equilibrium volume of this cell when exposed to 3x PBS, which can be used to predict the osmotically inactive volume fraction V_b.

Figure 2-8 shows volume excursion of macrophage cells perfused by 10% DMSO in 0.9% NaCl solution. The result shows that the cell shrinks first, and then expands gradually back to its original volume (may exceed its original isotonic volume a little). This phenomenon is caused by the co-existence of transport of water and permeable CPA.

When the cell is perfused by the CPA solution, the gradient of osmolality between intra- and extracellular environments drives mass transport across the cell membrane. Water flows out of the cell and the permeable CPA (DMSO) flows into the cell. Since generally the permeability to water is much higher than that to CPA, the transfer of water dominates in the beginning, such that the cell shrinks. After a period, water transport approaches its balance state, while the CPA concentration inside the cell is still much lower than that outside of the cell. So the CPA keeps flowing into the cell and the cell expands gradually. In this process, water will flow back into the cell slowly at the same time due to the increasing intracellular CPA concentration. This is the reason why the cell shrinks and then expands when exposed to permeable CPA solutions. So, according to the cell volume excursion history, the cell membrane permeabilities to water and CPA can be calculated.

The cell membrane permeabilities to water and CPAs were simulated by software MLAB. The results are shown in Table 2-3 and Table 2-4 for T cells and macrophages, respectively.

2.3.3 Osmotic tolerance limits of the T cells and macrophages

The results of osmotic tolerance limits to DMSO and propylene glycol for T cells (CD3+) and macrophages (CD18+) are shown in Figure 2-9. The results show that T cells are more vulnerable to the CPA solutions than macrophages. For example, in experiment 1, when 10% DMSO was added and removed, T cell viability percentage decreased from 65% to less than 30%, while macrophage viability decreased from 65% to 58%.

It's obvious that the higher CPA concentration, the more injuries to the cells. Considering the effects of cryoprotective functions and injuries to the cells by the CPAs, an optimal concentration of CPA exists. In this experiment, the results suggest that 10% (v/v) DMSO and 1.5M propylene glycol are acceptable.

2.3.4 Cytotoxicity of CPAs to the T cells and macrophages

The cytotoxicity of three types of CPAs (DMSO, propylene glycol and glycerol) to T cells and macrophages was tested. The results are shown in Figure 2-10. Once again, it shows that T cells are much more vulnerable to CPAs than macrophages. Glycerol is more cytotoxic than the other two CPAs.

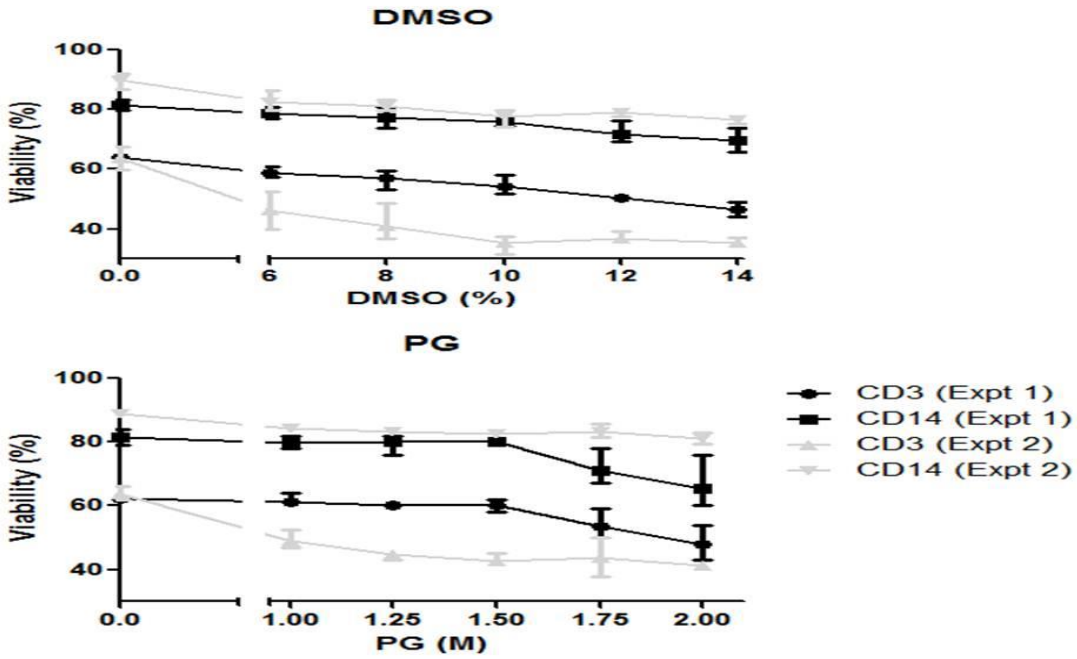

Figure 2-9 Osmotic tolerance tests of T cells and macrophages to CPAs (DMSO and Propylene glycol)

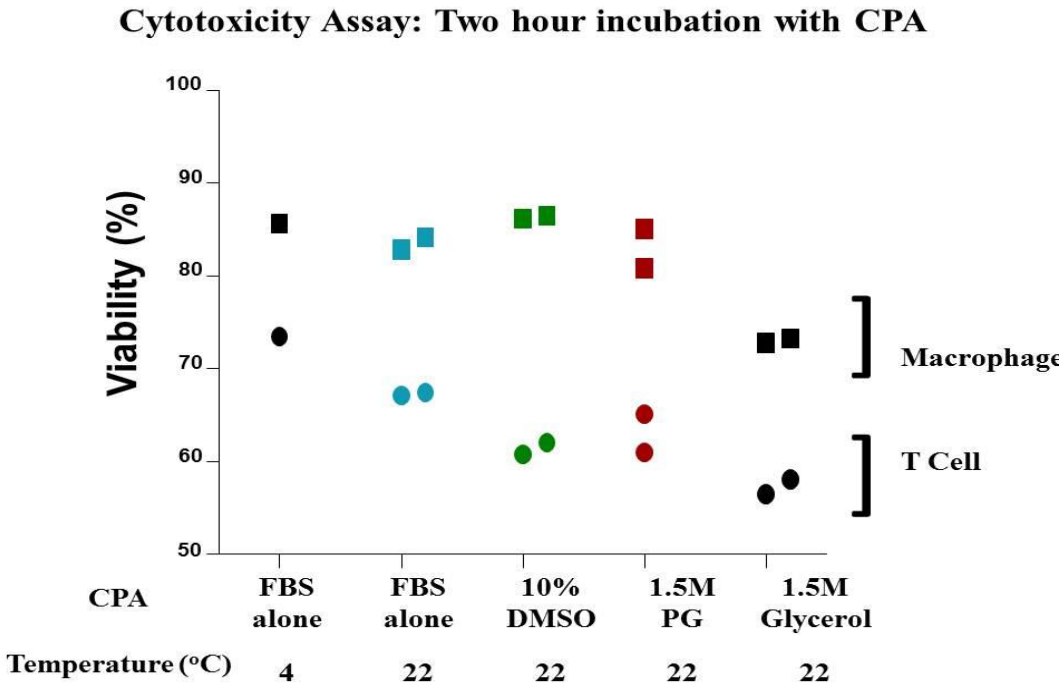

Figure 2-10 Cytotoxicity of CPAs (DMSO, Propylene glycol and glycerol) to the mucosal immune cells (T cells and macrophages)

2.3.5 Preliminary trial of cryopreservation of T cells and macrophages with slow cooling rate

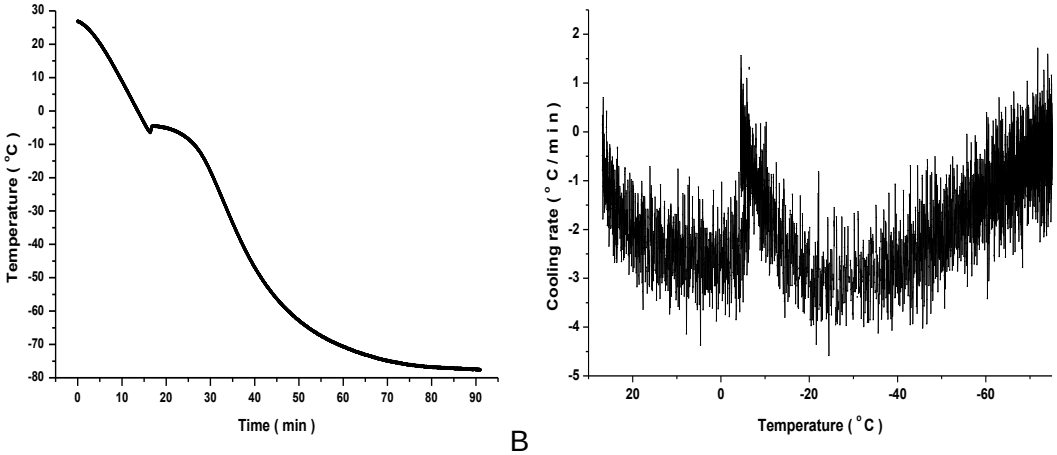

Figure 2-11 Temperature history and cooling rates for samples frozen in the Box-in-Box (BIB). (a) Temperature history of samples in BIB; (c) cooling rate of samples in BIB.

The sample temperature history and the cooling rates during freezing are shown in Figure 2-11. The cooling rate is about -1~-3.5 ℃/min. The cell viability results, including the absolute viable cell percentage and normalized cell viability compared to control are shown in Figure 2-12. Obviously, glycerol is the worst CPA among the three options. And DMSO is slightly better than propylene glycol. We can also see that, for T cells, too many cells have already lost their viability before freezing (low absolute viable T cell percentage in the control group). This implies that T cells are very vulnerable to the pre-freezing processing. The pre-processing protocol should be further optimized and the processing time should be shortened in the future.

2.4 Discussion

In this chapter, a microfluidic perfusion channel was optimized and applied to measure the membrane permeabilities to water and different CPAs of human vaginal mucosal immune cells. Some other types of cells have been tested by our group or others and the results are shown in Table 2-5. It shows that compared to some other cell types, the human vaginal mucosal immune cells have relatively lower Lp values than oocytes, cancer cells, and megakaryocyte cells, and similar to those of pancreatic islets and

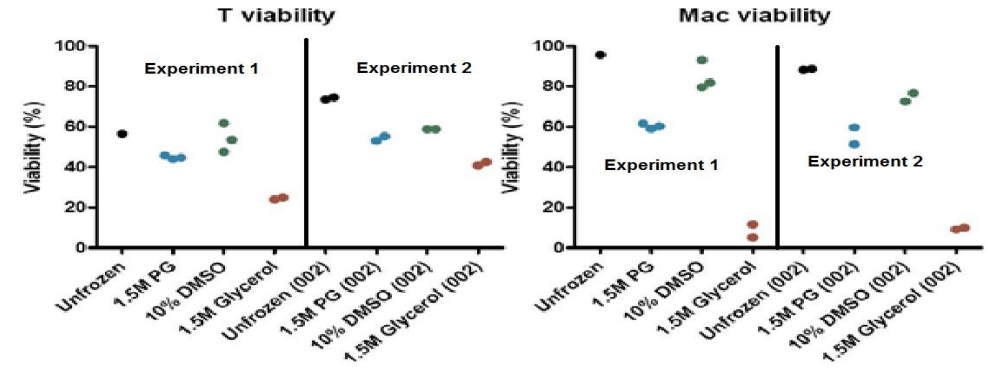

A

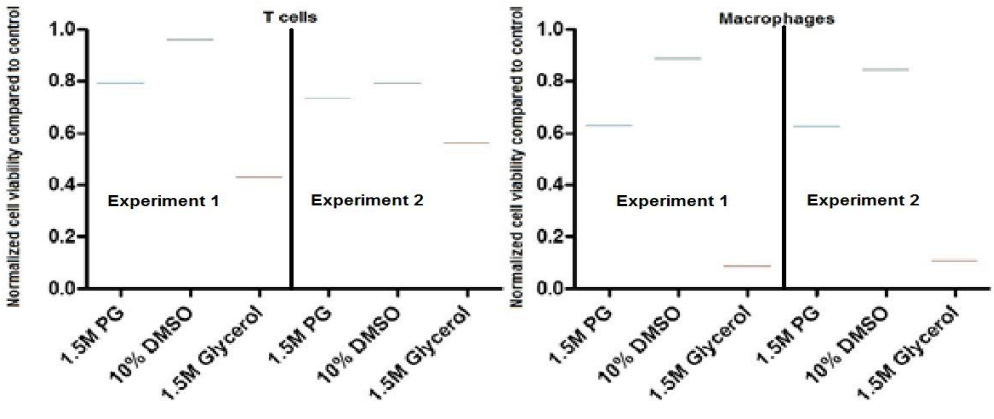

B

Figure 2-12 Viability of T cells and macrophages after cryopreservation with different CPAs at low cooling rate. (A) The absolute cell viability assessed by flow cytometry. (B) the normalized cell viability compared to control group (unfrozen)

Table 2-5 Lp and Ps of some types of cells presented in literatures

Cell type	Lp (um/min/atm)	Ps (x10^-3 cm/min)	Reference
Rat basophilic leukemia	0.38	0.49	(81)
Mouse ovum	0.43		(88)
Mouse oocyte	0.48		(92)
Mouse oocyte	0.45		(93)
Golden hamster pancreatic	0.27		(94)
Human prostate cancer cell	0.45		(95)
Mouse dendritic cell	0.17	0.63	(96)
Human megakaryocyte cell	2.26	1.8	(97)
Human vaginal T cells	0.21	0.47	Current study
Human vaginal macrophages	0.31	0.99	Current study

dendritic cells. This means that water transfers relatively slowly when the T cells and macrophages are frozen. It implies that the mucosal immune cells prefer to be frozen at lower cooling rate. This is the reason why we chose the box-in-box device to cryopreserve the cells with low cooling rate in our preliminary trials.

The microfluidic perfusion channel method can be used measure cell membrane properties at supra-zero temperatures. Many micro-channels can be easily mass-produced by microfabrication. Therefore this approach is cost-effective. However, it also has some disadvantages. It belongs to photomicrographic methods. The measurement accuracy depends on the quality of captured images and methods of image processing. It is applicable to only spherical cells because of the assumption in the conversion from 2-D image to 2-D volume. The measured results are not the average of bulk of cells, but of individual cells. Furthermore, it cannot be applied at sub-zero temperatures. Therefore, in the next chapter, another method will be proposed to measure the cell membrane properties at sub-zero temperatures. Combination of these two approaches will enable us to obtain the cell properties at any temperatures.

For the comparison among the four types of CPAs for mucosal immune cells, glycerol obviously has much lower permeability than the other three. So, glycerol is the worst option for the vaginal immune cell cryopreservation. This point was also approved by the cytotoxicity tests and the preliminary cryopreservation results. Ethylene glycol shows similar results for T cells, while for macrophages Ps to ethylene glycol is lower than that to DMSO and propylene glycol. Both T cells and macrophages have similar Lp and Ps values to DMSO and propylene glycol. The cytotoxicity tests and cryopreservation trials also had similar results for DMSO and propylene glycol. These two CPAs could be the best options. In the next work, more replicate experiments are needed to compare these two CPAs.

We also observed that T cells were always more susceptible to stresses than macrophages. In some experiments, just after tissue digestion and cell sorting, the T cell viability was low even without any treatments of CPA addition/removal and freezing. This indicates that there is still much work to do to improve the protocols of tissue processing and cell procurement.

2.5 Conclusions

In this chapter, a microfluidic perfusion channel was applied to measure the membrane permeabilities of T cells and macrophages to water and different CPAs. Cytotoxicity and osmotic tolerance limits of the cells to the CPAs were also tested. Results showed that DMSO and propylene glycol could be optimal options for the cryopreservation of human vaginal immune cells. Slow cooling rate is predicted to be preferred because of the relatively lower water permeability of these cells. Some predictions were demonstrated by the preliminary cryopreservation experiments. In the future, more experiments are needed to further compare the CPAs and optimize the cryopreservation protocol for these cells.

Chapter 3 Determination of cell membrane properties at sub-zero temperatures with differential scanning calorimetry (DSC)

3.1 Introduction

In Chapter 2, a microfluidic perfusion channel was applied to measure the cell membrane properties at room temperature, wherein, there was no temperature control device coupled with the perfusion channel. However, in order to precisely study the water transport across cell membrane during cooling, the cell membrane properties at different temperatures (including lower than zero degree Celsius) are needed.

The microfluidic perfusion channel system can be used to measure the properties at different temperatures (generally > 0 ℃); however, there are some technical difficulties in this approach. In order to achieve low temperatures, a cryo-stage (e.g., HCS601, Instec, Boulder, Colorado) is located under the microscopy, and the microfluidic channel is put on the cooling/heating pad of the cryo-stage (see Figure 3-1). The problems of this approach include: (1) The distance between the observation target (cells in the microchannel) and the lens is increased significantly. Lenses with extremely long working distances are needed, but it is difficult to manufacture lenses with long working distance and high magnification at the same time. (2) The spacing between the observation targets and the lens is complex in this situation. The microscopy working light should transmit through the two cryo-stage glass windows and the glass slide (for inverted microscopy) or the PDMS layer (upright microscopy). Two window glasses are needed in the cooling system for sealing and defrosting. Under this condition, the image quality was decreased dramatically because of the complex light pathway. This made it very difficult to get accurate cell volume excursion assessment in image analysis. (3) The cryo-stage was originally designed for thin sample films on glass slides. A cover can be screwed above the sample to seal the chamber, such that samples are cooled or heated in a closed environment. However, when the microfluidic device is mounted on the cooling/heating pad of the cryo-stage, the chamber cannot be closed. Therefore, it is hard to precisely control the temperature and prevent frost. (4) This approach is only applicable at supra-zero temperatures. If temperature goes below freezing point, ice

formation happens in the cell suspension, which makes the measurement of cell volume change very difficult.

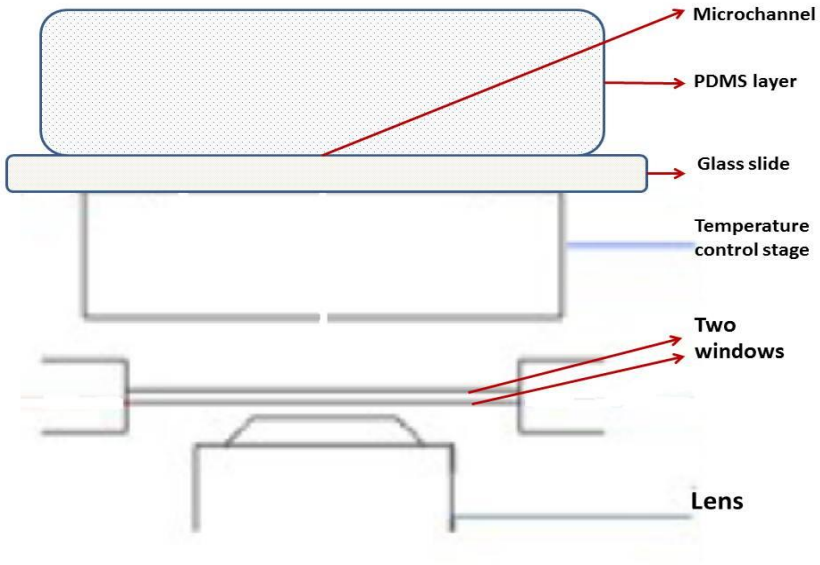

Figure 3-1 Microfluidic perfusion channel on the cryo-stage

In order to precisely evaluate the cell membrane properties at sub-zero temperatures, Differential Scanning Calorimetry (DSC) measurement is applied. The idea of using DSC to predict cell membrane properties was originally proposed by Devireddy and Bischof (98). Later the method was modified for cells with high permeability and high cytocrit by the Gao Group (99, 100). In this chapter, the DSC measurement will be applied to measure the membrane permeability to water of lymphocytes (T cells and monocytes) from human peripheral blood mononuclear cells (PBMC) at sub-zero temperatures.

3.2 Theory and mathematical formulations

3.2.1 Theory of the DSC measurements

The theory of measuring cell membrane properties based on DSC results was first developed by Devireddy and Bischof (98). Slow-Fast-Slow (SFS) cooling protocol is applied for the same cell suspension sample. The fate of cell and water during freezing is shown in Figure 3-2 (A-D). The assumptions for this study include:

- At a very slow cooling rate (such as -5 ℃/min), the possibility of intracellular ice formation can be ignored.
- The water diffusing from intracellular solution will mix into extracellular medium and then freeze totally outside of the cell.
- All components in the cell suspension have the same density of 1g/cm^3.
- The latent fusion heat of water ΔH_f is constant at various temperatures.
- All cells are alive (osmotically active) during the first slow cooling step and all cells are lysed after the fast cooling step (e.g., 200 ℃/min). In order to thoroughly kill the cells, repeated fast cooling will be applied in our experiment.

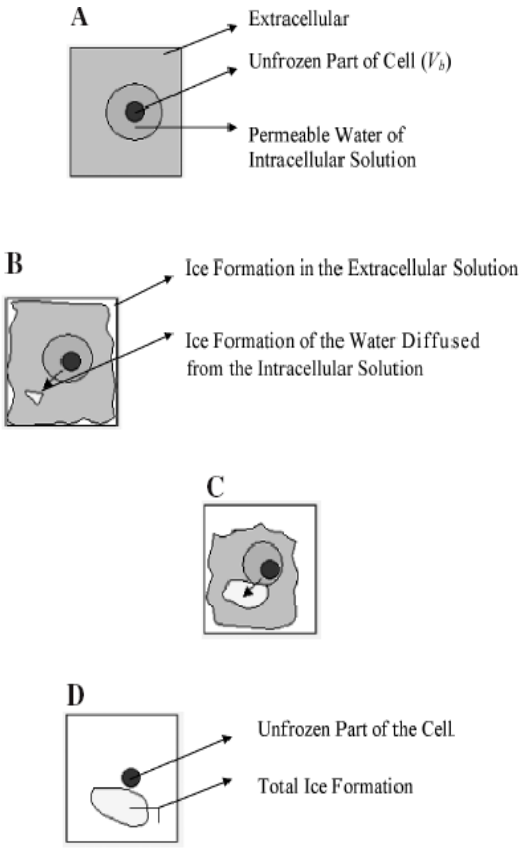

Figure 3-2 The fate of cell and water during freezing. (A) Cell and its isotonic solution before freezing. (B) Dehydration of the cell and two kinds of extracellular ice formation. (C) Ice growth during freezing. (D) The final state of the cell and ice. (Devireddy et al., 1998)

During the first slow freezing, the heat release in DSC data from the cell suspension is caused by two parts of water: the ice formation of water in the extracellular solution and water that diffuses from the intracellular solution to outside during freezing (Figure 3-2B&C). If the cell volume at temperature T is V(T), and the initial volume in isotonic environment is V_0, then the water diffusing out of one cell has the volume of V_0-V(T) at temperature T. Therefore, the heat release of one cell will be $\Delta H_f \cdot (V_0 - V(T))$ if we assume that all the extracellular water freezes, where ΔH_f is the latent heat of one unit mass of pure water. For a cell suspension with cytocrit of α, the heat release due to the freezing of the diffused water of all the cells in the control volume is $\alpha \cdot \Delta H_f \left(\frac{V_0 - V(T)}{V_0}\right)$.

For extracellular solution, the heat release of the ice formation is $(1-\alpha) \cdot q_{ec}(T)$, where $q_{ec}(T)$ is the heat release of one unit mass of extracellular solution at temperature T.

Therefore, for one unit mass of cell suspension in the first slow cooling process, the heat release (without intracellular ice formation) including the crystallization of extracellular solution and the water diffused from inside the cells is

$$\boldsymbol{q(T)_{ec+cw} = \alpha \cdot \Delta H_f \left(\frac{V_0 - V(T)}{V_0}\right) + (1-\alpha) \cdot q_{ec}(T)} \qquad (3\text{-}1)$$

The subscript "ec" and "cw" stand for extracellular water and cell water, respectively. Here, $q_{ec}(T)$ can be measured with DSC, and it is generally lower than the latent heat of pure water because of the water bound to the solute.

$$\boldsymbol{q_{ec}(T) = (1 - BF_{ec}) \cdot \Delta H_f < \Delta H_f} \qquad (3\text{-}2)$$

where BF_{ec} is the bound fraction. For example, the freezing heats of RPMI-1640 culture medium, PBS and pure water were measured as 259.55±4.50, 272.80±0.63, and 315.05±2.60, in J/g, respectively by DSC 8500 (Perkin Elmer, Waltham, Massachusetts) with cooling rate of 5 ℃/min.

All cells are assumed to be killed in the fast cooling step. Therefore, in the last slow cooling step, there is no water transport across the cell membranes. However, the bound fraction in the suspension includes dissolved solutes (ds), cell debris (cd) and the water bound to them. The heat release in this slow cooling step is

$$\boldsymbol{q_{ec+cw+cd}(T)} = (\mathbf{1} - \boldsymbol{BF_{ec+cw+cd}}) \cdot \boldsymbol{\Delta H_f} \quad (3\text{-}3)$$

It is hard to precisely quantify the term $BF_{ec+cw+cd}$, but the total heat release of the suspension at any temperature T, $q_{ec+cw+cd}(T)$, can be measured with DSC.

The difference of heat releases between the first and the last slow cooling steps is

$$\boldsymbol{\Delta q(T)_{DSC}} = \boldsymbol{q(T)_{ec+cw}} - \boldsymbol{q_{ec+cw+cd}(T)} \quad (3\text{-}4)$$

Substitute Eqation (3-1) into the equation above, we can get

$$\boldsymbol{\Delta q(T)_{DSC}} = \boldsymbol{\alpha \cdot \Delta H_f}\left(\frac{\boldsymbol{V_0 - V(T)}}{\boldsymbol{V_0}}\right) + (\mathbf{1} - \boldsymbol{\alpha}) \cdot \boldsymbol{q_{ec}(T)} - \boldsymbol{q_{ec+cw+cd}(T)} \quad (3\text{-}5)$$

After rearrangement and solving for cell volume V(T), we can get

$$\frac{\boldsymbol{V_0 - V(T)}}{\boldsymbol{V_0}} = \frac{\boldsymbol{\Delta q(T)_{DSC}}}{\boldsymbol{\alpha \cdot \Delta H_f}} \times \left[\mathbf{1} - \frac{\boldsymbol{(1-\alpha) \cdot q_{ec}(T) - q_{ec+cw+cd}(T)}}{\boldsymbol{\Delta q(T)_{DSC}}}\right] \quad (3\text{-}6)$$

On the right hand side, cytocrit can be assessed prior to the experiments, and the heat release terms, $\Delta q(T)_{DSC}$, $q_{ec}(T)$ and $q_{ec+cw+cd}(T)$ can be measured with the DSC.

Normalizing the Equation (3-6) with respect to the total change in cellular volume during dehydration (i.e., V(T)=V_b (osmotically inactive cell volume), $\Delta q(T)_{DSC}$=Δq_{DSC}, $q_{ec}(T) = q_{ec}$ and $q_{ec+cw+cd}(T) = q_{ec+cw+cd}$), we can get

$$\frac{\boldsymbol{V_0 - V(T)}}{\boldsymbol{V_0 - V_b}} = \frac{\boldsymbol{\Delta q(T)_{DSC}}}{\boldsymbol{\Delta q_{DSC}}} \cdot \boldsymbol{\kappa(T)} \quad (3\text{-}7)$$

Where

$$\boldsymbol{\kappa(T)} = \frac{\mathbf{1} - \frac{\boldsymbol{(1-\alpha) \cdot q_{ec}(T) - q_{ec+cw+cd}(T)}}{\boldsymbol{\Delta q(T)_{DSC}}}}{\mathbf{1} - \frac{\boldsymbol{(1-\alpha) \cdot q_{ec} - q_{ec+cw+cd}}}{\boldsymbol{\Delta q_{DSC}}}} \quad (3\text{-}8)$$

$\kappa(T)$ can be interpreted as a ratio of fractional inaccuracies to the total inaccuracies at temperature T in the conversion of measured heat release to volumetric information. In fact, $\kappa(T) \approx 1$, verified by the experimental data. Therefore,

$$\frac{V_0 - V(T)}{V_0 - V_b} \approx \frac{\Delta q(T)_{DSC}}{\Delta q_{DSC}} \quad (3\text{-}9)$$

Solving for V(T), one can obtain

$$\boldsymbol{V(T) = V_0 - (V_0 - V_b) \cdot \frac{\Delta q(T)_{DSC}}{\Delta q_{DSC}} \cdot \kappa(T)} \quad (3\text{-}10)$$

This is the volume response of a cell during freezing. This information is very important for the assessment of cell membrane properties at sub-zero temperatures.

In Chapter 2, microfluidic perfusion channel and image analysis were applied to get the volume excursion history of individual cells directly when perfused by solutions at room temperature. In this chapter, we are discussing applying DSC to evaluate the averaged cell volume history indirectly, but at any temperatures during freezing.

3.2.2 Water transport across cell membranes during cooling

After V(T) of cells is calculated, the cell membrane permeability to water at any temperature, $L_p(T)$, can be simulated according to the Mazur-Toner and Arrhenius equations as follows (101-103):

$$\boldsymbol{\frac{dV(T)}{dT} = \frac{L_p(T)A_cRT}{Bv_w}\left[ln\frac{V(T)-V_b}{V(T)-V_b+\phi_s n_s v_w} - \frac{\Delta H_f}{R}\left(\frac{1}{T_r} - \frac{1}{T}\right)\right]} \quad (3\text{-}11)$$

$$\boldsymbol{L_p(T) = L_{pg} * e^{-\frac{E_q}{R}\left(\frac{1}{T}-\frac{1}{T_r}\right)}} \quad (3\text{-}12)$$

Here, A_c is the cell surface area, R is the universal gas constant, B is the cooling rate, T_0 is the initial temperature, V_b is the osmotically inactive cell volume, n_s is the number of moles of salts, v_w is the specific molar volume of water, ϕ_s is the dissociation constant (=2 for NaCl), L_{pg} is the L_p at reference temperature T_r (generally =273.15K), and E_a is the activation energy of the dependence of L_p on temperature.

In Equation (2-1), it does not cover the temperature dependence of L_p. Here, Equation (3-11) & (3-12) cover the variation of L_p on temperatures. $L_p(T)$ is essential to predict the optimal cooling rate for the cryopreservation of cells.

3.3 Experimental study: materials and methods

3.3.1 Cell suspension sample preparation

In this study, lymphocytes, including CD3+ T cells and CD14+ monocytes from peripheral blood mononuclear cells (PBMC) were measured with the DSC. The PBMC units were cryopreserved with the recommended protocol by the HIV/AIDS Network

Coordination (HANC) in Fred Hutchinson Cancer Research Center (FHCRC) in Seattle. Before the DSC experiment, the frozen PBMCs were thawed quickly in 37 ℃ water bath. Then the lymphocytes were sorted by flow cytometry. Totally about 2 million T cells and 1 million monocytes were obtained from each unit of PBMC after sorting. The cells were washed with PBS to remove the proteins in the extracellular solution (culture medium). Finally the cells were resuspended in PBS to a concentration of about 2e7 cells/mL (based on the estimation of flow cytometry results) for both the T cells and monocytes. Then the cells were transported to the Gao Lab at University of Washington at 4 ℃.

The cell viability was assessed by Trypan blue staining. Cell suspension and the 0.4% Trypan Blue solution was mixed thoroughly with volume ratio of 1:1. After 2min incubation at room temperature, the cell suspension was spread on glass slides and observed under the microscopy. Viable cells remain unstained and cells with compromised membranes (we will call them "dead" cells here) are stained as blue. At least 200 cells were counted for the viability assessments. The process took no more than 15min for each sample because longer incubation time could lead to more cell death.

3.3.2 Assessment of cytocrit (α)

The cell sizes/volumes and concentrations were measured with the Scepter cell counter (Scepter^{TM} 2.0, EMD Millipore Corporation, Billerica, MA, USA). The results were then used to estimate the cytocrits of the cell suspensions.

3.3.3 Measurement of the osmotically inactive cell volume (V_b)

Hypertonic saline solutions (2xPBS or 3xPBS) were added into the cell suspension dropwise with final volume ratio of 1:1. The cells were equilibrated in these hypertonic solutions for 5min at 4 ℃, and then observed under upright microscope. Images were captured by a digital camera (Phantom v310, Vision Research). The cell sizes in isotonic and hypertonic PBS solutions were then used to estimate the osmotically inactive cell volume (V_b). The cell volumes were also measured with the Scepter cell counter (Scepter^{TM} 2.0, EMD Millipore Corporation, Billerica, MA, USA), which obtained the average volume of tens of thousands of cells.

3.3.4 Calibration of the DSC

DSC 8500 (Perkin Elmer, Waltham, Massachusetts) was applied in this study. Based on the second generation of HyperDSC ® technology, DSC 8500 is featured by its high sensitivity and accuracy. The device was calibrated carefully following the user manual, including the calibrations of temperature, heat flow and the furnace control.

For the choice of standard reference materials for the calibration, indium is always recommended by the user manual. Besides indium, two more reference materials, n-Octane and n-Dodecane, were also used to calibrate the temperature and heat flow because their freezing/melting temperatures are in the sub-zero temperature range, which is close to the freezing point of cell suspension and intracellular ice formation temperature. The expected and measured phase transition properties of these three standard materials after calibration are listed in Table 3-1. It shows that the accuracies of temperature and latent heat are excellent (temperature error< 0.2 ℃ and latent heat error<1%).

Table 3-1 Calibration of temperature and heat flow for the DSC device

	T-melting (℃)		Latent heat of fusion (J/g)	
	Expected	Measured	Expected	Measured
Indium	156.60	156.73	28.45	28.20
n-Octane	-56.76	-56.67	182.00	183.35
n-Dodecane	-9.65	-9.59	216.73	218.53

The furnace was calibrated in the temperature range of -80 ℃ to 200 ℃. After calibration, the differences between the real sample temperature and programed temperature were <0.05 ℃ in the isothermal equilibration step, and <0.5 ℃ in the scanning step with cooling rate lower than 10 ℃/min.

In the beginning of every experiment, the phase transition properties of the three standard materials were first measured to check the calibration. If the errors of temperature or heat flow exceed expectation (e.g., 0.2 ℃ and 2% of latent heat, respectively), calibration will be conducted again before the tests of cell suspensions.

3.3.5 Determination of cell membrane properties with DSC measurements

In Devireddy's approach, a "Slow-Fast-Slow" (SFS) DSC cooling program was run for the same cell suspension sample. Herein, the fast cooling step is supposed to induce intracellular ice formation and lead to cell death. To verify that the cells are dead before the last slow cooling step, the fast cooing step was repeated in our study, i.e., a "Slow-Fast-Fast-Slow" (SFFS) program was conducted. For each sample, 5-10 mg cell suspension was added to the aluminum pan. 0.1-0.2mg freeze-dried *Pseudomonas syringae* (ATCC, Manassas, VA) was added to each sample as ice nucleator to prevent/decrease supercooling. Then the pan was sealed with the crimper. The mass of each sample was precisely measured. In details, the DSC scanning program is described as below.

1. Isothermally holding at 4 ℃ for 1min.
2. Cooling from 4 ℃ to -6 ℃ at 5 ℃/min to induce extracellular ice formation. Since ice nucleator was added, crystallization happened before cooled down to -6 ℃, which was indicated by a heat release peak (generally at about -5.5 ℃). If without ice nucleator, the freezing temperature varied a lot and was generally lower than -18 ℃.
3. Heating from -6 ℃ to -0.53 ℃ (but not overshot) at 10 ℃/min.
4. Isothermally holding at -0.53 ℃ for 5min. Here, the holding temperature -0.53 ℃ is the theoretical melting temperature of isotonic saline solution (PBS). It is calculated by the relationship of$\Delta T = 1.858 * Osm$, where Osm=0.288 Osm/kg-H_2O is the osmolality of the PBS solution and $\Delta T = 273.15 - T$ (K) (104). Therefore, the melting temperature of the isotonic saline solution is -0.53 ℃. This holding step is very critical. Extracellular ice formation is induced and remains equilibrium in the suspension.
5. Cooling from -0.53 ℃ to -40 ℃ at 5 ℃/min. The thermogram from this cooling step is $q(T)_{ec+cw}$ (see Equation (3-1)), including crystallization of extracellular water and the water diffused out of the cells.
6. Heating from -40 ℃ to -0.53 ℃ at 100 ℃/min. Some cells could survive this thawing process as osmotically active, while some cells would be dead due to cryo-injury.

7. Cooling from -0.53 ℃ to -40 ℃ at 200 ℃/min, and then heating from -40 ℃ to -0.53 ℃ at 100 ℃/min. This fast cooling step is to induce intracellular ice formation and cryo-injury to lyse the cells.
8. Repeat the step-7 (fast cooling to -40 ℃ at 200 ℃/min and then heating to -0.53 ℃ at 100 ℃/min). This step is to ensure that almost all cells would be dead before the last slow cooling step.
9. Isothermally holding at -0.53 ℃ for 5min. Since all cells have compromised membranes, intracellular water, cell debris, proteins and salts are exposed in the solution. Ice is induced and remains equilibrium in the suspension at this holding temperature.
10. Cooling from -0.53 ℃ to -40 ℃ at 5 ℃/min. The thermogram from this cooling step is $q_{ec+cw+cd}$ (see Equation (3-3)), which is smaller than the thermogram of the first slow cooling (Step-5) because of the large bound fraction of the water.

3.3.6 Verification of assumptions proposed in the method

In the theory of DSC method, it is assumed that cells are killed by the fast cooling step. The heat release difference between the first and the last slow cooling steps is based on the fact that in the first slow cooling step, the heat release is due to crystallization of both extracellular water and the water diffused out of the cells. In the last slow cooling step cells are lysed such that proteins, salts and cell debris are exposed and bound to water, therefore crystallization heat release is reduced. In order to test these assumptions, PBMC lymphocytes were rapidly cooled in liquid nitrogen and thawed in 37 ℃ water bath twice, and then were assessed with Trypan blue staining for viability. The cooling rate was monitored by thermocouples.

In order to test the reliability of the DSC measurements of heat flow in the “SFFS” program, PBS ($\alpha=0$) and lysed cell suspension (by repeated rapid freezing, $\alpha>0$ but osmotically inactive) were scanned with the same program. The heat release difference between the first and last slow cooling steps for these two kinds of samples should be zero.

3.4 Results

3.4.1 Cell size, concentration, viability and cytocrit

The size, volume and concentration of T cells and monocytes from PBMC were measured with Scepter cell counter. The results are listed in Table 3-2. The cytocrit was calculated based on the cell volume and concentration. For example, T cells with volume of 169.181um^3 and concentration of 0.823e7cells/mL, the cytocrit (α) is

$$\alpha = 169.181\mu m^3 \times \frac{1.646e7}{mL} = 2.785e-3$$

For both the sorted T cells and monocytes, the viabilities were more than 90% before the DSC experiments.

Table 3-2 Cell size, volume, concentration and cytocrit

	T cell	Monocyte
Cell diameter (μm)	6.861	7.968
Cell volume (V_0, μm^3)	169.181	264.878
Cell concentration (cells/mL)	1.646e7	1.910e7
Cytocrit (α)	2.785e-3	5.059e-3

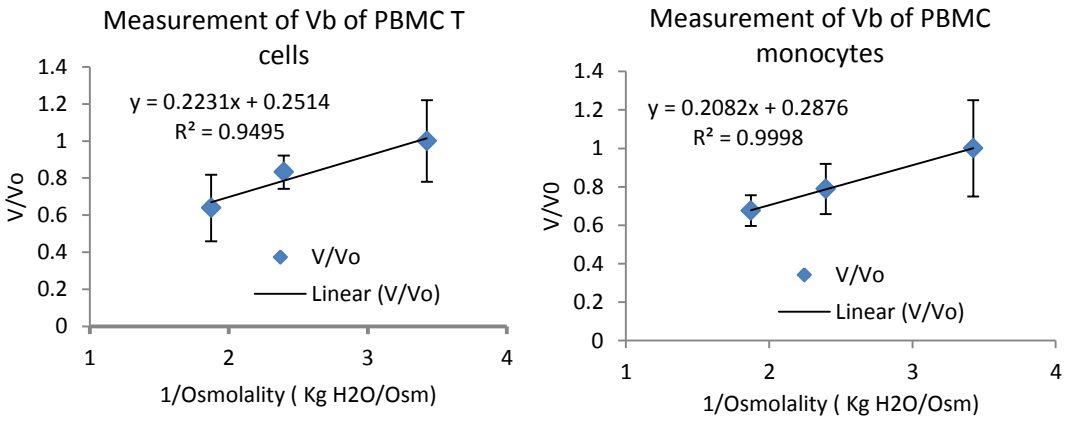

Figure 3-3 Determination of the osmotically inactive volume fraction (Vb) of PBMC T cells and monocytes

3.4.2 Osmotically inactive volume (V_b)

The Boyle van't Hoff plots of PBMC T cells and monocytes are shown in Figure 3-3. The inactive volume fractions (V_b) of T cells and monocytes are 25.1% and 28.8%, respectively, according to the y-intercepts.

3.4.3 DSC heat flow curves

A representative experimental DSC "heat flow (mW)-time (min)" curve for a cell suspension is shown in Figure 3-4. Basically, the program consists of nucleation of extracellular ice, slow cooling, fast cooling, fast cooling and then slow cooling. Before the first and the last slow cooling steps, samples are fully equilibrated at -0.53 ℃ for some time (5min). The thermogram difference between the two slow cooling steps (shown in Figure 3-5-A, gray part) is due to different statuses of cells (live or dead). At any temperature (T), the partial thermogram difference $\Delta q_{DSC}(T)$ (Figure 3-5B) can be calculated by the DSC data analysis software (Pyris, Perkin Elmer) and then be used to estimate the cell volume change history V(T) and water transport across cell membranes during cooling.

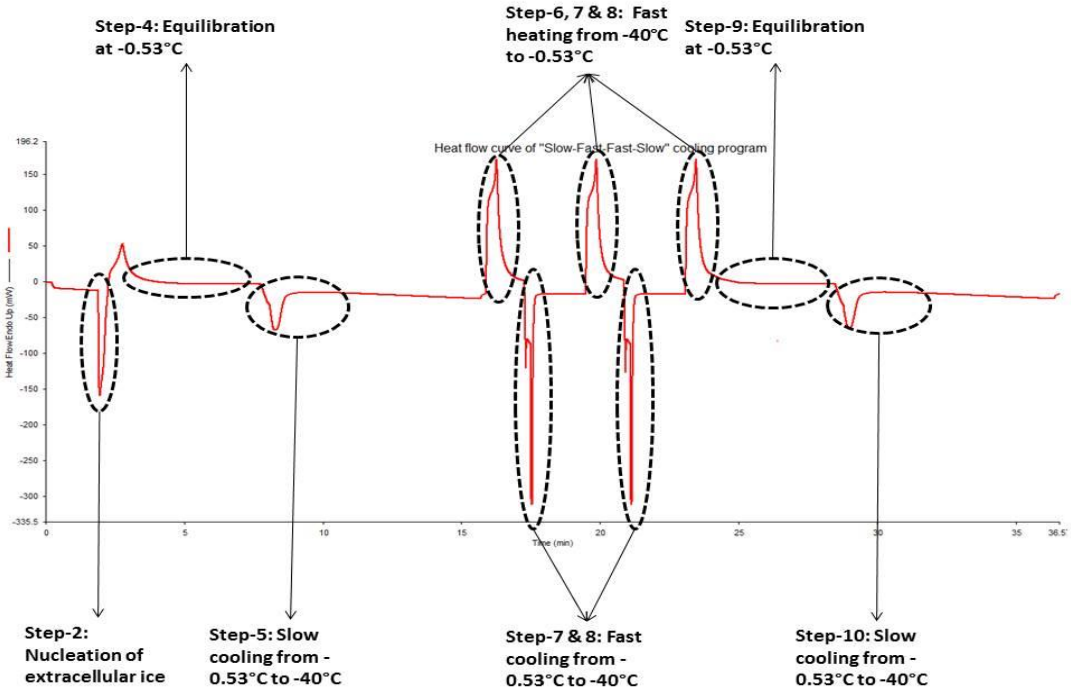

Figure 3-4 DSC heat flow curve of the "Slow-Fast-Fast-Slow" (SFFS) cooling program

3.4.4 Cell membrane properties (Lp and Ea)

From the total DSC thermogram difference Δq_{DSC} and partial difference at temperature T $\Delta q_{DSC}(T)$, the cell volume changing history during cooling, V(T), can be calculated by Equation (3-10). Since the cell viability before the first slow cooling step was lower than 100%, the cytocrit in Equation (3-10) (in the κ term) was modified by the result of that the cytocrit value (α value in Table 3-2) times the cell viability. One representative experiment result of V(T) is shown in Figure 3-6. The theoretical water transport model (equations (3-11) and (3-12)) was then applied to numerically determine the two parameters: cell membrane permeability to water at Tr (=273.15K) Lp and the activation energy Ea, by a nonlinear regression curve-fitting to the experimental V(T) data. MLab programming software (MLab for PC, Civilized Software Inc., Silver Spring, MD) was applied because of its power in curve fitting.

After Lp and Ea were obtained, V(T) was theoretically predicted by equations (3-11) and (3-12). The results are shown in Figure 3-7. The experimental V(T) data are presented as red circles, and the theoretically predicted data based on the obtained parameters (Lp and Ea) are shown as the black dots.

The estimated Lpg and Ea results of PBMC T cells and monocytes are shown in Table 3-3 (mean$\pm$STD).

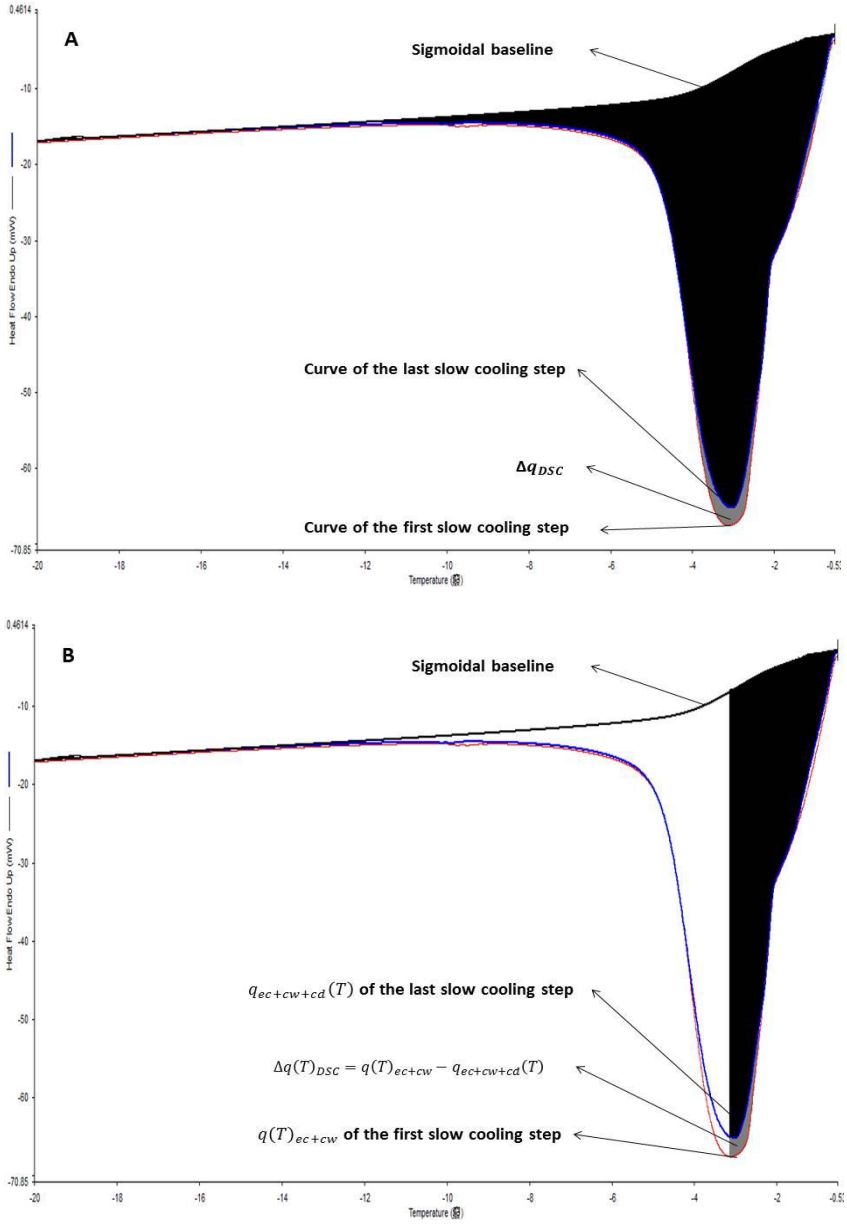

Figure 3-5 Heat flow thermogram obtained from the first and last slow cooling steps in the "Slow-Fast-Fast-Slow" (SFFS) cooling program. (A) Heat flow curves of the two slow cooling steps and the total thermogram difference between them (gray part). (B) Partial thermogram to any temperature (T) of the two slow cooling steps and the difference between them.

Table 3-3 Lpg and Ea of PBMC lymphocytes

	T cells (n=15)	Monocytes (n=9)
Lpg at Tr=273.15K (μm/atm*min)	0.119±0.0670	0.135±0.0204
Ea (kcal/mol)	46.939±16.296	52.189±6.729

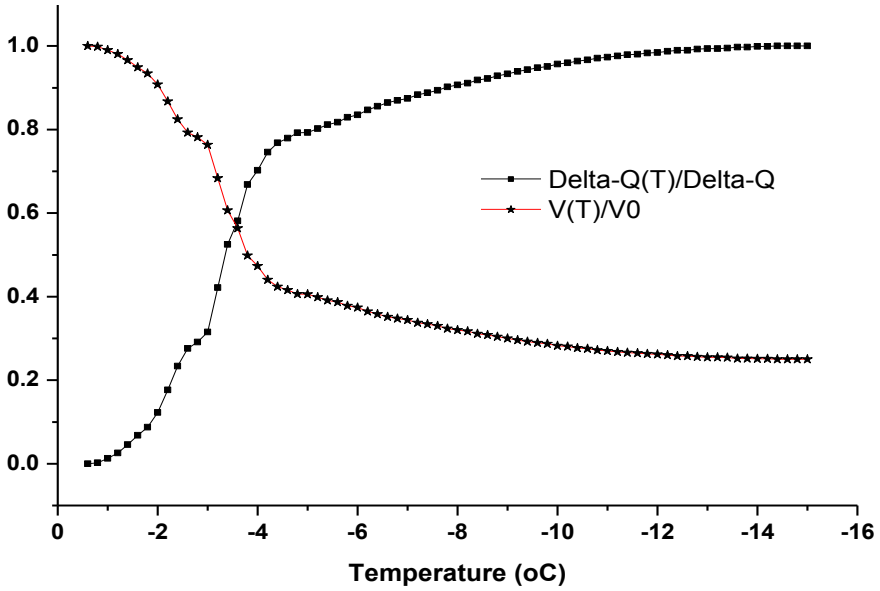

Figure 3-6 Cell volume changing history, V(T), during cooling based on analysis of DSC thermograms

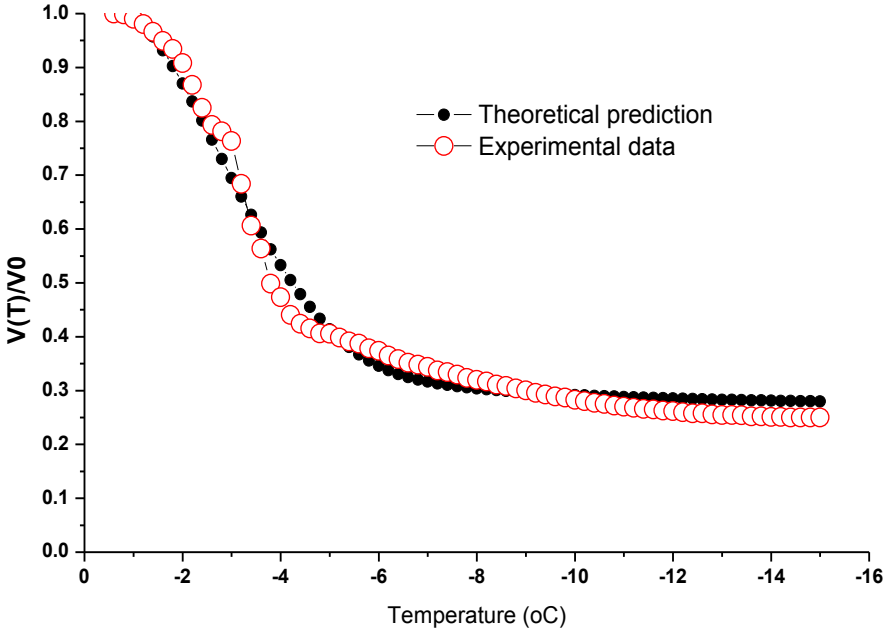

Figure 3-7 Simulation of Lp and Ea by curve-fitting of the cell volume during cooling (V(T)).

3.4.5 Prediction of optimal cooling rates for PBMC T cells and monocytes

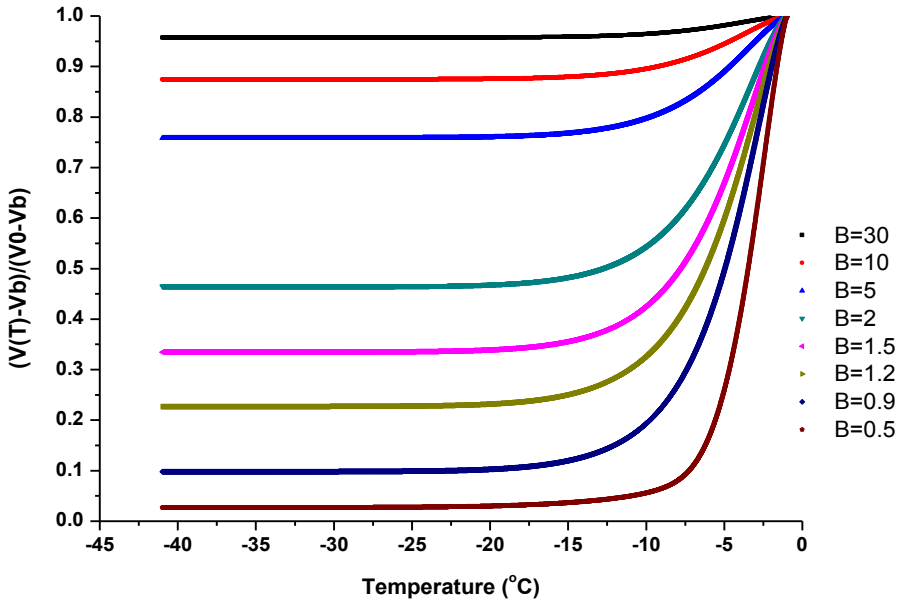

Figure 3-8 Prediction of the optimal cooling rate for PBMC T cells

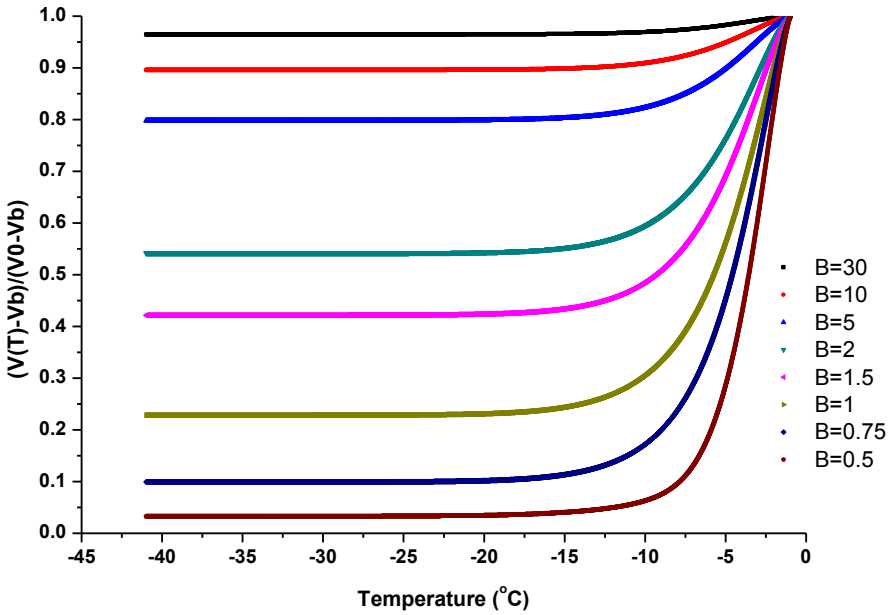

Figure 3-9 Prediction of the optimal cooling rate for PBMC monocytes

After the cell membrane permeabilities to water at any sub-zero temperatures, Lp (T), are obtained, water transport process for cells during cooling can be simulated. The optimal cooling rate can be roughly predicted by the cell dehydration results. The numerical

simulation results of optimal cooling rate prediction are shown in Figure 3-8 and Figure 3-9 for PBMC T cells and monocytes, respectively. It shows that cell dehydration generally halted at temperatures lower than -20 ℃ because the Lp decreases with temperature dramatically. For example, Lp of PBMC T cells at -20 ℃ decreases to 0.108% of the Lp at Tr (273.15K). From the results, we can see that at very low cooling rate, cells undergo severe dehydration, which may lead to the "solute injury" to the cells. At high cooling rate, cells do not dehydrate very much. Much water still remains inside the cell (e.g., >95% water remains inside cells for cooling rate B=30 ℃/min). Intracellular ice formation may happen when temperature goes down to the IIF temperature. This is the so-called "ice injury" in cryobiology. Therefore, optimal cooling rate exists for a specific cell type, which should be high enough to prevent solute injury and slow enough to prevent ice injury.

In cryobiology, it is generally suggested that about 10% intracellular water remaining inside the cells at the IIF temperature during cooling would be an optimal condition. The crystallization of this part of remaining water is "rescuable"; meanwhile this part of water can prevent the damage caused by severe cell shrinkage. If we choose 10% cellular water remaining inside cells at the IIF temperature as the criteria, the predicted optimal cooling rates for PBMC T cells and monocytes are 0.9 ℃/min and 0.75 ℃/min, respectively. This prediction matches the reality very well! In the standard operating procedure (SOP) for the HIV/AIDS Network Coordination (HANC), cooling rate of 1 ℃/min is applied for PBMC cryopreservation (105).

One more thing should be pointed out that the theoretical prediction results show that there is still much water remaining inside cells at low temperatures when cooling rate is 5 ℃/min. Although IIF probability at this cooling rate is very low, IIF can happen during cooling, which may break the assumption of no IIF for the DSC method. Furthermore, at such cooling rate, cells are not fully dehydrated even at very low temperatures. This implies that 5 ℃/min may not be slow enough for PBMC lymphocytes in the DSC method. Lower cooling rate could be better for more cell dehydration. However, the DSC experiments will take much longer time if cooling rate is decreased. Solute injury may also be potentially induced in slower cooling.

3.4.6 Verification of assumptions proposed in the method

One important assumption in the "Slow-Fast-Fast-Slow" DSC cooling method is that the cells are lysed after the two fast cooling steps. In order to validate this assumption, PBMC T cells and monocytes were cooled in liquid nitrogen and thawed in 37 ℃ water bath twice. The cell viability was assessed by Trypan blue staining. The results showed that 97.8% T cells and 96.9% monocytes were dead, which verified the assumption.

In order to test the accuracy and reliability of the DSC heat flow measurements, two solutions were scanned with the "Slow-Fast-Fast-Slow" program. One was PBS solution (no cells, α=0), and the other one was the T cell suspension with concentration of 1.646e7 cells/mL but the cells had been killed by rapid cooling and thawing twice. The thermograms of the first and the last slow cooling steps were compared. Results showed that, for both PBS and the suspension with dead cells, the thermogram difference between the two slow cooling steps was less than 2J/g, which is within the measurement error limit of the DSC. For suspensions with live cells, the thermogram difference was generally larger than 10 J/g.

3.5 Discussion

In Chapter 2, a microfluidic perfusion channel was applied to measure the cell membrane permeabilities to water and CPAs at room temperature. The results are very important for the CPA selection. Meanwhile, the membrane permeability results are also helpful for the estimation of cell water transport during CPA addition/removal and cooling of cell suspension. However, this method can only be used to measure the cell membrane properties at temperatures above freezing point. For more precise study of the cell water transport during cooling and prediction of optimal cooling procedure for a cell suspension, cell membrane properties at sub-zero temperatures are needed.

In this chapter, an approach based on DSC measurements was applied to assess the cell membrane permeability to water at any temperatures lower than freezing point. This method has some distinct merits. (1) This method gives the average response of large number of cells, compared to the results of individual cells obtained by cryomicroscopy. (2) Cell membrane properties at sub-zero temperatures can be measured. (3) This method does not depend on the cell shape and size. For methods based on cryomicroscopy and

image observation, only spherical cells with relatively large sizes can be investigated in order to achieve high image quality and enough accuracy in conversion from 2D image to 3D volume. (4) This method can be applied to tissues. Properties of a tissue, instead of individual cells in the tissue, are very important for the cryopreservation of tissue (104, 106-109). (5) When CPAs exist in the cell suspension or tissue, this DSC method can also be applied (110, 111).

However, there are also some limitations in this DSC approach. In the "Slow-Fast-Fast-Slow" cooling program, it is assumed that all cells are lysed by the fast cooling steps. In order to ensure the cell damage before the last slow cooling step, fast cooling was applied twice in this study. However, in reality, this assumption may be not correct for some cell types because DSC cannot achieve such high cooling rate to kill all the cells with freezing. For a cell type with large membrane permeability to water, the cooling rate causing fatal intracellular ice formation could be as high as thousands of degrees Celsius per minute. For example, the "optimal" cooling rate for human red blood cells is about 1,000 ℃/min (31). Currently, there is no DSC device that can achieve cooling rates higher than 1,000 ℃/min to lyse red blood cells. Furthermore, it has been found that some types of cells, like red blood cells, the compromised membranes of cells (ghosts), which are caused during rapid cooling step, can be self-resealed during the thawing step before the last slow cooling step. For these types of cells, the "Slow-Fast-Fast-Slow" DSC scanning method does not work.

In order to exclude the assumptions that are made in the "Slow-Fast-Fast-Slow" method, a modified DSC method was developed by the Gao group (99, 100). In the modified method, only one slow cooling scan is done for a sample, but different samples with different cytocrit values are tested. The absolute thermogram values of the slow cooling step are proportional to the cytocrit (see Equation (3-1)). Based on the proportionality (slope and intercept), cell volume history can be calculated and membrane permeabilities can be assessed accordingly. The modified approach does not require the assumption of cell lysis by fast cooling, therefore can be applied to cells with high permeability (e.g., red blood cells). However, high cytocrit is necessary for this modified approach to get accurate measurements. If the cytocrit is very small (such as the case of PBMC

lymphocytes in this study), a tiny error in cytocrit measurement may cause large error in the slope calculation of the "heat flow-cytocrit" curves. So, in cryobiological studies, the original "Slow-Fast-Slow" cooling method and the modified approach should be selected according to different conditions.

3.6 Conclusions

In this chapter, a "Slow-Fast-Fast-Slow" cooling DSC method was applied to measure the membrane properties of PBMC lymphocytes (T cells and monocytes) at sub-zero temperatures. Intracellular ice formation temperatures of these cells were also assessed by relatively fast cooling. Based on the measurements, optimal cooling rates were predicted, which are very consistent with that applied in conventional SOPs. The results proved that this DSC method is a very good approach to measure the cell membrane properties at sub-zero temperatures. Combined with the method of microfluidic perfusion channel in Chapter 2, cell membrane properties at any temperatures (above and below freezing point) can be obtained. They are very important for CPA selection, CPA addition and removal and prediction of optimal cryopreservation protocols.

Chapter 4 An automated multifunctional cell processor for cell concentration and CPA addition/removal

4.1 Introduction

As mentioned in Chapter 1, there are some challenges in cellular therapy. One problem is cell concentration or cell suspension volume control. For example, after cell culturing/expansion, the cell suspension volume could be very large, as high as about 10L. In order to achieve transplantable volume and population, it should be concentrated to a specific volume (e.g., 200mL). Currently, this is performed by centrifugation, which is time consuming, may cause cell clumping and damage, and increases the risk of contamination.

Another challenge in cellular therapy is the successful cryopreservation of the cells. Cryopreservation of cells includes addition of CPA, cooling, storage, thawing, and removal of CPA. In Chapter 2 and 3, measurements of cell membrane properties at supra-zero and sub-zero temperatures were discussed. The results can be applied to select the optimal CPA and predict the optimal cooling protocol. Besides these, addition and removal of CPA can also cause severe osmosis injury to cells.

CPAs are needed to eliminate cryo-injury to cells during freezing, however, they should be removed before transplantation due to their side-effects (see review in Chapter 1). During CPA addition and removal, osmotic injuries may happen to the cells if suboptimal procedures are applied. When CPA with high concentration is added to or removed from cell suspension, due to intra- and extracellular osmolality gradients, cells will shrink or expand dynamically. This cell volume excursion can cause injury to cells (60). So far, CPA is added to cell suspension dropwise and slowly. For CPA removal, centrifugation is generally used (112-116).

In CPA removal, isotonic solution is added to the cell-CPA suspension, equilibrated, and then the mixture is centrifuged to remove CPA in the supernatant. This procedure usually needs to be repeated for a few times before the CPA concentration is reduced to an acceptable level. However, this method has many disadvantages, such as intense labor and time consumption, high possibility of contamination, osmotic and mechanical injury

to the cells, clumping of cells due to centrifugation, and possible activation of stem cells, etc. Thus, it would be highly desirable to find safer and more reliable methods for CPA removal.

Thus far, a few alternative approaches have been developed for cryoprotectant removal. Dialysis mass transfer in hollow fibers has been tried in some researches (71, 72, 117, 118). However, the large osmolality gradient across the hollow fiber membranes can cause severe osmotic damage to the cells, especially at the beginning of the mass transfer process when cell suspension and diluent solution meet in the dialyzer. Thus, priming of the dialyzer with hyperosmotic solution first is generally required, which still introduces extra complexity and time consumption. Meanwhile, due to the nonuniform distribution of osmolality gradient across hollow fiber membranes along the fibers, mass transfer in the dialyzer is very complicated and hard to control. These problems prevent dialysis method being an effective and reliable approach of CPA removal. Recently, Hubel et al. developed a method based on mass diffusion in microfluidic flows for CPA removal (73, 119). However, the mass transfer rate is very low since passive diffusion due to concentration gradient is the driving force. This system is hard to scale up for large volume samples.

Real-time monitoring of CPA concentration during CPA addition and removal is not performed on a routine basis during cell processing operations. In order to assess CPA concentration in cell suspension after washing, a few methods have been applied by researchers, such as capillary zone electrophoresis (20), high-performance liquid chromatography (HPLC) (120), and gas chromatography (121). However, all these approaches are time-consuming, expensive and need special chemical agents, apparatuses and expertise.

In this chapter, we will propose a novel system based on mass transport across hollow-fibers to conduct the cell concentration and addition/removal of CPA without shortcomings mentioned above. We construct a prototype of a multifunctional cell processing device based on hollow-fiber cartridges and peristaltic pumps. This device, currently built and operated as a breadboard system can perform cell concentration and CPA addition and removal with a single device and with almost the same settings (tubing,

cartridges, and pumps). Operation modes will be optimized to increase the cell processing efficiency and decrease cell loss. The advantages of the device include: (1) high cell recovery rate, (2) low cost, (3) low processing time, (4) reduced labor, (5) ease of operation, (6) closed aseptic system with low risk of contamination, and the most important, (7) realization of all the 3 cell processing goals on one single device. In terms of long-term commercialization, this device has the potential to become alternative basic equipment used for any situations in research laboratories and hospitals where related cell processing is done frequently.

In this chapter, we will also apply a novel approach to assess CPA concentration in CPA solutions based on the measurements of electrical conductivity (**EC**). On-site and real-time monitoring of the CPA concentration can be done by this low-cost and easy-to-operate method.

4.2 Standard data of electrical conductivity (EC) of CPA solutions

4.2.1 Materials and methods

4.2.1.1 Measurements of EC standard data of DMSO-NaCl-water ternary solutions

The ternary solutions used in this study consisted of DMSO (100% pure, Mallinckrodt Baker, Inc., Phillipsburg, NJ), NaCl Crystal (99.6% pure, Mallinckrodt Baker, Inc., Phillipsburg, NJ), and deionized (DI) water generated from Milli-Q (Millipore Corporation, Billerica, MA). When preparing the ternary solutions, NaCl crystal powder was first dissolved in DI water by weight to obtain final concentrations of 0.9, 1.8, 4.5, and 9 wt%, which were presented as r=1, 2, 5 and 10, respectively. Herein, r is the normalized concentration of NaCl with respective to that in isotonic NaCl solution. Secondly, DMSO was added to NaCl-water solutions with volume percentages of 0, 2.5, 5, 7.5, 10, 20, 30, 40 and 50%. The solutions with different NaCl and DMSO concentrations were prepared for the EC measurements.

A conductivity meter (Orion 4-Star, Thermo Fisher Scientific Inc., Waltham, MA) was employed to collect EC of sample solutions. All the experiments were performed at room temperature (22 ± 0.5℃). The cell constant of the conductivity meter was calibrated every twenty measurements following the instrument's instruction manual. The AUTO-

READ measurement mode was applied when the measurement was conducted. After each measurement, the conductivity probe was rinsed with DI water, and blotted dry before the next measurement. Each individual sample was measured three times.

4.2.1.2 Measurements of EC standard data of glycerol-NaCl-water and ethylene glycol-NaCl-water ternary solutions

Since glycerol and ethylene glycol are the other two types of CPAs that have been widely used in cryopreservation, in this part, the standard data of the EC of the these two types of CPA solutions will be measured. Similar to the procedures mentioned above, the ternary solutions used in this study consisted of glycerol or ethylene glycol (Mallinckrodt Baker, Inc., Phillipsburg, NJ), NaCl and deionized (DI) water. When preparing the ternary solutions, NaCl crystal powder was first dissolved in DI water by weight to obtain final concentrations of 0.9, 1.8, 4.5, and 9 wt%, which were presented as r=1, 2, 5 and 10, respectively. Second, glycerol or ethylene glycol was added to NaCl-water solutions with different volume percentages from 0 to 50% (v/v). When preparing the glycerol solution, mass weighting was applied to precisely control the glycerol volume since small volume of glycerol was hard to be prepared due to its high viscosity. Then the solutions with different NaCl and CPA concentrations were measured at room temperature for EC. For each solution, the measurement was performed at least for three times.

4.2.1.3 Effect of albumin on the electrical conductivity of the NaCl-albumin-water ternary solutions

Albumin usually exists in blood, culture medium and cell products. In order to investigate the influence of albumin on the EC of the solution, NaCl-albumin-water ternary solutions were prepared. Similar to the procedure above, 0.9% (w/v) NaCl solution was prepared first. Then bovine serum albumin (Sigma-Aldrich) was added to the NaCl solution with different final concentrations: 0%, 2%, 4%, 6%, 8%, and 10% (w/v). Then the EC of these solutions was measured at room temperature. Each solution was measured for three times.

4.2.1.4 Effect of DMSO on the electrical conductivity of the NaCl-albumin-DMSO-water quaternary solutions

In a real situation of cell cryopreservation, cells may be in the NaCl (or other salts)-albumin-DMSO-water solution after thawing. During DMSO removal, DMSO

concentration decreases while albumin remains in the suspension. Sometimes, in order to apply the EC measurement to predict the DMSO concentration, we may need to consider the influence of albumin on the EC data.

In this part, NaCl-albumin-DMSO-water solutions with different DMSO concentrations were prepared and measured. Briefly, a ternary solution of 0.9% (w/v) NaCl-5% (w/v) albumin-water was prepared first. Here 5% albumin concentration was chosen because this concentration was generally used in cell culture media. Then this ternary solution was mixed with DMSO to make NaCl-albumin-DMSO-water solutions with different DMSO concentrations (0%, 2.5%, 5%, 7.5%, 10%, 20%, 30%, 40%, 50% (v/v)). When preparing these solutions, they were immersed in ice and the mixing was performed slowly such that the solution temperature was not heated up too much. Then the EC of these solutions was measured at room temperature. Each solution was measured at least for three times.

4.2.2 Results

4.2.2.1 Standard electrical conductivity data of DMSO-NaCl-water ternary solutions

The EC data of DMSO-NaCl-water ternary solutions are shown in **Figure 4-1**. Obviously the EC depends on both the concentrations of NaCl and DMSO. The higher of NaCl concentration (larger r value) or the lower of DMSO concentration, the higher will be the EC of the solution. From the data, it shows that the dependence of EC on DMSO and NaCl concentrations can be written as an exponential function:

$$\boldsymbol{EC = A * e^{B*C}} \quad (4\text{-}1)$$

Where EC: electrical conductivity of the ternary solutions (mS/cm); C: concentration of DMSO (v/v, %); A and B are constants. It's interesting that B=-0.036, the same for different r values (different NaCl concentrations) (except B=-0.035 for r=1). A is determined by NaCl concentration (shown in Figure 4-2) and can be estimated by

$$\boldsymbol{A = -0.3777r^2 + 15.828r} \quad (4\text{-}2)$$

Accordingly, the EC of DMSO-NaCl-water ternary solutions can be estimated by

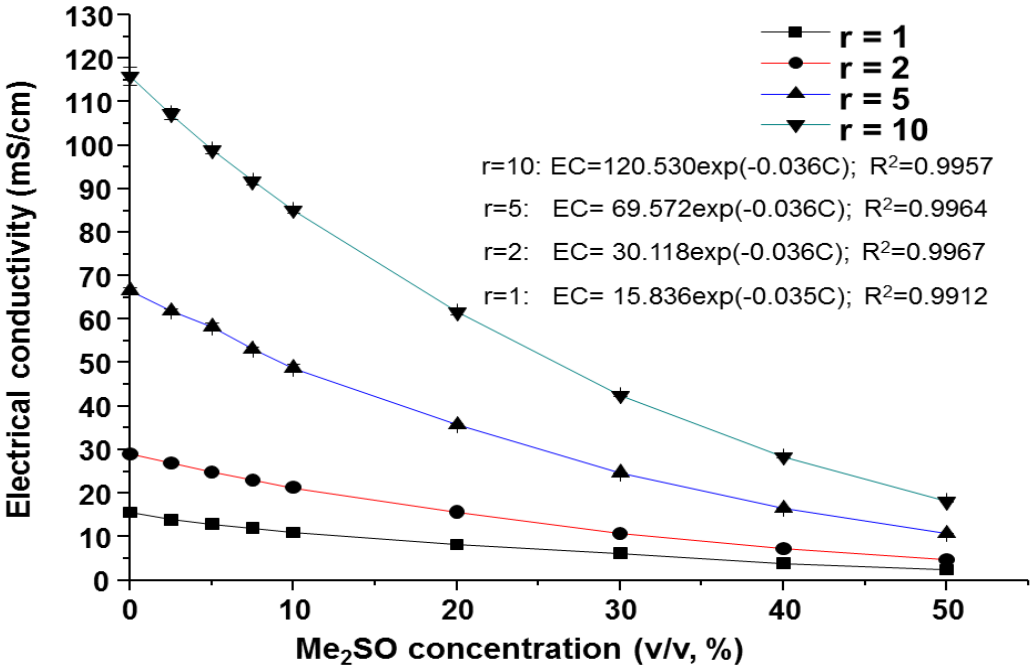

Figure 4-1 Electrical conductivity of DMSO-NaCl-water ternary solutions

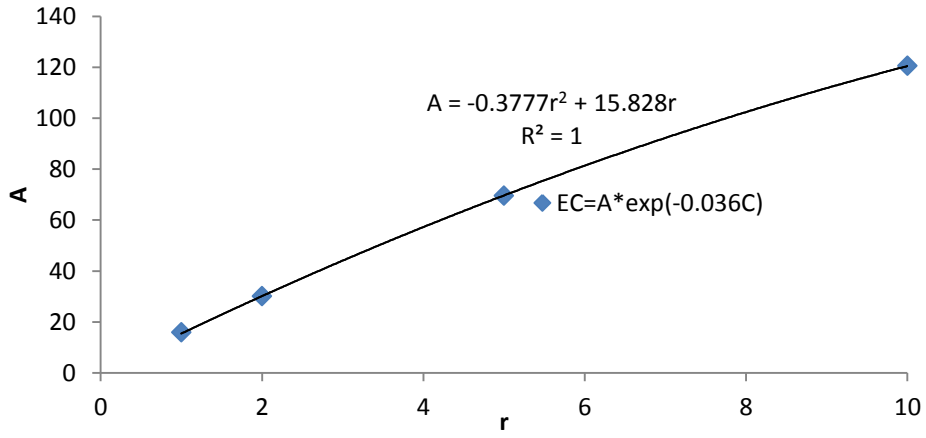

Figure 4-2 Dependence of A on NaCl concentration

$$\boldsymbol{EC} = (\boldsymbol{-0.3777r^2 + 15.828r}) * \boldsymbol{e^{-0.036*C}} \quad (4\text{-}3)$$

Specifically, for DMSO-0.9% NaCl- water ternary solutions (r=1), the dependence of EC on DMSO concentration can be fitted by

$$EC = 15.836 * e^{-0.035*C} \quad (4\text{-}4)$$

4.2.2.2 Standard electrical conductivity data of glycerol-NaCl-water and ethylene glycol-NaCl-water ternary solutions

The EC results of glycerol-NaCl-water and ethylene glycol-NaCl-water ternary solutions are shown in Figure 4-3 and Figure 4-4. Obviously when CPA concentration increases or salt concentration decreases, the EC of the solutions decreases. The dependence of CPA concentration on the EC can be also fitted with exponential equations.

For glycerol, it can be presented as:

$$EC = A * e^{-0.045C} \quad (R^2 > 0.99) \quad (4\text{-}5)$$

For ethylene glycol, the EC can be predicted as:

$$EC = A * e^{-0.036C} \quad (R^2 > 0.99) \quad (4\text{-}6)$$

A is determined by the salt concentration.

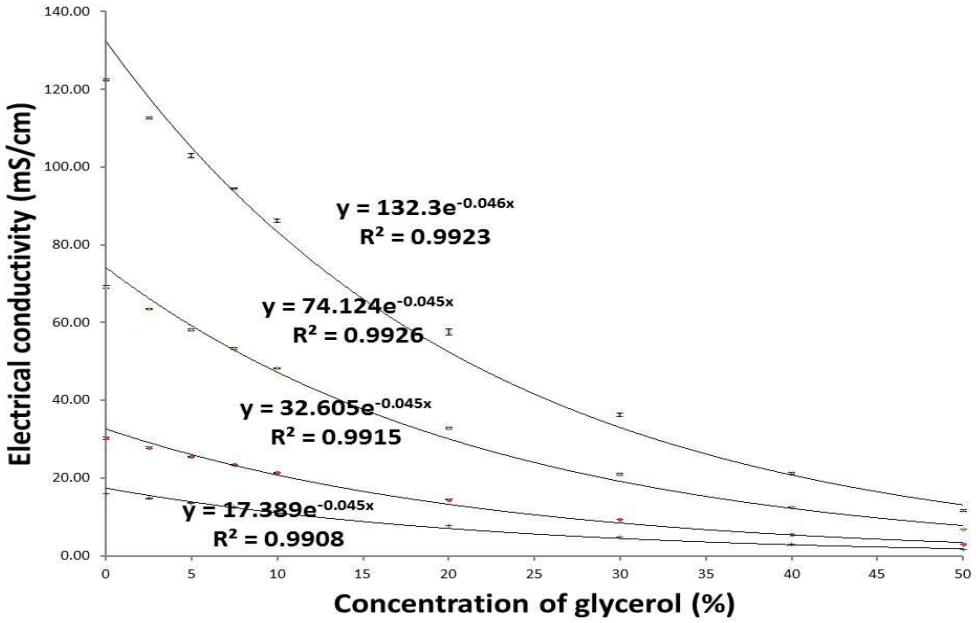

Figure 4-3 Electrical conductivity of glycerol-NaCl-water ternary solutions

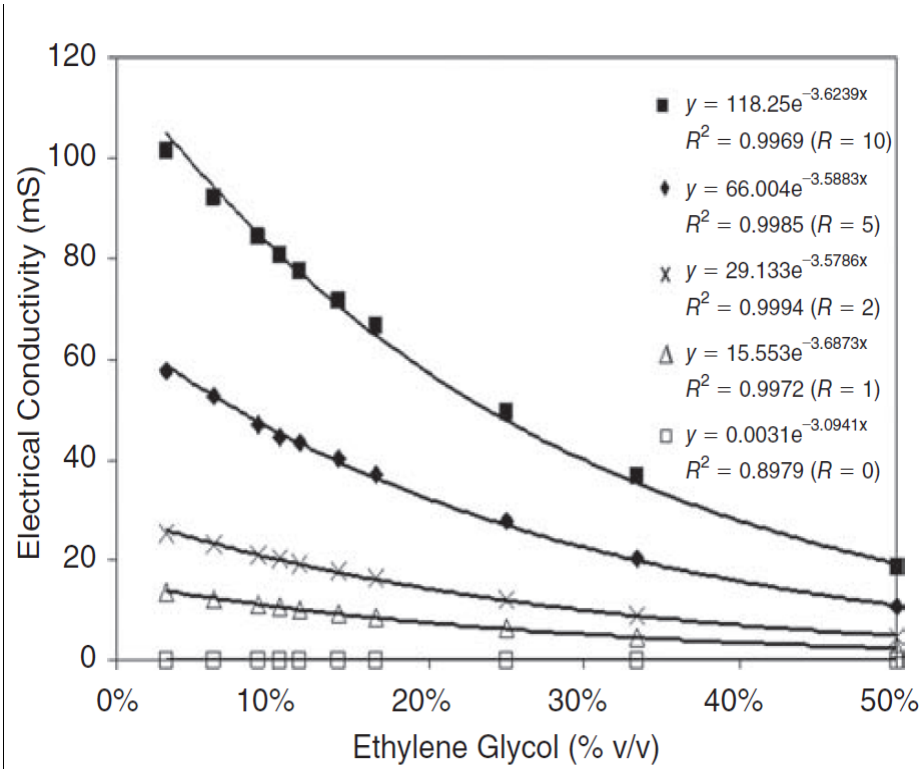

Figure 4-4 Electrical conductivity of ethylene glycol-NaCl-water ternary solutions

4.2.2.3 Effect of albumin on the electrical conductivity of the NaCl-albumin-water ternary solutions

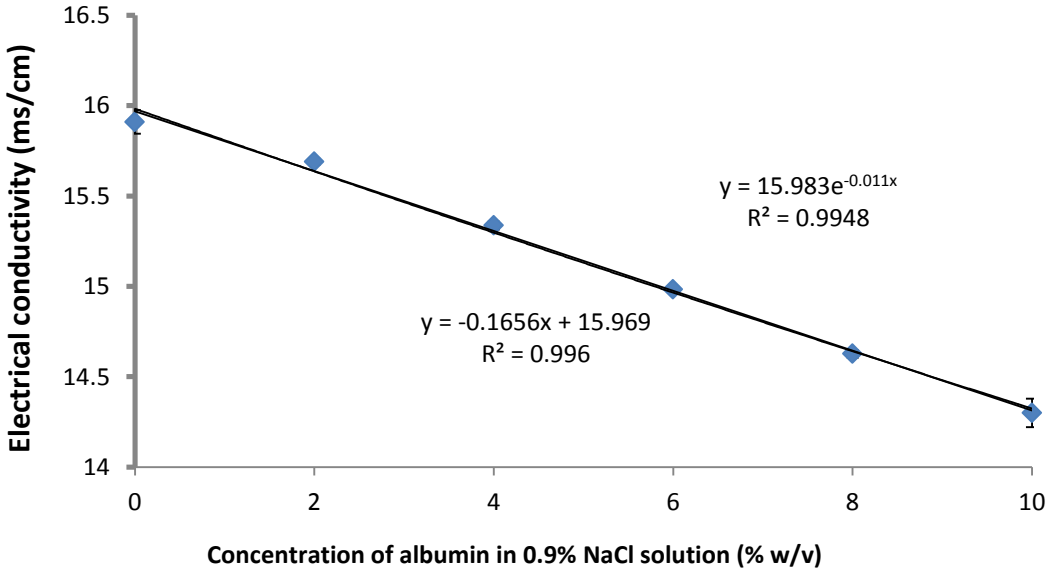

Figure 4-5 Effect of albumin on the electrical conductivity of albumin-NaCl-water ternary solutions

The effect of albumin on the EC of albumin-NaCl-water ternary solutions is shown in Figure 4-5. In this experiment, the concentration of NaCl in the solutions was constant (0.9% w/v), and albumin concentration changed from 0 to 10% (w/v). Obviously when the concentration of albumin increases, the EC of the solution decreases. The data can be fitted linearly as

$$\boldsymbol{EC = -0.1656 * C + 15.969 \quad (R^2 = 0.996)} \tag{4-7}$$

Where, C is the concentration of albumin (w/v%).

The data can also be fitted exponentially as

$$\boldsymbol{EC = 15.983 * e^{-0.011C} \quad (R^2 = 0.9948)} \tag{4-8}$$

Compared to Equation (4-3), it implies that albumin and DMSO decrease the EC of the solutions with similar exponential ways, yet with different decreasing rates. For DMSO, the exponential constant B is -0.036, and for albumin the constant is -0.011.

4.2.2.4 Effect of DMSO on the electrical conductivity of the NaCl-albumin-DMSO-water quaternary solutions

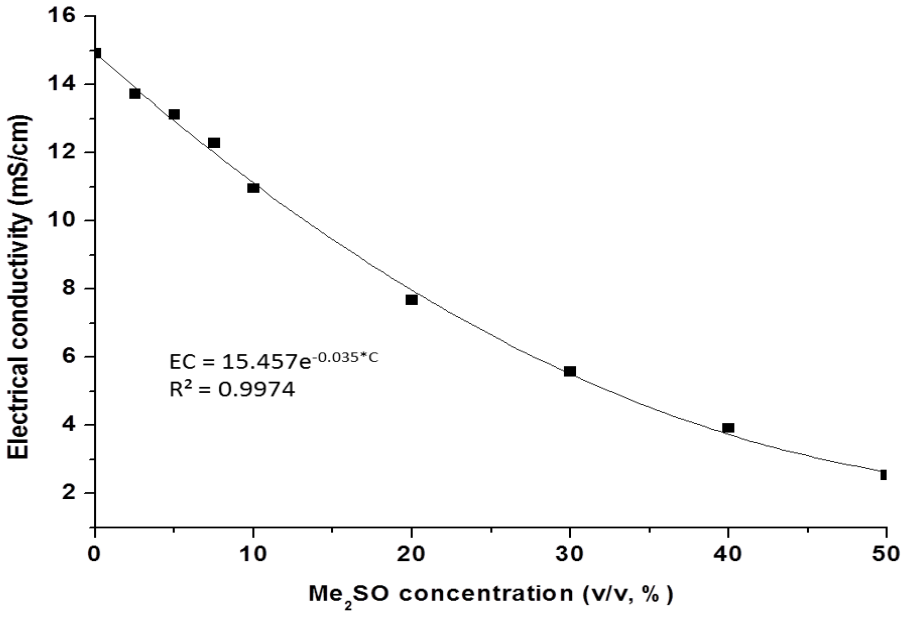

Figure 4-6 Effect of DMSO on the electrical conductivity of DMSO-5% albumin-NaCl-water solutions

In the DMSO-albumin-NaCl-water quaternary solutions, only the concentration of DMSO was changed. Its effect on the EC of the solutions is shown in Figure 4-6. Once again, we can see that the data can be well fitted by an exponential function as

$$\boldsymbol{EC = 15.457e^{-0.035C}} \quad (\boldsymbol{R^2 = 0.9977}) \tag{4-9}$$

Where, the exponential constant is -0.035, very close to the constant in Equation (4-3).

4.2.3 Discussion

In order to evaluate the residual CPA concentration (DMSO, glycerol, and ethylene glycol), the standard curves of "CPA concentration-EC of the CPA solutions" were obtained. For CPA-NaCl-water ternary solutions, EC can be well represented by exponential equation: $\mathrm{EC} = \mathrm{A} * \mathrm{Exp}(\mathrm{B} * \mathrm{C})$. Interestingly, A is determined only by salt concentration and B is constant for any salt concentrations (B=-0.036, -0.036 and -0.045 for DMSO, glycerol and ethylene glycol, respectively. Concentration unit: %, v/v). A similar effect of albumin on the EC of albumin-NaCl-water ternary solutions was also found with an exponential constant of -0.011. This indicates that the effects of CPA, albumin and salt on the EC values are not coupled. This might be due to the fact that CPA, albumin and salt cannot combine or interact in the solutions.

These standard curves can be used to predict the residual CPA concentration in the solutions during CPA removal. This will be demonstrated in the following parts. Compared to other methods, EC measurements have many advantages including low cost, ease of operation, and fast measurement. Another significant advantage is that the measurement can be done without contact with the cell suspension when coupled with the following "dilution-filtration" method of CPA removal, which can reduce the contamination risk dramatically.

4.3 Design of the multifunctional cell processor

The working schematic for the multi-functional cell processing device is shown in Figure 4-7. A hollow-fiber cartridge and three peristaltic pumps compose the key parts of the device. This design can achieve all of, but not limited to, the three goals of cell processing: cell concentration, CPA addition and CPA removal. The pump settings for different cell processing goals are listed in Table 4-1.

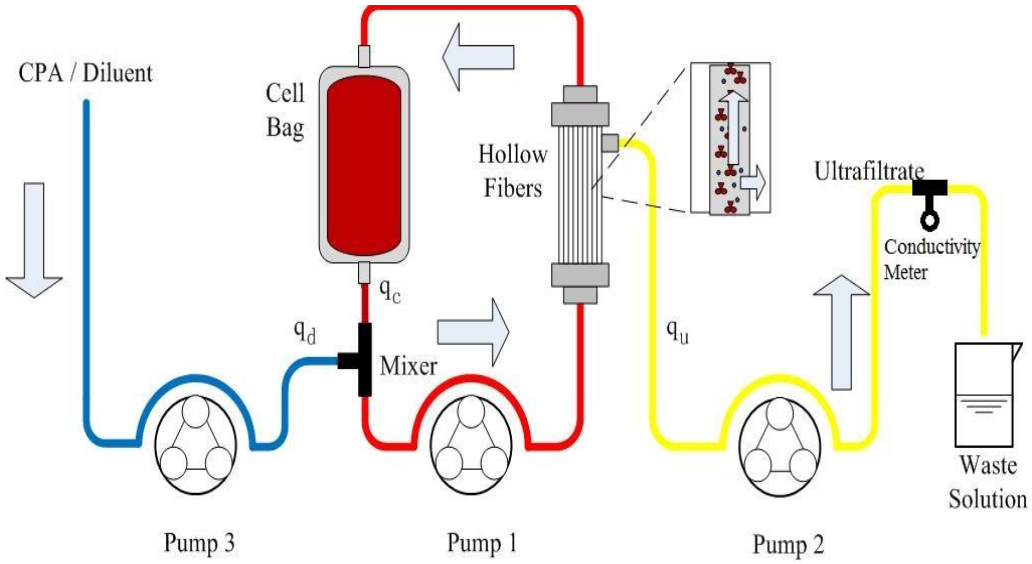

Figure 4-7 Working schematic of the multifunctional cell processing device

Table 4-1 Pump settings for different cell processing goals

Cell processing	Pump 1	Pump 2	Pump 3
Cell concentration	→	→	off
CPA addition	→	off	→
CPA removal	→	→	→
Cell retrieval	←	off	off

For cell concentration: shut down pump 3 and run pump1& 2.

For CPA addition: shut down pump 2. Run pump 1& 3 with a specific flow rate ratio (e.g., 11:1). The "T" shape connector and pump 1 also work as mixers.

For CPA removal: run pump 1 and pump 3 with a specific flow rate ratio (e.g., 11:1) to add washing buffer solution into cell suspension gradually and slowly. Meanwhile run pump 2 with the same ultrafiltration rate as flow rate of pump 1 to remove CPA. This also helps to keep the volume of cell suspension constant.

For cell retrieval (after processing): run pump 1 reversely with slow velocity.

4.4 Concentration/volume control of cell suspension with the multifunctional cell processor

This part demonstrates the feasibility of cell concentration with hollow fibers. A cartridge composed of cellulose acetate hollow fibers (CA-50, Baxter Healthcare Co., Deerfield, IL 60015) was chosen for the preliminary trial of cell concentration because of its small priming/hold-up volume (about 30mL). The experiment schematic is shown in Figure 4-7 and Table 4-1. Lymphoblast cell line (LCL) was used as model cells. The cells were cultured, expanded for 8-12 days at Fred Hutchinson Cancer Research Center and then 1 litter of the cell suspension in culture medium was harvested for the later experiment of volume reduction. The cell concentration and viability before concentration were assessed with hemocytometer and Trypan blue as 8.3e6 cells/mL and 91%, respectively.

The operation procedure included:

① Priming of cartridge and tubing with isotonic phosphate buffer saline (PBS) (pump-1= 200mL/min).

② Concentration of cells with different ultrafiltration rates. The ultrafiltration rate was adjusted by pump-2. Pump-1 was run at a constant rate of 200mL/min.

③ Retrieval of cells from tubing and hollow fibers. Pump-1 was run reversely with different flow rates (20 and 300mL/min).

Results showed that:

① Cell viability rate after concentration was 87.9-89.2%.

② In Step-3, when flush the hollow fibers with larger flow rate (300mL/min), cell population recovery rate was 50.0%. Lots of bubbles and foaming were formed and many cells remained in hollow fibers. On the contrary, if low flow rate (20mL/min) was applied, the cell population recovery rate was much higher (82.2%). We hypothesize that this could be due to that the liquid moving front face in the cartridge may be non-flat (curved). When pump-1 runs reversely, since the pressure distribution on the cross-section of the cartridge is not uniform, liquid in the hollow fibers in the center part of cartridges moves faster, while liquid in

the outer part moves more slowly. Once the liquid in the center line of the cartridge is retrieved, the hollow fibers are filled with only gas, accordingly the resistance wherein decreases dramatically. This forms the "leaky channel" in cartridge, which prevent the retrieval of liquid in the outer part of the hollow fibers. This hypothesis can be evaluated by observing the liquid moving front face with magnetic resonance imaging (MRI) in the future.

③There was no difference of cell viability after concentration when different ultrafiltration rates were applied (50~200mL/min).

4.5 Removal of CPA with the multifunctional cell processor

4.5.1 Introduction

Conventional methods of removing CPA from cell suspensions based on centrifugation have seldom changed since 1970s. Nowadays the most widely used procedure was proposed by Rubinstein et al. in 1995 (122). This process can result in cell clumping and loss, stem cell activation, and risk of contamination etc.. It's also time-consuming and labor intensive. Some devices have been commercially available for CPA removal such as CytoMate^{TM}, Sepax S-100 and Cobe-2991. CPA can be removed by these automated devices using user-definable programs. So labor consumption is reduced significantly. Risk of contamination can also be decreased due to the closed fluid path. However, these devices are basically based on centrifugation or spinning membranes. Thus severe cell loss can also happen. Fleming et al. developed a microfluidic channel for CPA washing based on diffusion, which introduced the booming field of lab-on-chip to CPA removal (73, 74). However, this method is not efficient and not suitable to be scaled up for samples with large volumes. Ding et al. proposed the method of dialysis using hollow fiber modules with semi-permeable membranes (71, 72). Since the modules have been widely applied in clinical treatments (artificial kidney) and proved by Food and Drug Administration, this method is potentially easy to be commercialized. But the challenge is that the first mixing process of washing solution and cell suspension cannot be well controlled, which may cause severe cell loss.

In Table 4-2, working mechanism, pros and cons of a few methods and devices used for CPA removal are presented. Some CPA removal solutions are listed in Table 4-3.

In this part, we will apply the multi-functional cell processing system for CPA removal by using a dilution-filtration method.

Quantification of residual CPA concentration

One easy way to estimate the residual CPA concentration after washing is through calculation according to the dilution procedure, sample concentrations and volumes. However, this is an indirect estimation and cannot get precise CPA content. Osmolality measurement is a precise approach to detect colligative property of the cryopreservation medium, but the data give the comprehensive effects of all vehicles in the medium including CPA, salt, electrolytes and macromolecules. Furthermore, osmolality measuring device—osmometer is generally expensive. Capillary zone electrophoresis (20, 123, 124) and chromatography, such as high-performance liquid chromatography (HPLC) (67, 120) and gas chromatography (121), were proposed to directly measure residual CPA concentration and also applied in clinical practice. But these methods also have some disadvantages including using special chemical agents and devices, complex procedures and intensive time consumption.

In this work, electrical conductivity measurement will be applied for on-site and real-time monitoring of the residual CPA concentration in the cell suspension. As shown in the part of Chapter 4.2, CPA concentration and EC of the solution have a deterministic correlation, which can be used to estimate the CPA concentration by the simple, fast and cheap EC measurement.

Table 4-2 Methods and devices for CPA removal

Methods or devices	Mechanism	Comments, pros and cons	References
Centrifugation	Centrifugation	Standard procedure of CPA removal so far. • Pros: using regular devices available in most labs. • Cons: high time and labor consumption, causing cell clumping, stem cell activation and cell loss, high risk of contamination, etc..	(9, 14, 20, 25, 120, 122, 123, 125-127)
CytoMate™	Filtration by spinning membrane	• Pros: allowing a step-by-step user definable programming, low risk of contamination because of closed fluid path, time-effective. • Cons: the first step of dilution process is not well controlled; cell aggregation and clumping.	(20, 69, 121)
Sepax S-100	Consisting steps of dilution and centrifugation using a rotating syringe	• Pros: automated processing, low risk of contamination because of closed system, fast removal of CPA. • Cons: Cell loss and clumping due to centrifugation.	(120, 126)
Cobe 2991	Centrifugation	• Pros: automated processing, low risk of contamination because of closed system, fast removal of CPA. • Cons: Cell loss and clumping due to centrifugation.	(12, 123, 128)
Microfluidic channel	Diffusion-based extraction of CPA molecules from cell stems in microfluidic channels	• Pros: automated processing, suitable for cell suspension with small volume. • Cons: Low efficiency of CPA removal due to diffusion-based extraction, not suitable to be scaled up for samples with large volume.	(73, 74)
Dialysis through hollow-fiber dialyzer	Dialysis across semi-permeable hollow fiber membranes	• Pros: automated processing, low labor consumption, effective CPA removal, low risk of contamination because of closed system, suitable for samples with large volumes • Cons: the first step of dilution process is not well controlled; cell loss and cell clumping, special modifications needed for samples with very small volumes.	(71, 72)

Table 4-3 Solutions for CPA removal

Solutions for CPA removal	References
10% dextran-40 and 5% HSA in saline	(127)(129)
PBS supplemented with 5% dextran 40, 5% ACD-A and 1% HSA.	(20)
10% ACD in saline	(9)(123)
7.5% dextran-40 and 5% human albumin in saline	(120)
One-third ACD-A anticoagulant+two thirds albumin 4%	(125)
Saline solution with 10% acid citrate dextrose anticoagulant	(12)
2.5% w/v HSA and 5% w/v Dextran 40 in isotonic saline	(122)(122)
15% ACD-A in RPMI-1640 medium	(14)
5% dextran, 2.5% human albumin, 10% acid citrate dextrose (ACD-A)	(126)

- HES: hydroxyethyl starch; ACD-A: acid citrate dextrose.

4.5.2 Materials and methods

"Dilution-filtration" system for CPA removal

The "dilution-filtration" system for CPA removal is presented in Figure 4-7. It mainly consists of three peristaltic pumps (400F/M1, Watson-Marlow), one hollow fiber dialyzer (Hemoflow, F5HPS, Fresenius Medical Care), a T-shape connector, and silicon tubings (985-75, Pall). Pump 1 and pump 3 cooperate to control the flux of diluent (q_d) and cell suspension (q_c). Diluent and cell suspension are mixed in the T-shape connector and tubing, pass through the hollow fibers, and then return to the cell suspension container. Pump 2 controls the ultrafiltration rate (q_u). Filtrated solution is collected in the waste solution container. Herein the diameter of the tubing perfectly matches the pumps. When the pump stops, it can also function to clamp the loop, which prevents pressure loss inside the dialyzer. The dialyzer made of polysulfone was chosen in this work because of its large cross-membrane flux capability and high efficiency of clearance. Macromolecules (such as proteins), cell debris and cells cannot pass through the fiber membranes, which leads to the simplicity of the waste solution composition and benefits the monitoring of CPA concentration by electrical conductivity measurements.

DMSO removal with the "dilution-filtration" system

200mL 10% DMSO (v/v)-0.9% NaCl-water ternary solution was used to mimic cell suspension with CPA. Isotonic NaCl solution was used as diluent. The actual pumping rates of the three pumps were calibrated before experiments. The "dilution-filtration" mode program was set as follows:

Step 1: Adjust pump 1 and pump 3 to achieve q_c=200mL/min and q_d=20mL/min. Adjust pump 2 to achieve filtration rate of q_u=20mL/min. Herein q_d=q_u such that the volume of "cell suspension" keeps constant. Agitate the cell bag for better mixing. Repeat step 1 for 45 times. Run the program for 1min each time.

Step 2: Stop pump 2 and pump 3. Run pump 1 slowly (20mL/min) in reverse direction for 3min to retrieve the "cell suspension" in the tubings and dialyzer back to the cell suspension container.

Real-time monitoring of DMSO concentration

In the program mentioned above, after each dilution-filtration cycle (i.e., 1min), the EC of the newly collected "waste solution" in Step 1 (volume: ~20mL) was measured. The osmolality of the waste solution was also measured by a vapor pressure osmometer (Wescor Inc., Logan, UT). Then the newly collected waste solution was pooled to another big container. The EC and osmolality of the "cell suspension" in this experiment were also measured after each cycle. All the measurements were conducted twice.

Glycerol removal from cryopreserved red blood cells with hollow fibers

Ten units of red blood cells (~200mL/unit) were cryopreserved (glycerol concentration was 40%, w/v)) and deglycerolized by the dilution-filtration method with hemofilter cartridge (Plasmflo TM AP-05H/L, ASAHI) with the similar operation procedures as mentioned above.

4.5.3 Results

4.5.3.1 DMSO removal from DMSO-0.9% NaCl-water ternary solution by "dilution-filtration"

The experiment results of DMSO removal from DMSO-0.9% NaCl-water ternary solution by "dilution-filtration" system are shown in Figure 4-8. After processing for

45min, the volume of "cell suspension" was 196mL, which was very close to the original volume (200mL). Totally 860mL isotonic NaCl solution was used as diluent. Figure 4-8A shows the EC and osmolality of the waste solution that were obtained every minute. According to Equation (4-4), EC data were converted to DMSO concentrations of the waste solution, shown in Figure 4-8B. The DMSO concentration decreased to <1% (v/v) after 35min. The results also show that DMSO concentrations estimated by EC measurements match the osmolality data very well, which implies EC measurement can be used to monitor the DMSO concentration during processing.

The EC data and converted DMSO concentrations of "cell suspension" and waste solution are shown in Figure 4-8C&D. After about 10min, the difference between "cell suspension" and waste solution was very small. After 20min, they were almost identical to each other. The discrepancy between "cell suspension" and waste solution in the beginning was caused by the experiment design and sample procurement method. In the first 2 minutes, waste solution was cumulated in the dialyzer end for priming and its DMSO concentration was high. At the 3rd minute, waste solution sample could be procured out of the dialyzer and measured; herein the waste solution sample was actually the mixture of that achieved in the first 3 minutes. Therefore it had higher DMSO concentration and lower EC than the "cell suspension". After a few minutes, the waste solution in the dialyzer and tubing was replaced. The cumulative effect disappeared and the readings of "cell suspension" and waste solution became identical.

For the theoretical prediction of the concentration of DMSO in the "cell suspension", it is a mixing-dilution problem. The DMSO concentration (C_{DMSO}) can be estimated by the governing equation:

$$\boldsymbol{V_{Cell} * \frac{dC_{DMSO}}{dt} = -\frac{m}{m+1} * f_{Diluent} * C_{DMSO}} \quad (4\text{-}10)$$

Where, VCell is the volume of "cell suspension" (mL), t is time (min), m is the flux ratio of cell suspension to diluent, and fDiluent is the flow rate of diluent (mL/min).

Solving this equation, the concentration of DMSO can be estimated as

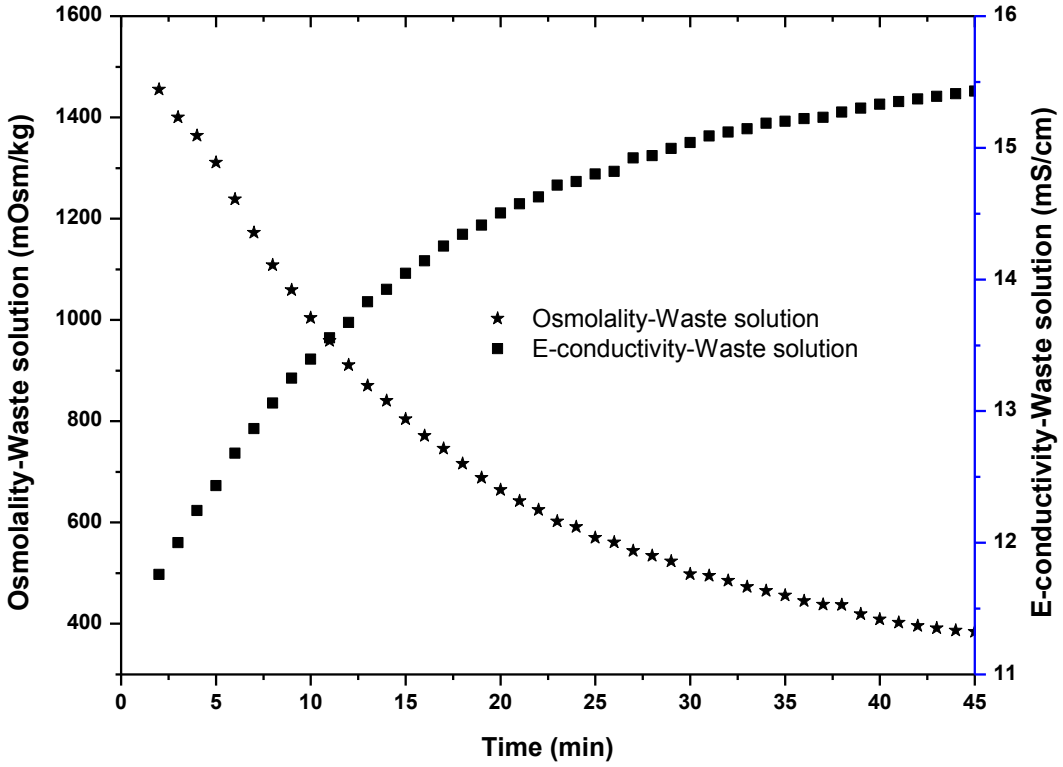
Osmolality-Waste solution (mOsm/kg)
E-conductivity-Waste solution (mS/cm)
Time (min)
Osmolality-Waste solution
E-conductivity-Waste solution

A

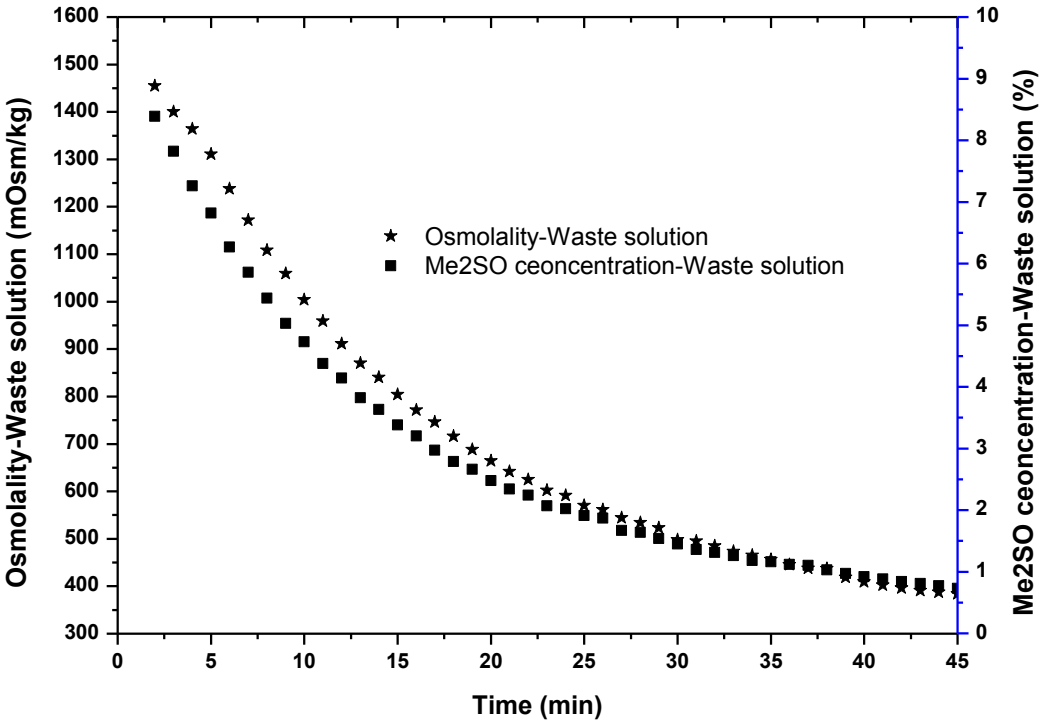
Osmolality-Waste solution (mOsm/kg)
Me2SO ceoncentration-Waste solution (%)
Time (min)
Osmolality-Waste solution
Me2SO ceoncentration-Waste solution

B

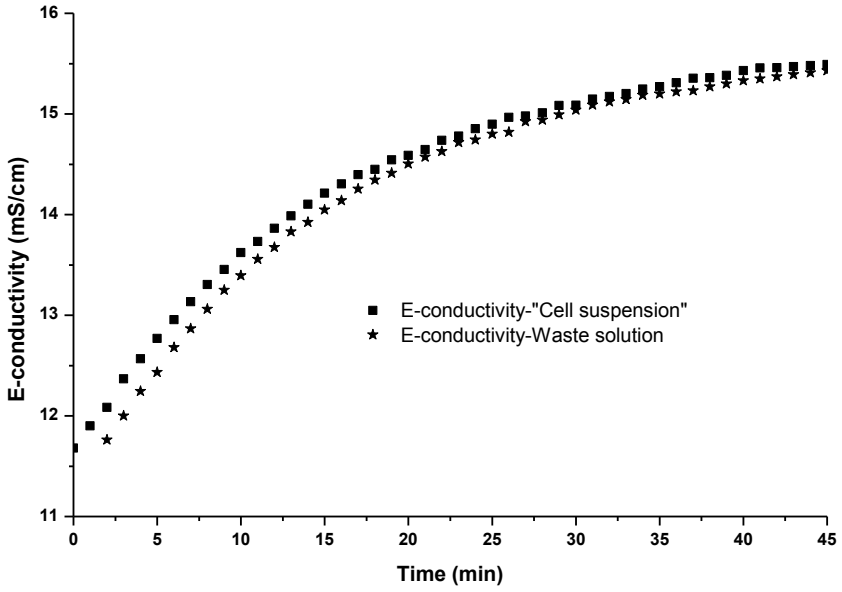

C

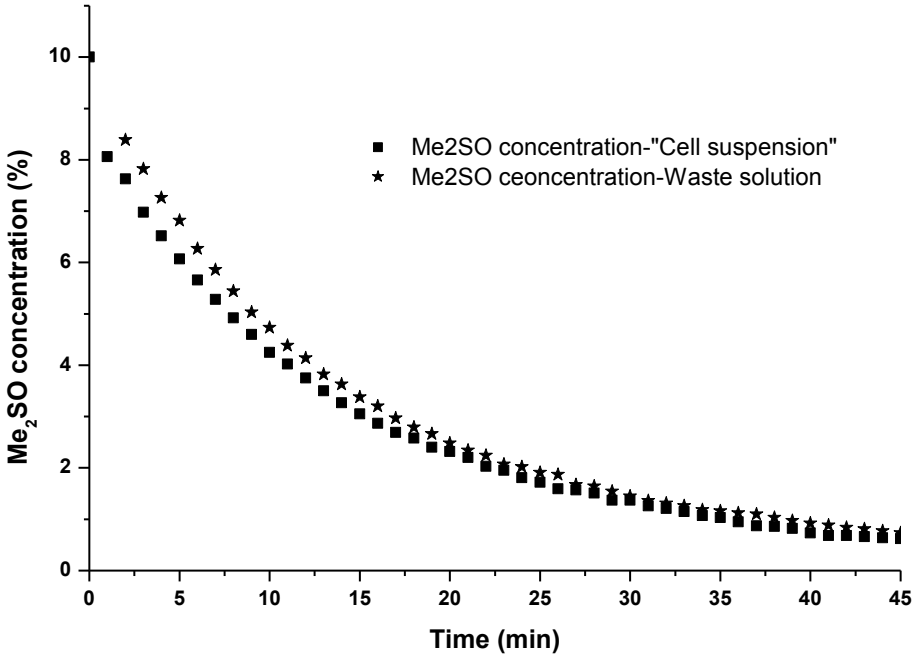

D

Figure 4-8 DMSO removal from DMSO-NaCl-water ternary solution by “dilution-filtration”. (A) Conductivity and osmolality of waste solution; (B) DMSO concentration and osmolality of waste solution; (C) Conductivity of “cell suspension” and waste solution; (D) DMSO concentration of “cell suspension” and waste solution. (Me_2SO=DMSO)

$$\boldsymbol{C_{DMSO}(t) = C_{DMSO}(t=0) * e^{-\frac{f_{Diluent}}{V_{Cell}} * \frac{m}{m+1} t}} \quad (4\text{-}11)$$

In our experiment, the initial concentration is $C_{Me2SO}(t = 0) = 10\%$, flux of diluent was 20mL/min, m=10, and volume of "cell suspension" was 200mL. So, theoretically, the DMSO concentration in "cell suspension" is

$$\boldsymbol{C_{DMSO}(t) = 10 * e^{-\frac{20}{200} * \frac{10}{11} t} = 10 * e^{-0.091t}} \ (\%) \quad (4\text{-}12)$$

According to the results presented in Figure 4-8 D, actually the DMSO concentration in "cell suspension" during the whole removal process (45min) can be fitted as $C_{Me2SO}(t) = 10e^{-0.07t}$ ($R^2 = 0.9741$), which was close to but a little different with theoretical prediction. The discrepancy may be caused by the fact that the fluxes of "cell suspension", diluent and filtration cannot be precisely controlled as programmed after longer time running since the engagement between tubing and pumps may get worse due to fatigue of the plastics. This hypothesis can be proved by the fact that in the first 10min of the experiment (with good engagement and precise flux control), the DMSO concentration data of "cell suspension" can be fitted as $C_{DMSO}(t) = 10e^{-0.091t} (R^2 = 0.9372)$, which perfectly matches the theoretical prediction.

4.5.3.2 DMSO removal from DMSO-5% BSA-0.9% NaCl-water quaternary solution by "dilution-filtration"

The results of DMSO removal from DMSO-5%BSA-0.9% NaCl-water quaternary solution by "dilution-filtration" system are shown in Figure 4-9. Figure 4-9A shows the EC and osmolality of the waste solution that were obtained every minute. According to Equation (4-4), EC data were converted to DMSO concentrations of the waste solution, shown in Figure 4-9B (no BSA in waste solution!). The DMSO concentration decreased to <1% (v/v) after 35min. The EC data and converted DMSO concentrations of "cell suspension" and waste solution are shown in Figure 4-9C&D. ECs of "cell suspension" were always lower than those of waste solution due to the existence of BSA in "cell suspension". After certain time of processing (~10min), the difference of DMSO concentration between "cell suspension" and waste solution was very small, which implies that measurements of waste solution can be applied to monitor the status of "cell suspension".

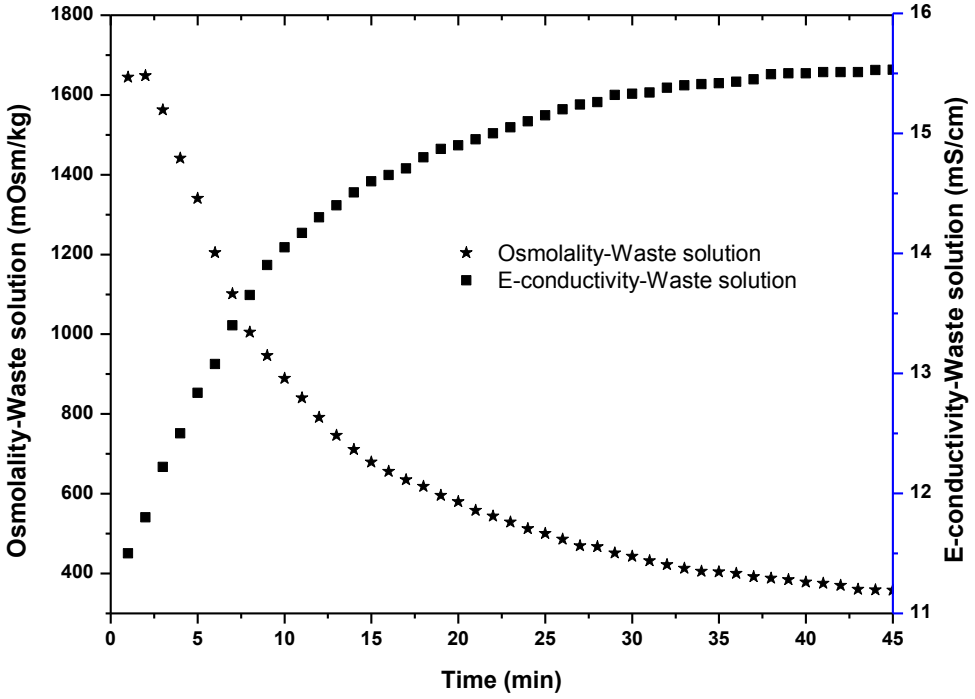
Osmolality-Waste solution (mOsm/kg)
E-conductivity-Waste solution (mS/cm)
Time (min)
Osmolality-Waste solution
E-conductivity-Waste solution

A

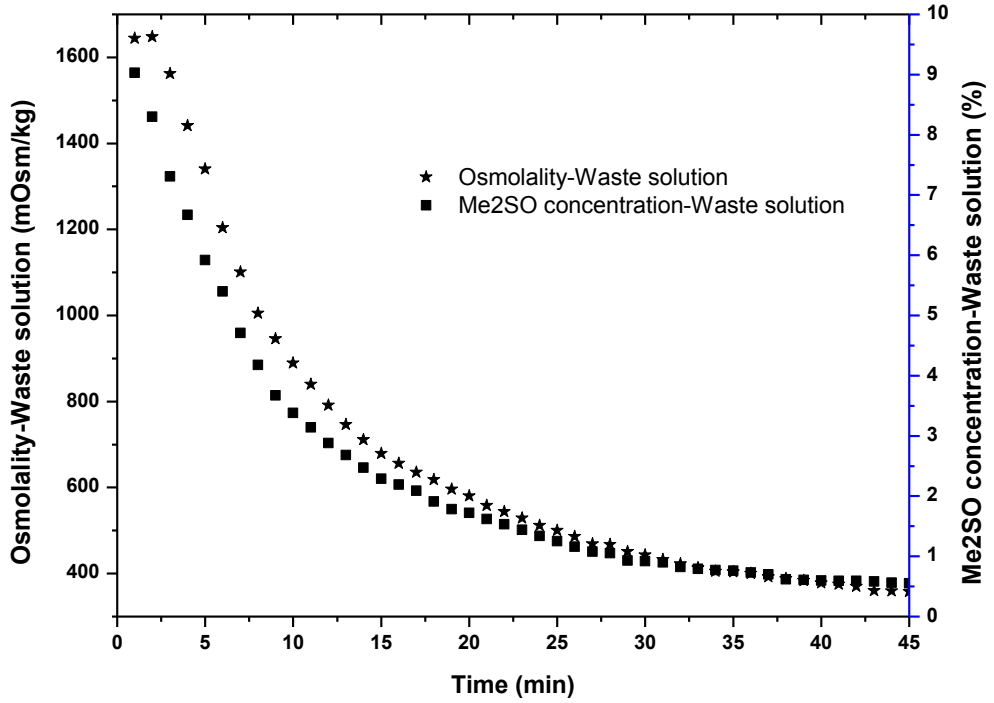
Osmolality-Waste solution (mOsm/kg)
Me2SO concentration-Waste solution (%)
Time (min)
Osmolality-Waste solution
Me2SO concentration-Waste solution

B

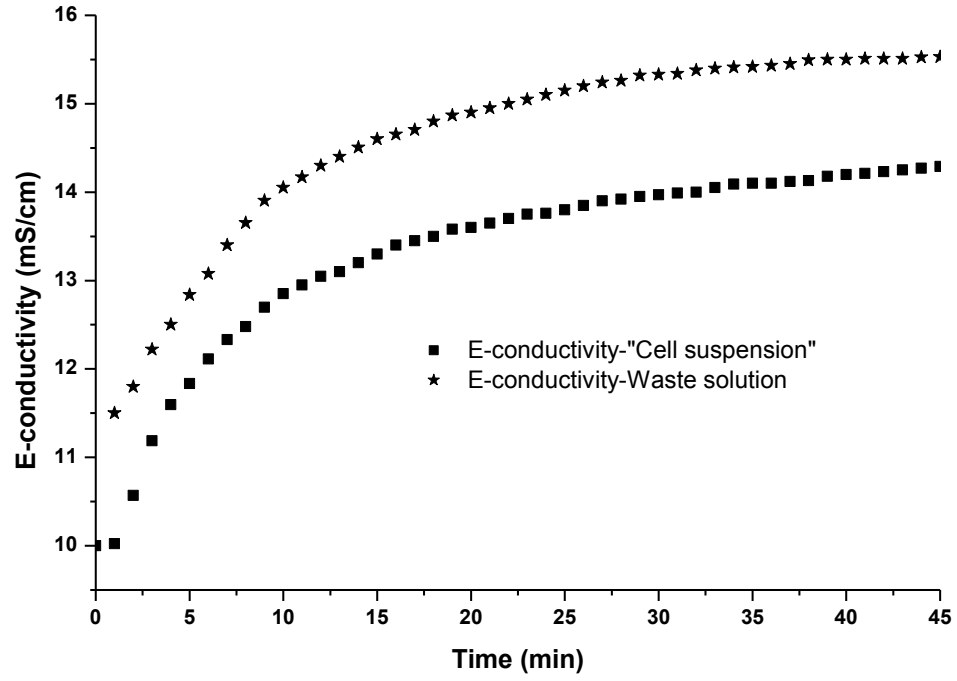

C

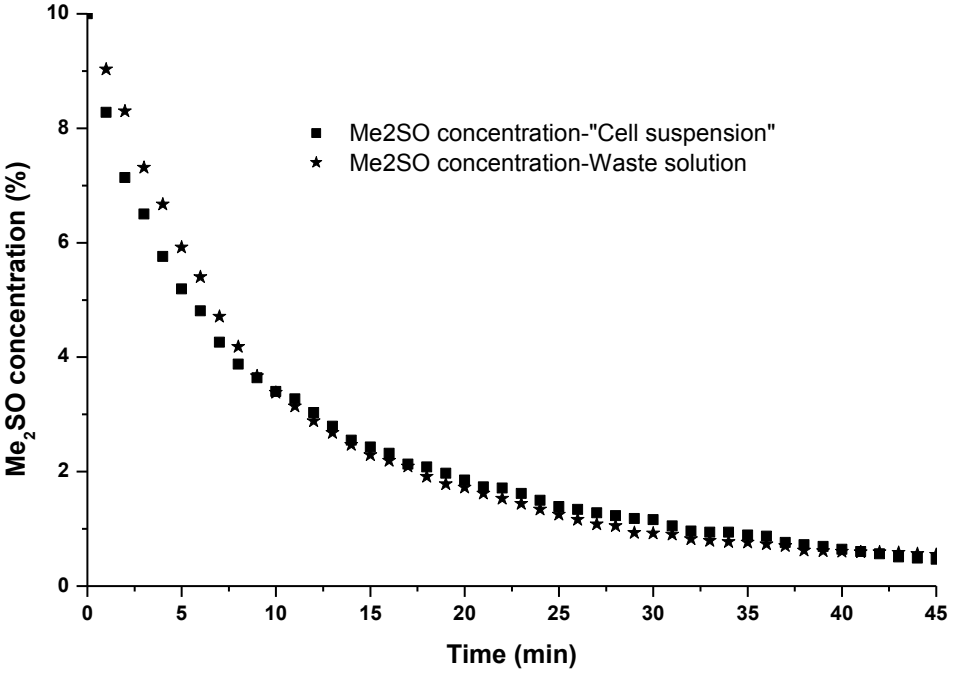

D

Figure 4-9 DMSO removal from DMSO-BSA-NaCl-water quaternary solution by “dilution-filtration”. (A) Conductivity and osmolality of waste solution; (B) DMSO concentration and osmolality of waste solution; (C) Conductivity of “cell suspension” and waste solution; (D) DMSO concentration of “cell suspension” and waste solution.

4.5.3.3 Glycerol removal from cryopreserved red blood cells

The results are shown in Table 4-4. The residual glycerol concentration (5.57 ± 2.81 g/L, n=10) is lower than the standard value (10g/L) required by American Association of Blood Banking (AABB). The cell count recovery rate was 91.19 ± 3.57% (n=10). Each of the unit was processed within one hour, which is similar to the automatic centrifuging method. Comparing to the reported methods (dialysis method, no in vitro data has been presented; manual centrifuging method: >80%, and automatic centrifuging method 89.4 ± 3.0%), the results indicate an obvious advantage of our method in cell safety. Furthermore, the operation procedure here was not optimal, even better results can be expected after optimization.

Table 4-4 Deglycerolization of blood with dilution-filtration method

UNITS	Thawed Blood Vol (ml)	Thawed Blood Hct (%)	Cell Count Recovery (%)	Residual Glycerol (g/L)
1	221.8	30	93.64	2.60
2	204.1	27	85.92	3.39
3	229.8	29	91.64	12.26
4	219.0	23	90.91	4.90
5	217.6	25	91.38	3.39
6	210.0	28	90.76	6.56
7	216.7	24	81.60	3.80
8	200.5	29	94.18	7.34
9	204.5	21	92.24	5.35
10	205.0	30	93.80	6.08
Mea	212.9	27	91.19	5.57
S.D.	9.49	3	3.57	2.81

4.5.4 Discussion

In this work, a "dilution-filtration" system was successfully applied to remove DMSO from DMSO solutions efficiently. In the present study, flux ratio of "cell suspension" to diluent was 10:1. This large ratio can decrease the cell volume excursion and osmotic injury to cells. The CPA removal procedure can be further optimized to prevent osmotic injury and increase CPA removal efficiency as follows: apply larger flux ratio of cell suspension to diluent (m value) in the beginning, and then decrease the ratio gradually when the CPA concentration in cell suspension declines.

Compared to the traditional centrifugation method of CPA removal, the "dilution-filtration" can decrease labor and time consumption, eliminate mechanical injury due to

centrifugation, avoid cell packing and clumping, and prevent contamination. The volume of diluent solution needed for CPA removal is also decreased dramatically in the "dilution-filtration" method.

Compared to the method of dialysis using hollow fibers, the "dilution-filtration" method also has many other advantages: (1) in the beginning of the dialysis process, the cell suspension has to be exposed to diluent in the dialyzer. This process is generally hard to control and severe osmotic injury can happen. In order to decrease the osmotic shock to cells, sometimes hyperosmotic nonpermeable solutions are applied to prime the dialyzer first. This can improve cell recovery but cause complexity and this nonpermeable material eventually needs to be removed. In "dilution-filtration" method, the mixing of cell suspension and diluent can be well controlled in the "dilution" step (adjust the m value). (2) In dialysis method, CPA clearance is due to the passive diffusion transport across the fiber membranes caused by the CPA concentration gradient, while in "dilution-filtration" method, CPA is removed by active filtration. So the CPA removal efficiency can be improved dramatically. (3) In dialysis method, the CPA gradient across the membranes is not uniform along the fibers. So mass transport is not uniform and cells experience different osmotic stresses along the fibers. This increases complexity and thus makes it harder to achieve optimal conditions. (4) It is much easier to control and manipulate the final cell suspension volume and cell concentration with the "dilution-filtration" method.

EC measurement can be a very good method to assess CPA concentration. Compared to direct osmolality measurement by osmometer, its advantages include low cost, ease of operation, real-time and on-line monitoring, and broad working range (CPA concentration).

For the CPA-salt-water ternary solution, once the salt concentration is fixed, the CPA concentration can be determined by its EC. This is generally the case of CPA removal after cell cryopreservation with fixed salt concentration. The hollow fibers selected in this work can block macromolecules from crossing the fiber membranes, such that the waste solution is CPA-NaCl-water ternary solution. Meanwhile, salt concentrations in cell suspension and diluent are isotonic, this leads to the fact that salt concentration

everywhere, including in waste solution, is isotonic. Accordingly, EC change of the waste solution is determined only by the CPA concentration change. In order to further evaluate the validity of predicting CPA concentration in cell suspension with the data of waste solution, the measurements of "cell suspension" were conducted and compared with those of waste solution. The results show that after a short period of priming solution removal, the EC, CPA concentration and osmolality of "cell suspension" and waste solution were almost identical to each other. This proves that assessment of waste solution is a good measure of the real-time state of the cell suspension. Measuring the waste solution, instead of cell suspension, has at least two advantages: first, waste solution is generally simpler than cell suspension without effect of proteins, cell debris, etc.; secondly, this can prevent direct contact of the EC probe with the cell suspension, keep the cell loop closed, and reduce the risk of contamination. A probe can be mounted in the waste solution loop to achieve real-time, on-line monitoring of CPA concentration during CPA removal.

4.6 Conclusion

In this chapter, a multi-functional cell processor was developed and applied for cell concentration (volume reduction), CPA addition and CPA removal. Compared to methods that are applied traditionally (centrifugation) or proposed recently (dialysis, diffusion in microfluidic device), the operation system has many advantages including low time and labor consumption, low osmotic injury to cells, high effectiveness, ease to control the final suspension volume and low risk of contamination. This device potentially can become alternative basic equipment used in research laboratories or hospitals where related cell processing is done frequently.

A simple approach based on electrical conductivity measurements was also developed for the quantification and monitoring of the residual CPA concentration. Standard data of a few CPAs solutions (DMSO, glycerol, ethylene glycol) were obtained. Coupled with the multi-functional cell processing system, this method can be used to measure the EC of waste solution and predict the real situation in cell suspension. This way can prevent contamination and achieve on-site and real time monitoring of the CPA concentration.

Chapter 5 Cryopreservation of bacteria and freeze-drying of proteins: an application of biopreservation in diagnosis of *Mycobacterium tuberculosis*

5.1 Cryopreservation of *Mycobacterium tuberculosis*

5.1.1 Introduction

Tuberculosis (TB) is the second leading cause of death from an infectious disease worldwide (only after HIV/AIDS). Millions of people die of this disease every year (1.2-1.5 million deaths in 2010). An active TB patient can infect 10-15 persons in a year without restriction or treatment. TB prevention and control, including diagnosis, treatment and drug development is one of the major tasks of World Health Organization (WHO) and many governments, especially in developing countries (130).

Timely and correct diagnosis of TB is still a challenge. Often collected samples must be shipped to centers with clinical laboratory facilities, well-trained personnel and specialized working environments for biosafety. In this context, cryopreservation can be a useful option (131). Biobanking of *Mycobacterium tuberculosis* (MTB) is also important in fundamental biological research and for the development of new drugs, vaccines, biomarkers and diagnostic tests. Clinical and laboratory samples are often exchanged among institutions for comparative multicenter studies. Therefore quality control of transported samples is a very important issue.

There have been few studies on the optimization of MTB cryopreservation. Clinical MTB samples such as sputum are stored at room temperature, but only for a few days (132-134). Viability of some bacteria, such as MTB and *M. bovis,* can be severely affected by storage conditions during shipping (135). Papers published a few decades ago demonstrated long-term preservation of MTB samples at -70 ℃, but little information on optimization of the cryoprotective medium and freezing procedure was provided (135-139). Therefore, optimization of MTB cryopreservation remains an unfilled need, especially for situations requiring quantification of viable MTB cells in samples with low cell density.

Since *M. bovis* Bacillus Calmette-Guérin (BCG), a non-virulent strain of the *M. tuberculosis* complex, is very close to *M. tuberculosis* in terms of cell physiology, it was

used as the model to optimize the cryopreservation protocol in the first part of this study. Common cryopreservation media, effect of a cryoprotective agent (glycerol) and cooling rate were studied. It has been suggested that transient incubation of cells in broth medium after exposure to stress environments, such as heating, freezing/thawing or ultraviolet (UV) light, helps to repair the injury for some cell types (140-143). Therefore, the effect of transient incubation (preincubation) on cryopreserved BCG cells was also explored. To conclude the study, the optimized protocol was applied to *M. tuberculosis* H37Ra cells spiked into a natural, undefined sample matrix, namely human sputum.

5.1.2 Materials and Methods

BCG cell preparation and concentration assessment

BCG cells were cultivated to late log/early stationary phase in 15 ml conical tubes containing 5 mL Difco Middlebrook 7H9 broth with 10% ADC enrichment and 0.05% Tween 80 (BD Diagnostics, Sparks, MD) (henceforth referred to as 7H9) at 37 ℃ without agitation for 3-4 weeks. Cells were harvested by centrifugation for 5 min at 5000rpm and then resuspended in an equal volume of fresh 7H9. Cell concentration was assessed by optical density measurement at 580 nm with a spectrophotometer (Molecular Devices Spectramax Plus, Sunnyvale, CA). According to previously published growth measurements an A_{580} of 0.1 units is equivalent to $6.3x10^7$ CFU per mL Mycobacterium cells (144).

BCG cryopreservation

BCG cells were cryopreserved in three different media: Phosphate-buffered saline (PBS), 7H9, and 7H9 + glycerol (EMD Chemicals, INC., Gibbstown, NJ). For PBS and 7H9, BCG cells were diluted in PBS or 7H9 respectively to an estimated cell density of 1e8 CFU/mL (based on optical density). For 7H9 + glycerol, BCG cells were first diluted with 7H9 to 5e8 CFU/mL, and then 7H9 + glycerol (pre-cooled to 4 ℃) was slowly added dropwise to final volume ratio of 4:1. The final glycerol concentration in the freezing sample was 4% [v/v]. The cell suspension was agitated gently for osmotic equilibration during medium addition. After medium addition, the cell suspension was stored at room temperature for 15 minutes for equilibration before cryopreservation. For

all three groups, the final cell concentration was 1e8 CFU/mL. This high cell density is typical of many cryopreserved samples and it enabled Live/Dead staining and microscopic analysis. Cryogenic freezing vials (2 mL, Fisher Scientific, Pittsburgh, PA) were used for cryopreservation, each containing 0.5 mL of the cell suspension.

For comparison between different cooling rates, two freezing methods were implemented. One was slow cooing in a "Box-in-Box" (BIB) system (see Figure 2-5) that was developed in our group, and the other was rapid cooling by direct immersion of samples into liquid nitrogen (LN2). For cryopreservation in BIB, vials were placed in the slots cut into the polyethylene foam. The system was then closed and placed into a -80 ℃ freezer overnight. Dummy samples with only cryoprotective medium were treated the same way. T-type thermocouples (SA-1T; Omega, Stamford, CT) were inserted inside the dummy samples to record temperature history during cooling. After equilibrium in the -80 ℃ freezer overnight, the samples were transferred into liquid nitrogen (LN2). The protocol for fast cooling was to immerse the sample vials into LN2 directly, and record temperature history via dummy samples.

Thawing of cryopreserved BCG cells

For sample thawing, the frozen samples were removed from LN2 and quickly immersed into a 37 ℃ water bath. They were agitated gently until no crystals remained. Then the cells were assessed for viability by microbiological culture and live/dead staining as below.

Microbiological culturing, with and without preincubation

The thawed cells were diluted with 7H9 broth to a concentration of 4000 CFU/mL. Before culturing, the cells were divided into two groups. One group was plated on 7H10 agar directly (without preincubation), and the other was pre-incubated in 7H9 at 37 ℃ with 5% CO_2 and 100% humidity for 20 hours before plating in order to study the preincubation effect. For plate culturing, Difco Middlebrook 7H10 agar with 10% (v/v) OADC enrichment (BD Diagnostics, Sparks, MD) (7H10) was used. Cell suspension of 250 μL with a predicted concentration of 4000 CFU/mL was spread on each plate. Plates were sealed in plastic bags (BD GasPak EZ; BD Diagnostics, Sparks, MD) and incubated

at 37 ℃ with 5% CO_2, and 100% humidity. After incubation for about 24 hours, the petri dishes were inverted in order to prevent agar from desiccation during extended culture.

These experiments were repeated three times with three separate batches of BCG cells. CFUs were counted at several time points post-inoculation.

Live/Dead staining assessment

A BacLight Live/Dead staining kit (Invitrogen, Grand Island, NY) was used to assess cell envelope integrity of cryopreserved cells. The staining was performed as specified by the user manual, briefly: 1.5 μL live/dead staining reagent was added to 0.5 mL cell suspension, which was vortexed, incubated at room temperature for 15 minutes, and then observed under fluorescence microscopy (Nikon Instruments INC, Melville, NY).

Cryopreservation of M. tuberculosis H37Ra cells in sputum

The experimental design of H37Ra cryopreservation in sputum is illustrated in Figure 5-1. H37Ra cells were spiked into sputum samples that had been collected for diagnostic purposes from anonymous human donors with no tuberculosis exposure (Bioreclamation Inc, Hicksville, NY). Estimated final cell concentrations were 1e7 CFU/mL. Then the samples in cryogenic freezing vials (0.5 mL in each vial) were frozen with three different methods: Putting vials in the BIB and then BIB in a -80 ℃ freezer, putting vials in a -80 ℃ freezer directly, or immersing vials in liquid nitrogen (LN2) directly. After fast-thawing in a 37 ℃ water bath, samples were treated with N-acetyl-L-cysteine and sodium hydroxide (NALC-NaOH) following the standard digestion-decontamination procedures for TB specimen processing (145). The samples were centrifuged at 3000g for 20 min, and the pellets were resuspended in 7H9 for microbiological culturing as described above. The experiments were repeated twice.

In order to differentiate the effects of NALC-NaOH treatment and cryopreservation, three control experiments were conducted, as shown in Figure 5-1. In Control 1, H37Ra cells were spiked into 7H9 and then cultured (without cryopreservation, NALC-NaOH treatment, or centrifugation). In Control 2, H37Ra cells were spiked into 7H9, and the

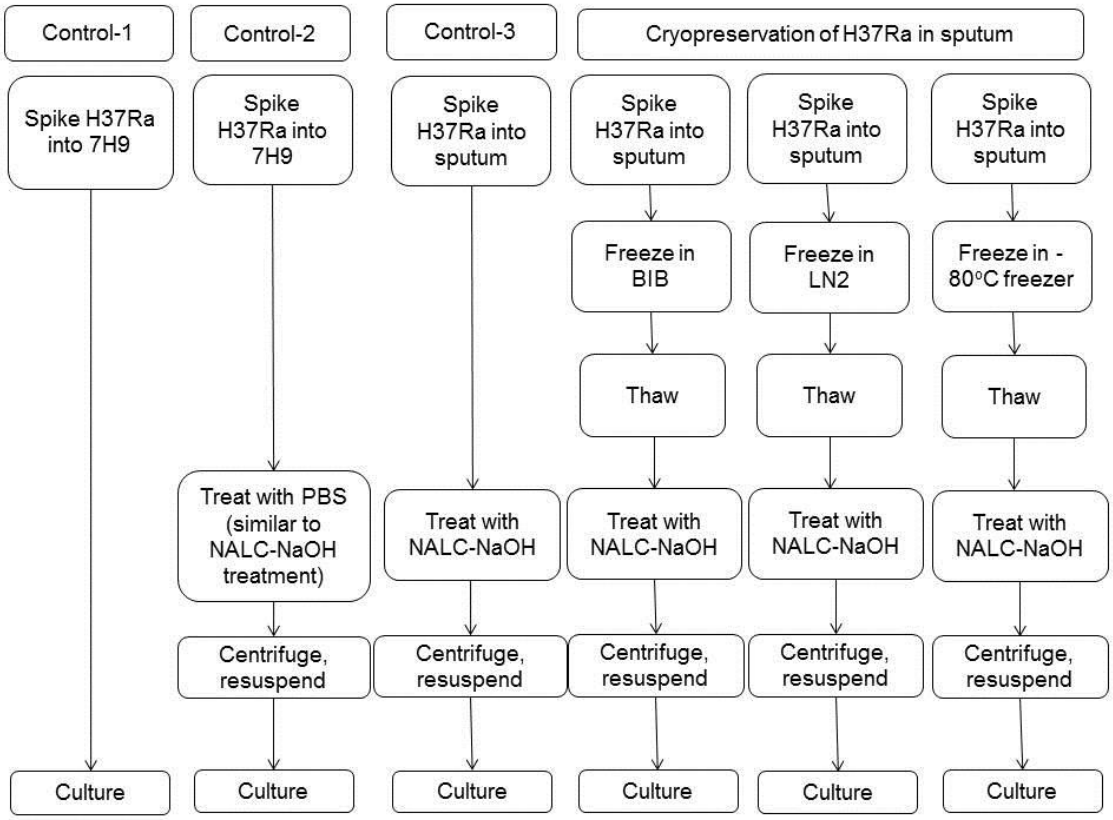

Figure 5-1 Experiment design of H37Ra cryopreservation in sputum

samples were treated with PBS buffer following the procedure of NALC-NaOH treatment (with PBS in place of NALC-NaOH), centrifuged, and then cultured (without cryopreservation and chemical influence of NALC-NaOH). The difference between Control 1 and Control 2 is the effect of centrifugation on cell loss. In Control 3, H37Ra cells were spiked into sputum, and the samples were treated with NALC-NaOH, centrifuged, and then cultured without cryopreservation. Comparison between Control 2 and Control 3 indicates the effect of NALC-NaOH treatment.

Surface antigen check of the cryopreserved BCG cells

In MTB diagnosis, many methods are based on the function of the cell surface antigen. In order to check whether the MTB cells can be used for diagnosis after cryopreservation, the function of the cell surface antigen was assessed as follows.

BCG cells were cryopreserved in 7H9, PBS buffer, or in 7H9+5% glycerol. Box-in-box was applied to provide slow cooling rate. In order to study the effect of cooling rate on the surface antigen, fast cooling by immersing vials in liquid nitrogen (LN) was also applied. The preservation procedure was similar to that mentioned above.

After thawing, the BCG cell surface antigen function was checked by enzyme immunoassay with a 96-well filter (Filter EIA). The experiment is similar to enzyme-linked immune-sorbent assay (ELISA). The experiment details are as below.

1) 100uL BCG cell suspension (cryopreserved and fresh control) was added to each microwell of the 96-well plate (BD Biosciences).
2) The cell suspensions in microwells were washed/flushed with 200uL PBS for 3 times.
3) 100uL primary antibody (6855-C and IgY-6855) solution (10ug/mL in PBS) was added into each well. Here the antibody 6855-C is the non-specific binding control antibody, and IgY-6855 is the antibody specific to BCG cells. Both antibodies were provided by Soelberg and Furlong Lab in the Department of Medicine-Division of Medical Genetics at University of Washington.
4) The plate was sealed with cover, put into incubator and incubated at 37 ℃ for 1 hour. The binding reaction between the antibody and cell surface antigen can be accelerated at this higher temperature.
5) 200uL PBS was added to wash each well. This washing step was repeated for 4 times.
6) 50uL secondary rabbit antibody (Rabbit anti-IgY-Horse radish Peroxidase (HRP) Conjugate, Thermo) (1:500 diluted in PBS) was added into each well.
7) The plate was sealed and incubated at 37 ℃ again for 1 hour.
8) Each well was washed with 200uL PBS twice, and then washed with 200uL PBS+0.1% Tween 20 once, and with 200uL PBS once again.
9) 100uL Thermo ABTS Substrate solution was added into each well. The plate was then incubated at room temperature for 5min.
10) Vacuum was applied to suck all the solution in each well through the filter to another plate.

11) The optical density of the solutions in each well was measured by spectroscopy at 405nm (Beckman Coulter InC, Indianapolis IN).

In order to precisely check the surface antigen function after cryopreservation, flow cytometry (BD Biosciences) was also applied to assess the signals. In this test, BCG cells in 7H9 were cryopreserved with Box-in-Box system (slow cooling rate) or immersing in liquid nitrogen, respectively.

Statistical analysis

The results are presented as average ± standard deviations. The statistical analysis was performed with a two-way ANOVA test for the comparison between different conditions. The level of significance was set as $p<0.05$.

5.1.3 Results

Temperature record and cooling rate during freezing

Typical temperature profiles in the cooling process were recorded for dummy samples in the BIB system, in liquid nitrogen (LN2), and in a -80 ℃ freezer directly, and the cooling rates were computed. In the BIB system, a slow cooling rate of -1 to -3.5 ℃/min was observed. When samples were immersed into LN2 directly, the cooling rate ranged between -100 and -400 ℃/min. For samples in a -80 ℃ freezer directly without BIB, the cooling rate ranged between -10 and -20 ℃/min. Under this condition, the cooling rate was variable and depended on the location of the samples and heat transfer situation inside the freezer.

Viability of BCG cells after freezing and thawing

CFU numbers were counted at various time points after plating. After incubating for two weeks, colonies started emerging, while after four weeks the CFU numbers reached stability. There was little or no additional colony formation between 4 and 8 weeks culture.

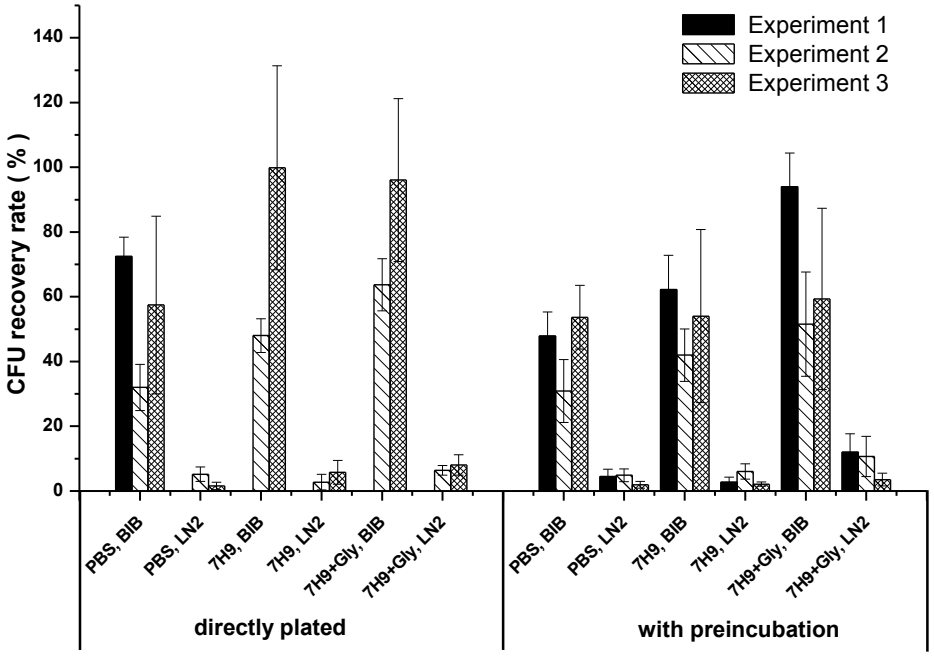

Figure 5-2 Microbiological culture results of cryopreserved and thawed BCG cells.

The CFU recovery rates compared to control samples are shown in Figure 5-2. (In the first experiment cells were cultured for three weeks and in the second and third experiments for four weeks). The results indicate that the cooling rate is one of the most critical factors for BCG cells to survive freezing and thawing. A slow cooling rate enabled about one order of magnitude greater CFU recovery than a fast cooling rate ($p<0.05$) in all freezing media tested. There was no significant difference between any of the three freezing media ($p=0.06\sim0.87$).

CFU counts of cryopreserved BCG with and without preincubation before plating are also shown in Figure 5-2. For cryopreserved BCG cells, preincubation did not significantly enhance the cells' recovery ($p=0.14\sim0.71$).

In conclusion, among the experimental conditions examined, only cooling rate exhibited a significant and consistent effect on BCG cryopreservation.

Live/Dead staining of BCG cells

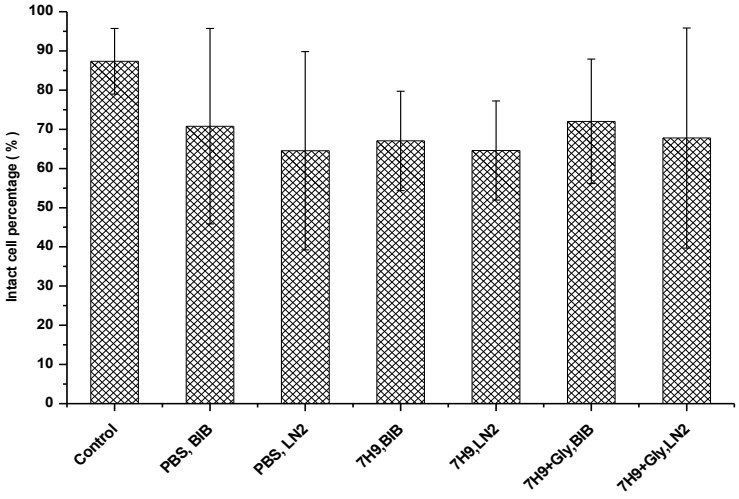

Figure 5-3 Intact BCG cell percentages after cryopreservation assessed by live/dead staining (mean±STD, n=14). Control: fresh cells.

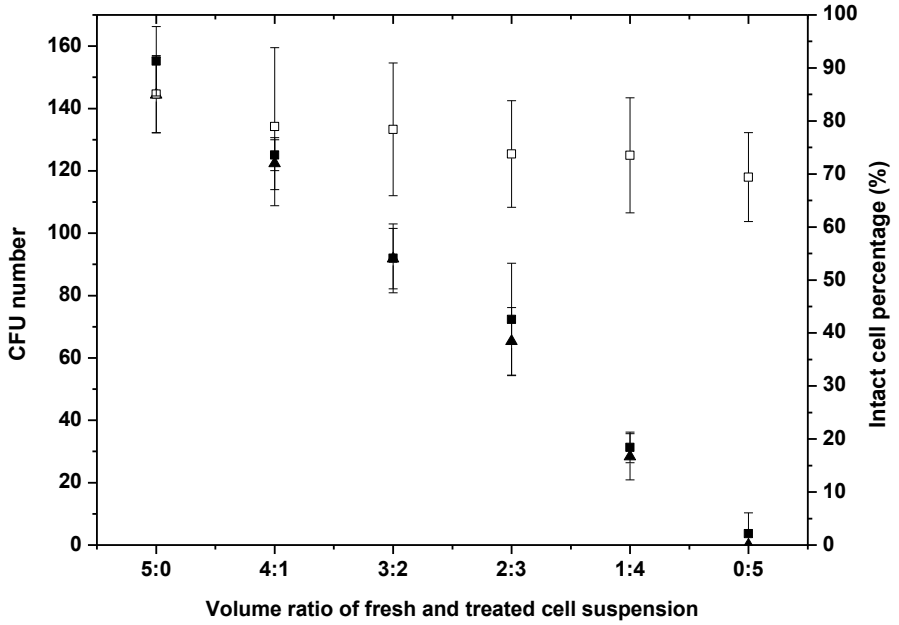

Figure 5-4 Correlation between live/dead staining and microbiological culturing results when applied to heat-treated (at 80 °C for 35 min) and cryo-killed (fast cooled in liquid nitrogen) BCG cells. (▲)CFU numbers for mixtures of fresh and heat-killed BCG cells ; (■)Intact cell percentage for mixtures of fresh and heat-treated BCG cells ; (□)Intact cell percentage for mixtures of fresh and cryo-treated BCG cells.

The BacLight Live/Dead staining kit, which differentially stains bacteria with intact vs. compromised cell envelopes, was used to assess cell envelope integrity of cryopreserved

cells. For all treatment groups, the percentage of intact cells after cryopreservation and thawing was evaluated with the BacLight live/dead staining kit (Figure 5-3). Among different freezing media and cooling rates, there was no significant difference in the percentage of intact ("live") cells ($p=0.14\sim0.99$). Compared to controls (fresh cells without cryopreservation), percentages of intact cells appeared high under all conditions, despite the sharply reduced viability (assessed by culture) of cells that were rapidly frozen in LN2.

The live/dead staining kit indirectly assesses viability in terms of cell envelope integrity. To validate the kit's performance on BCG cells, it was also applied to mixtures of fresh and heat-treated BCG cells and compared with the results of microbiological culturing. BCG cells were heated at 80 ℃ for 35 min (inactivated cells), and then the treated cell suspension was mixed with fresh (viable) cells. The two cell suspensions had the same cell concentrations (estimated by optical density) and were mixed with varying volume ratios of 0:5, 1:4, 2:3, 3:2, 4:1 and 5:0. The mixtures were divided into two groups. One was assessed by BacLight Live/Dead staining, and the other one was cultured on 7H10 agar. For microbiological culturing, each plate received 250 µL of cell suspension with a predicted starting concentration of 4000 CFU/mL (i.e. 1000 cells/plate, including both fresh and heat-treated). The CFU numbers were counted after culture for 28 days. As shown in Figure 5-4, live/dead staining yielded results that closely correlated with microbiological culturing results for heat-treated BCG cells. In contrast, a similar experiment of live/dead staining for the mixtures of fresh and cryo-killed BCG cells (fast cooled in LN2) was also conducted. However, the results did not show significant difference among the mixtures of fresh and cryo-killed cells with different volume ratios (0:5, 1:4, 2:3, 3:2, 4:1 and 5:0) (Figure 5-4).

Viability of M. tuberculosis H37Ra cells after cryopreservation in sputum

The CFU counting results of cryopreserved H37Ra cells in sputum are presented in Figure 5-5. The results show that treatment with NALC-NaOH, centrifugation, and freeze-thaw processing can result in viable cell loss. Comparison between Controls 1, 2 and 3, indicates that treatment with NALC-NaOH and centrifugation can each cause viable cell loss by about one decade. As the results of BCG cryopreservation in defined

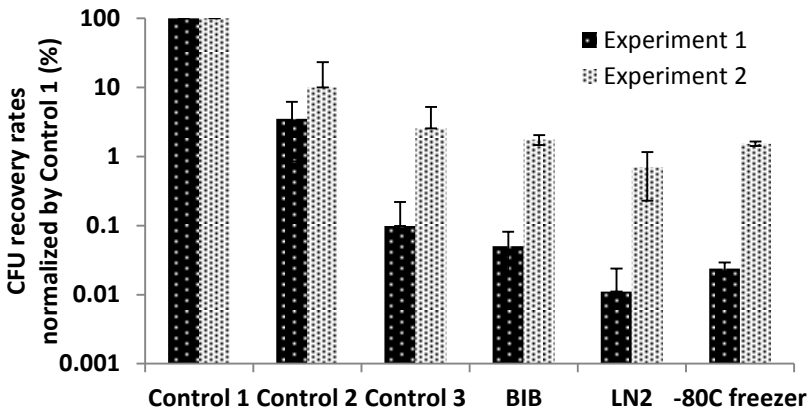

A

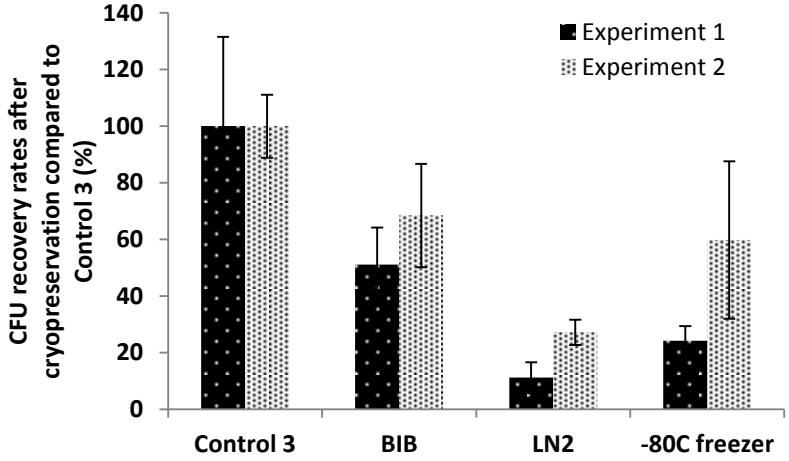

B

Figure 5-5 CFU results of cryopreserved and treated H37Ra cells. (A) CFU recovery rates (%) after cryopreservation, NALC-NaOH treatment and centrifugation, normalized by control 1. (B) Influence of cooling rate on CFU recovery rates (%) after cryopreservation, normalized by control 3. (n=6)

matrices, cooling rate was a critical factor for MTB cryopreservation in sputum. Fast cooling in LN2 reduced viability of MTB cells to a greater extent than slow cooling in BIB ($p<0.05$).

Direct freezing of MTB samples in a -80 ℃ freezer has been used in clinical trials and research due to its low cost and convenience. MTB cell recovery rate after cryopreservation was compared between direct freezing in BIB, and direct LN2

immersion. Of these conditions, the higher survival was observed when BIB was used ($p<0.05$). However, the difference between freezing in BIB and directly in the -80 ℃ freezer was significant in the 1st experiment ($p<0.05$), but not in the 2nd experiment ($p=0.73$). This might be due to the fact that freezing rates of samples in a -80 ℃ freezer vary significantly with location inside the freezer, freezer operation, and heat transfer conditions. The BIB system can provide a more reproducible slow-cooling environment for cryopreservation.

Surface antigen check of cryopreserved BCG cells

The function of surface antigen of BCG cells after cryopreservation was assessed and presented in Figure 5-6 A&B. After cryopreservation, the signal ratio of specific and non-specific antibodies decreased a little, but was still higher than 1. For comparison among different cryopreservation situations, cooling rate and solution matrix had little influence. This was inconsistent with the cell culturing results. It has been demonstrated that fast cooling rate (in LN2) killed many cells during freezing; however, in this part of study, there was no significant difference between fast and slow cooling rates. This implies that fast cooling may damage the cell viability of growing, but doesn't influence the surface antigen much. Once again, this indicates that we should be very careful when we talk about the term of cell "viability".

The signal ratio of specific and non-specific antibody was also not high even for fresh BCG cells. So, the antibody design may need further optimization, or more precise assessment methods should be applied. Therefore, flow cytometry was also applied to assess the cell surface antigen function.

The flow cytometry results are shown in Figure 5-7 A&B. Figure 5-7-A shows the absolute mean fluorescence intensity (MFI) signals, and B shows the signal ratio of MFI of specific 6855 antibody and non-specific antibody 6855-C. It's shown that the signal ratio of specific antibody and non-specific body decreased significantly after cryopreservation, but still may be acceptable for MTB diagnosis.

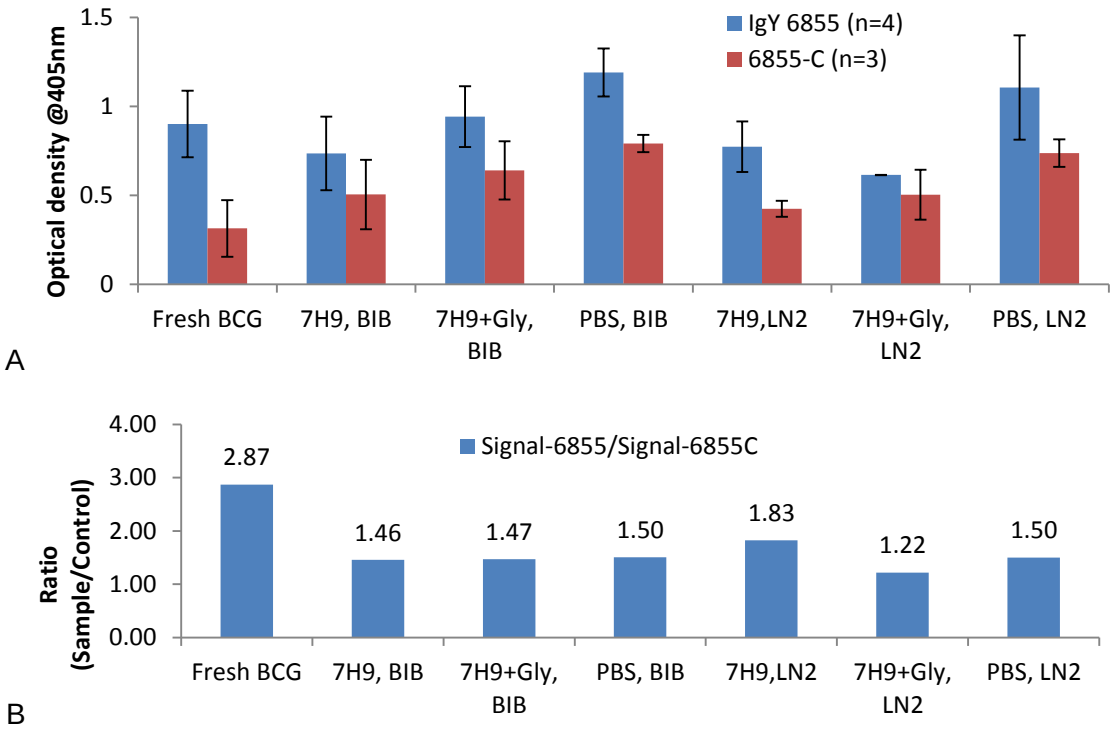

Figure 5-6 Function of BCG cell surface antigen after cryopreservation. (A) Absolute optical density; (B) normalized optical density (signal ratio of specific antibody and non-specific control antibody)

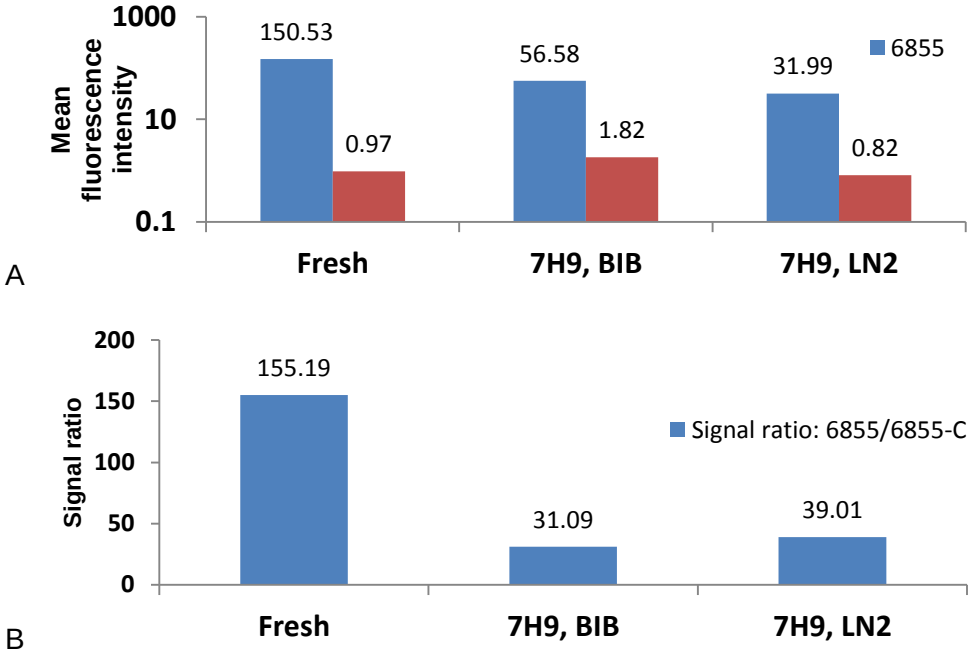

Figure 5-7 Flow cytometry results of IgY binding to cryopreserved BCG cells

5.1.4 Discussion

Currently there is no explicitly standardized protocol for the cryopreservation of clinical TB samples. Samples are often placed directly into a -80 ℃ freezer. However, this practice leads to variable cooling rates dependent on many factors including the sample container, volume of samples and heat transfer condition inside the freezer. Also the cooling rate in the freezer is not slow enough for MTB cryopreservation, as shown in the results. In this work, we employed a simple passive cooling device—"Box-in-Box", which enables a consistent and reproducible slow cooling rate. The BIB method is inexpensive, easy to operate, reliable, and delivers a reproducible cooling rate. The BIB device has been successfully used for cryopreservation of stem cells (91, 146, 147). The results in this paper showed that it delivers the highest recovery of MTB after cryopreservation.

In cryopreservation, according to the "two factors" hypothesis, cryoinjury to cells during freezing consists of "ice injury" and "solution injury" (30, 42). Many parameters might influence the cell recovery rate after freezing and thawing, e.g. cooling rate, the presence of cryoprotective agent (CPA), CPA addition and removal, and thawing process. The optimal procedure also depends on cell properties, such as the cell membrane permeability to water and CPA, the ratio of cell membrane area to cell volume (A/V), and osmotically inactive intracellular volume fraction (V_b). The results of this work showed that slow cooling is much better than fast cooling for cryopreservation of MTB cells. This may be explained by the properties of MTB cells. The *Mycobacterium* cell envelope has low permeability to most compounds including water ("permeability barrier"), because its outer leaflet is composed of giant saturated fatty acids with extremely low fluidity (148, 149). During freezing, extracellular water is frozen first, which causes the osmolality of extracellular solution to increase. Due to the imbalance of water chemical potential between the intra- and extracellular environments, intracellular water transports across the cell membrane and wall to the outside. This increases the osmolality of the intracellular solution, decreasing its freezing point, and hindering intracellular ice formation (IIF). For MTB cells, water may permeate across the cell envelope more slowly than the envelopes of other cell types. More time would be required to reach equilibrium between the inside and outside of the cells during freezing. Slow cooling

might mitigate the intracellular ice injury in MTB cryopreservation. Further research on MTB cell membrane and wall properties, including quantitative cell membrane permeability to water, would be helpful for cooling protocol optimization and interpretation.

The cryopreservation medium and specific CPAs are additional important factors that may influence the cell recovery. Generally CPAs such as glycerol are added before freezing to reduce intracellular ice formation. The standard formulation of 7H9 broth contains glycerol, but at a very low concentration (0.2%, v/v). Due to its widespread use in cryopreservation, glycerol was evaluated as the CPA in this study. However, the results revealed no significant benefits of glycerol ($p=0.11\sim0.87$). In the future, additional CPAs (such as dimethyl sulfoxide) may be tested.

Compared to PBS, 7H9 broth is a complex medium with differences in composition, pH, and osmolality. It contains many kinds of electrolytes, a low concentration of glycerol, and nutrients with pH=6.8 and osmolality of about 168mOsm/Kg H_2O. In contrast, PBS is pH=7.2~7.4, and its osmolality is about 290mOsm/Kg H_2O. The osmolality was measured by vapor pressure osmometer (Wescor INC., Logan, Utah). Despite these differences, we did not find out a significant difference between BCG cells cryopreserved in 7H9 and PBS ($p=0.11\sim0.84$). Compared to cooling rate, cryopreservation medium and CPA had limited impact. The results indicated that for convenience and simplicity, MTB cells could be cryopreserved well in 7H9, PBS, or possibly other media, as long as the cooling rate is slow (generally recovery rates >50%). This eliminates the steps of CPA addition and removal before and after cryopreservation, which add complexity and increase the risk of sample contamination.

When cells are exposed to stressful environments, e.g., cooling, heating, radiation, or desiccation, cellular functions may be impaired. It has been observed that for some cells, preincubation in broth or liquid medium for some time after exposure to the stress may help repair the injuries (140-143), however others doubt its effectiveness (150). In the present work, preincubation did not improve the recovery of cryopreserved BCG cells from cryoinjury.

The mechanism of cryoinjury during rapid cooling did not appear to involve severe damage to the cell envelope. By live/dead staining, rapidly cooled cell suspensions with low viability did not significantly differ from slowly cooled suspensions with high viability. The BacLight live/dead staining kit contains SYTO 9 and propidium iodide (PI). PI can penetrate only cells with compromised cell envelope integrity, while SYTO 9 can penetrate both intact cells and cells with compromised cell envelopes. Thus, intact cells emit green fluorescence while compromised cells emit red fluorescence under fluorescence microscopy, i.e., the live/dead staining kit indirectly assesses viability in terms of cell envelope integrity. After suboptimal (rapid) freezing and thawing, many BCG cells might retain intact walls and membranes, while sustaining enough intracellular injury to compromise their ability to grow. This contrasts with BCG cells heated at 80 ℃ for 35 minutes. For these heat-killed cells, live/dead staining and microbiological culture results correlated with each other, consistent with cellular inactivation mechanisms that include cell envelope damage. The commercially available BacLight live/dead staining kit was designed primarily for use on bacteria, but lacks enough information on efficacy when applied to MTB cells. It was previously reported that the staining pattern of the kit depends on the bacterium type, and even the way of treatment to the bacteria (such as heating, UV exposure), especially for cells in intermediate states between viable and inactivated states (151-153). Additional evaluation for the kit should be conducted for MTB viability assessment.

After cryopreservation, the BCG/MTB cell surface antigen function was decreased according to the results of filter plate and flow cytometry, but the function may be still acceptable for MTB diagnosis based on antigen-antibody binding. The inconsistence of cooling rate influence on cell growth capability and surface antigen implies that fast cooling can damage cell viability, but doesn't influence the cell surface antigen very much. This indicates that the term of cell "viability" should be used with extreme caution. In the next step, the design of more specific antibody should be further optimized. Furthermore, diagnosis of MTB with cryopreserved cells can be tested, such as with micro-tip immunoassay approach that was developed by Kim et al. (154).

5.1.5 Conclusions

Among the variables tested, cooling rate was the most critical factor for the cryopreservation of *Mycobacterium tuberculosis* complex cells. MTB complex cells were well cryopreserved in PBS buffer, Middlebrook 7H9 with and without added glycerol, or sputum if a slow cooling rate was applied. Preincubation of frozen/thawed BCG cells in 7H9 broth before culturing on solid 7H10 agar did not help the cells repair cryoinjury. Cell inactivation by fast cooling was not associated with a compromised cell envelope, as indicated by the results of microbiological culture and live/dead staining. After cryopreservation, the MTB cell surface antigen can still work for MTB diagnosis.

5.2 Freeze-drying and long-term preservation of MTB-IgY antibodies

5.2.1 Introduction

In the diagnosis, treatment, drug development and drug efficacy test of MTB disease, MTB specific antibodies play a very important role. For example, recently we developed a novel micro-tip immune sensor to diagnose MTB (154). The basic working principle is that first, micro-tips are functionalized with surface coating by layers of polyethyleneimine (PEI) (or poly-l-lysine), biotin-conjugated BSA, streptavidin, and biotin-conjugated capturing antibody specific to MTB complex cells; secondly, MTB cells are attracted to the tip surface and the cells are bound to the tip; thirdly, the tip surface is coated with detection fluorescence-antibody specific to the MTB complex cells; and finally, the tip can be analyzed by fluorescence signal intensity compared to negative control. In this approach, the function of the MTB specific antibodies is vital to successful diagnosis. In the future potential commercialization of this approach, antibodies should be provided to customers as necessary diagnosis kit supply. Therefore, successful and easy long-term preservation/transportation of the antibodies is very important.

Freeze-drying may be the best option for antibody storage. After freeze-drying, the residual moisture content (RMC) of the sample is low enough that any bio-reaction with the antibodies is suppressed or even stopped. The freeze-dried samples can be stored at room temperature, thus there is no need of equipment and power supply to provide cold-

chain during storage and transport. Furthermore, the weight of freeze-dried samples decreases dramatically.

However, after freezing and drying, the function of the antibodies may be impaired. In this part, freeze-drying will be applied to long-term preservation of MTB antibodies. After storage, the antibodies will be rehydrated and the function will be assessed. For freeze-drying, trehalose and dextran have been proved to be effective to prevent drying injuries (155-165). So, in this study, trehalose or dextran was added to antibody samples as lyophilization protective agent.

5.2.2 Materials and methods

5.2.2.1 Preparation of different lyophilization solutions

Four conditions of different lyophilization solutions (IgY in PBS only, PBS+trehalose with different concentrations, and PBS+trehalose+dextran) were tested. First, three stock solutions were prepared: 5% trehalose in PBS, 5% dextran in PBS, and 7.6 mg/mL IgY-fluorescence antibody in PBS. Then they were mixed with different procedures to make four different freeze-drying conditions as follows. They are marked as 1, 2, 3, and 4. The 2mL freeze-drying glass vials were used in this test. In each vial, 100uL solution was lyophilized. The details of preparation of lyophilization solutions for each vial are as follows:

1. 50uL IgY-fluorescence stock solution was mixed with 50uL PBS.
2. 50uL IgY-fluorescence stock solution was mixed with 50uL trehalose stock solution. So the final trehalose concentration was 2.5%.
3. 50uL IgY-fluorescence stock solution was mixed with 12.5uL trehalose stock solution and 37.5uL PBS. So the final trehalose concentration was 0.625%.
4. 50uL IgY-fluorescence stock solution was mixed with 25uL trehalose stock solution and 25uL dextran stock solution. So the final trehalose concentration and dextran concentration were both 1.25%.

In these four situations, the final concentration of IgY-fluorescence antibody in the lyophilization solutions was the same (3.8mg/mL).

5.2.2.2 Freeze drying of the samples

A delicate freeze-dryer (AdVantage EL. Virtis, Stone Ridge, NY) was used for this experiment. In this device, vacuum pressure and the shelf temperature can be controlled very precisely. First the vials containing 100uL solution in each one were put on the shelf. Then they were frozen and dried with the following protocol:

1. Freezing: The shelf temperature was ramped to -40 ℃, and then was held at -40 for 30min.
2. Primary drying: The primary drying was divided to a few steps as below. The vacuum pump kept running to precisely control the chamber pressure.
    a. T-shelf=-40C, vacuum pressure=200mTorr (266Pa), drying for 30min.
    b. T-shelf=-30C, vacuum pressure=200mTorr (266Pa), drying for 30min.
    c. T-shelf=-20C, vacuum pressure=200mTorr (266Pa), drying for 30min.
    d. T-shelf=-10C, vacuum pressure=200mTorr (266Pa), drying for 30min.
    e. T-shelf= 0C, vacuum pressure=200mTorr (266Pa), drying for 30min.
3. Secondary drying

    T-shelf= 10C, vacuum pressure=200mTorr (266Pa), drying for 30min.

The total lyophilization time was about 4 hours.

5.2.2.3 Storage of freeze-dried samples

When the freeze-drying procedure was done, the vials were sealed tightly and quickly with vial covers and Parafilm. Then the vials were put into two plastic bags. One bag was stored at room temperature, and the other one was stored in refrigerator. Desiccant was put in each bag to absorb moisture in the environment.

5.2.2.4 Rehydration and function assessment of the freeze-dried samples

Before tests, 100uL PBS was added to each vial to rehydrate the samples. After full rehydration, the function of the antibodies was tested with the Filter EIA method, which was similar to the procedure mentioned in the BCG cell surface antigen check. Briefly,

- 100 uL BCG suspensions (12 week growth) were added in each well (with the same cell populations) of a 96-well filter (0.45 micron) plate. Liquid passed the filter and BCG cells remained by applying vacuum.

- The cells were washed by flushing with 200uL PBS for three times to remove proteins in the cell suspension.
- 100 μL rehydrated IgY-fluorescence antibody solution (3.8mg/mL) was added to each well. Two controls were also prepared.
  - Positive control: IgY-Fluorescein Antibody (not frozen-dried)
  - Negative control: chicken pre-immune antibody (not for BCG)
- The samples were incubated with primary antibody for 1 hour at 37℃. Then vacuum was applied to remove liquid.
- The cells were washed by flushing with 200uL PBS four times to remove proteins in the cell suspension.
- 50uL secondary rabbit antibody (Rabbit anti-IgY-Horse radish Peroxidase (HRP) Conjugate, Thermo) (1:500 diluted in PBS) was added into each well.
- The samples were incubated at 37℃ for 1 hour to form 3 layers: BCG cells+IgY+rabbit anti-chicken IgY.
- The samples were washed with 200ul PBS twice, then with 200ul PBS+tween20 (0.1%) once to remove non-specific binding, then with 200ul PBS again.
- Thermo ABTS Substrate (stored in 4℃ refrigerator) was warmed up to room temperature. Then 100uL Thermo ABTS Substrate was added to each well. The samples were incubated for 10 min at room temperature, and then the liquid was filtered into receiver plate
- The receiver plate was put into spectrometer. The optical density was read at 405nm.

The function of the freeze-dried IgY-fluorescence antibodies were assessed after different storage times (1 week, 2 weeks, 3 weeks, 8 weeks, 34 weeks and 59 weeks.)

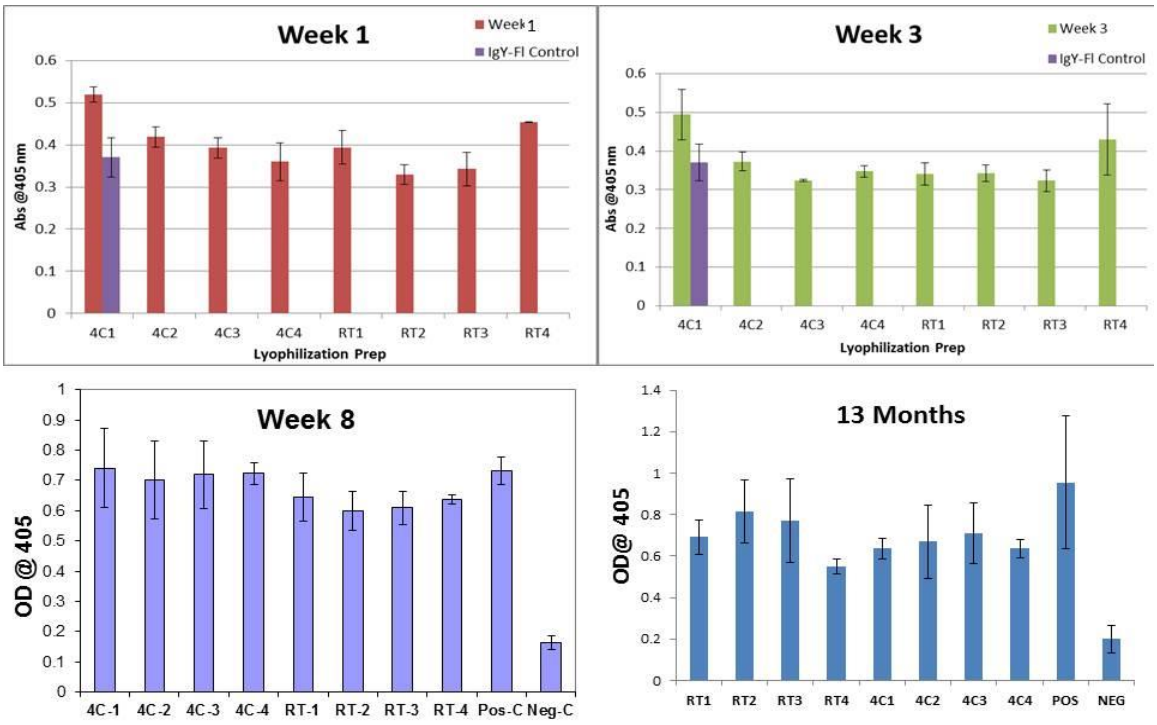

4 solution matrixes: 1) PBS; 2) 2.5% Trehalose; 3) 0.625% Trehalose; 4)1.25% Trehalose + 1.25%Dextran.
RT1: Sample freeze-dried in solution 1 and then stored at room temperature.
IgY-FL control: not lyophilized, stored at 4°C.

Figure 5-8 Function of freeze-dried BCG IgY antibody after storage for different times at different temperatures (n=6 for each data)

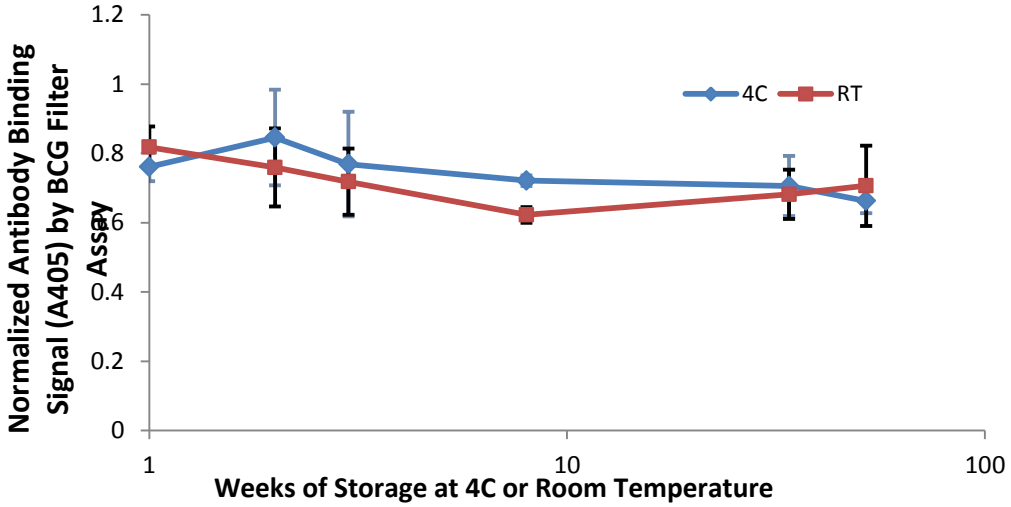

Figure 5-9 Normalized function of freeze-dried IgY antibody after storage for different times at different temperatures. (Mean value and standard error of the results of the four lyophilization solution matrixes.)

5.2.3 Results

After storage at different temperatures (4℃ and room temperature) for different storage durations (1 week, 2 weeks, 3 weeks, 8 weeks, 34 weeks and 59 weeks) , the samples were rehydrated and assessed for the antibody function. The results are shown in Figure 5-8. In the figure, each data was the mean value of the readings of 6 replicate wells. IgY-control (or named as positive control) was the function of non-freeze-dried IgY antibody (in liquid and stored at 4℃). Results show that freeze-drying didn't affect the antibody function much. Meanwhile, the different lyophilization solution matrixes (trehalose, dextran, PBS, etc.) didn't influence significantly. For simplicity, in the future the antibody can be just freeze-dried in PBS buffer.

In the results after week 8, the signal of negative control (antibody non-specific to BCG) was also assessed and showed. The much lower value indicates that the specificity of our antibody was still very high even after long-term storage.

In order to compare with the positive control, normalized signal (signal ratio of freeze-dried antibody and positive control) was calculated and shown in Figure 5-9. In this figure, the results of four lyophilization solution conditions were combined and averaged. So each data was the mean value of 24 readings (4 solution conditions x 6 replicate wells for each solution condition). Different storage temperatures (4℃ or room temperature) were also compared in Figure 5-9. With the increasing of storage duration, the function of freeze-dried IgY antibody decreased a little very gradually. The storage temperature (room temperature or 4°C) didn't influence the performance.

5.2.4 Discussion and conclusions

A successful and easy method for long-term preservation of MTB antibodies is a very important issue in MTB diagnosis and treatment. Lyophilization could be the best option for antibody preservation due to its advantages. In this part, the preliminary data showed that after freeze-drying and storage, the function of the antibody was preserved very well even after 13-month storage.

After long term storage the function of the antibody degraded very little and very slowly. The degradation trend was not influenced by the storage temperature. This may indicate that the residual moisture content (RMC) in the freeze dried samples was low enough.

Due to the lack of device, the RMC was not precisely measured in the tests. In the future, some methods, such as Karl-Fisher titration, can be applied to assess the RMC of the samples.

One limitation of the experimental design may be the “positive control” (IgY-control). In this study, IgY stored at 4 ℃ in liquid state was selected as positive control because the manufacturer of IgY claims that this antibody can be well preserved at 4 ℃ for two years, or in the freezer (-20 ℃) with glycerol for 10 years. However, this hypothesis needs to be proved. In the future, more work will be done to find the best control group.

Chapter 6 Conclusions and future work

6.1 Conclusions

Health is the eternal theme of human beings. To fight disease, innumerable efforts have been made from fundamental biological and pathological research to clinical trials by not only biologists and medical scientists, but also engineers. In the last few decades, cellular therapy has been proved effective or promising in the treatment of many diseases. The applications and commercial market size of cellular therapy have thrived and are predicted to keep growing fast in the near future. The increasing applications in cellular therapy cause greater challenges and needs in this field at the same time. One of the most significant challenges is the successful cryopreservation of biological samples (DNA/RNA, proteins, bio-fluids, cells, tissues and organs). Specifically speaking, the challenges include selection of the optimal cryoprotective agents (CPAs), addition of CPA, optimization of the cooling protocol, removal of CPAs after thawing, and designing related instruments. The optimal cryopreservation protocol of a bio-sample is determined by its inherent cryobiological characteristics. In this dissertation, a few novel approaches were developed to measure these fundamental properties and solve these challenges in cryopreservation.

In order to assess the cell membrane properties, two methods were studied in this dissertation. Firstly, cell membrane properties at room temperature were measured with the developed microfluidic perfusion channel. Human vaginal mucosal immune cells, including T cells and macrophages, were selected as the tested cells due to their emerging needs in the study of HIV. The cell membrane properties include the permeabilities to water and different CPAs. The results show that DMSO and propylene glycol have much higher membrane permeabilities than glycerol for both T cells and macrophages, which means that they might be the better options for the cryopreservation of T cells and macrophages. According to the cytotoxicity tests, they were further proved to be much better than glycerol. T cells were more susceptible to stresses than macrophages. The relatively low Lp values (cell membrane permeability to water) indicate that slow cooling rate could be suitable for the cryopreservation of mucosal immune cells. Some results of the preliminary freezing-thawing trials confirmed this prediction; however, at the same

time, they also indicated that further optimization is needed. For example, the cell viability was low before cryopreservation. Besides the optimization of cryopreservation protocols, the cell processing protocol including tissue digestion and cell sorting should be improved too.

Secondly, a “Slow-Fast-Fast-Slow” DSC cooling method was applied to measure the membrane properties at sub-zero temperatures of PBMC lymphocytes (T cells and monocytes). Intracellular ice formation temperatures of these cells were also assessed by relatively fast cooling (30 ℃/min). Based on the measurements, optimal cooling rates were predicted, which are very consistent with that applied in conventional SOPs. The results proved that this DSC method is a very good approach to measure cell membrane properties at sub-zero temperatures.

Combining the methods of microfluidic perfusion channel and DSC measurements, cell membrane properties at any temperature (above and below freezing point) can be obtained, which are very important for CPA selection, CPA addition and removal, and the prediction of optimal cryopreservation protocols.

In order to solve the problems in CPA addition/removal and cell concentration, a multifunctional cell processor based on active (instead of passive diffusion) mass transfer across semi-permeable hollow fibers was developed. A “dilution-filtration” working principle was proposed, which was proved to work effectively. This cell processor can achieve cell concentration (volume control of cell suspension), addition and removal of CPA media. A novel method based on electrical conductivity assessment was also proposed to achieve the on-line real-time monitoring of the residual CPA concentration during CPA removal process. Compared to other methods, this cell processing system is automatic (with low labor consumption), low-cost, easy to operate, safe for cells with decreased cell injuries, and has a closed fluid path system with low risk of contamination.

Cryopreservation of bacteria and freeze-drying of proteins were also discussed in this dissertation. MTB was selected in the study. Successful MTB cell preservation is vital for precise MTB diagnosis and drug development. Due to the small size of MTB cells and the cell wall/membrane configuration, it is challenging to measure the MTB cell

membrane permeabilities to water or CPAs precisely. Instead, many MTB cryopreservation trials were performed directly to optimize the preservation variables, such as CPA selection, cooling rate, and microbiological culturing with or without preincubation. The results showed that cooling rate was the most critical parameter for MTB cryopreservation. Slow cooling rate was necessary and sufficient for acceptable cryopreservation results, no matter whether CPA was added or not. Preincubation didn't help the cells overcome cryoinjuries. The MTB surface antigen can still work well after cryopreservation. In order to support the successful MTB diagnosis, the long-term preservation of MTB/BCG IgY antibodies was done. Freeze-drying was applied for the antibody preservation. The results showed that up to 13 months, the function of lyophilized IgY antibodies can be retained, regardless of the storage temperature of the dried samples (4 ℃ or room temperature).

6.2 Future work

We are currently unable to cryopreserve collected mucosal specimens without loss of viable immune cells and their functionality in HIV research and clinical trials, so a multi-center research team has been established to optimize the cryopreservation of mucosal immune cells and tissues for the use in assessing HIV vaccines and microbicides. Besides the Hladik and McElrath Group at Fred Hutchinson Cancer Research Center, the laboratories of Dr. Dezzutti at University of Pittsburgh and Dr. Shacklett at UC-Davis will provide us both the colorectal and the vaginal mucosal cells and their expertise in HIV research. DSC experiments will be done for these cells to measure the cell membrane properties at sub-zero temperatures. Combining them with those results at supra-zero temperature (Chapter 2), the cryopreservation of human mucosal immune cells will be optimized. The optimized protocol will be evaluated at all the participating laboratories. Their feedback will be applied to optimize the cryopreservation protocol further.

Tissue cryopreservation will be another main objective in our next plan. The DSC method will be applied to measure the fundamental cryobiological properties of human mucosal tissues based on the Krogh cylinder model. Combining the properties of the tissues and the cells in the tissues, cryopreservation of tissues will be optimized.

Besides cryopreservation, vitrification of tissues will be studied because of its ice-free advantage. In vitrification, the cryoprotective media, achieving fast cooling for vitrification and designing optimal warming technique to prevent de-vitrification will be the main challenges.

For the multi-functional cell processor, a few more steps will be taken to optimize the system setting and operation procedures for samples with smaller volumes. When the sample volume is small, such as $\leq$25mL, the portion of cells remaining in the tubing, hollow fibers and dialyzer ends is large, such that the cell population recovery rate could be low. In order to solve this problem, smaller dialyzers with much lower priming and dead filling volume may be helpful.

References

Literature Cited

1. McKernan, R., J. McNeish and D. Smith 2010. Pharma's developing interest in stem cells. Cell Stem Cell. 6, 517-520.

2. Trounson A, Thakar RG, Lomax G and Gibbons D 2011. Clinical trials for stem cell therapies. BMC Medicine. 9.

3. Evers, P. .2009.Advances in the stem cell industry. Business Insights,.

4. Mason C. and Manzotti E. 2010. Editorial: Regenerative medicine cell therapies: Numbers of units manufactured and patients treated between 1988 and 2010. Regenerative Med.Regenerative Medicine. 5, 307-313.

5. Young, R. R. 2012. Adult stem cell fact sheet. 7th annual stem cell summit. New York.

6. Shaw R. 2010. Industrializing stem cell production. BioProcess Int.BioProcess International. 8, 10-15.

7. POLGE C, SMITH AU and PARKES AS 1949. Revival of spermatozoa after vitrification and dehydration at low temperatures. Nature. 164.

8. Thomas, E. D., H.L. Lochte, W.C. Lu and J.W. Ferrebee 1957. Intravenous infusion of bone marrow in patients receiving radiation and chemotherapy. N. Engl. J. Med. 257, 491-496.

9. Akkök, Ç. A., M.R. Holte, J.M. Tangen, B. Østenstad and Ø. Bruserud 2009. Hematopoietic engraftment of dimethyl sulfoxide-depleted autologous peripheral blood progenitor cells. Transfusion. 49, 354-361.

10. Bakken, A. M., O. Bruserud and J.F. Abrahamsen 2003. No differences in colony formation of peripheral blood stem cells frozen with 5% or 10% dimethyl sulfoxide. Journal of Hematotherapy & Stem Cell Research. 12, 351-358.

11. Cordoba, R., R. Arrieta, A. Kerguelen and F. Hernandez-Navarro 2007. The occurrence of adverse events during the infusion of autologous peripheral blood stem cells is related to the number of granulocytes in the leukapheresis product. Bone Marrow Transplant. 40, 1063-1067.

12. Foïs, E., M. Desmartin, S. Benhamida, F. Xavier, V. Vanneaux, D. Rea, J.-. Fermand, B. Arnulf, N. Mounier, M. Ertault, J.-. Lotz, L. Galicier, E. Raffoux, M. Benbunan, J.-. Marolleau and J. Larghero 2007. Recovery, viability and clinical toxicity of thawed and washed haematopoietic progenitor cells: Analysis of 952 autologous peripheral blood stem cell transplantations. Bone Marrow Transplant. 40, 831-835.

13. Hidalgo, J., R. Krone, M. Rich, K. Blum, D. Adkins, M. Fan, R. Brown, S. Devine, T. Graubert, W. Blum, M. Tomasson, L. Goodnough, R. Vij, J. DiPersio and H. Khoury 2004. Supraventricular tachyarrhythmias after hematopoietic stem cell transplantation: Incidence, risk factors and outcomes. Bone Marrow Transplant. 34, 615-619.

14. Hirata Y., Kishino K., Onozaki F., Nakaki Y., Yamamoto C., Matsuyama T., Mori M., Ozawa K., Muroi K., Fujiwara S.-I., Sato K. and Ozaki K. 2011. Use of cryoprotectant-depleted allogeneic peripheral blood stem cells for transplantation. Hematology Hematology. 16, 221-224.

15. Donmez, A., M. Tombuloglu, A. Gungor, N. Soyer, G. Saydam and S. Cagirgan 2007. Clinical side effects during peripheral blood progenitor cell infusion. Transfusion Apheresis Sci. 36, 95-101.

16. Otrock Z.K., Beydoun A., Barada W.M., Masroujeh R., Bazarbachi A. and Hourani R. 2008. Transient global amnesia associated with the infusion of DMSO-cryopreserved autologous peripheral blood stem cells. Haematologica Haematologica. 93, e36-e37.

17. Junior, A. M., C.A. Arrais, R. Saboya, R.D. Velasques, P.L. Junqueira and F.L. Dulley 2008. Neurotoxicity associated with dimethylsulfoxide-preserved hematopoietic progenitor cell infusion. Bone Marrow Transplant. 41, 95-96.

18. Hentschke, S., M. Hentschke, K. Hummel, H.J. Salwender, D. Braumann and A. Stang 2006. Bilateral thalamic infarction after reinfusion of DMSO-preserved autologous stem-cells. Leuk. Lymphoma. 47, 2418-2420.

19. Mueller, L. P., S. Theurich, M. Christopeit, W. Grothe, A. Muetherig, T. Weber, S. Guenther and G. Behre 2007. Neurotoxicity upon infusion of dimethylsulfoxide-cryopreserved peripheral blood stem cells in patients with and without pre-existing cerebral disease. Eur J Haematol European Journal of Haematology. 78, 527-531.

20. Calmels, B., P. Houze, J. Hengesse, T. Ducrot, C. Malenfant and C. Chabannon 2003. Preclinical evaluation of an automated closed fluid management device: Cytomate™, for washing out DMSO from hematopoietic stem cell grafts after thawing. Bone Marrow Transplant. 31, 823-828.

21. Martin-Henao, G. A., P.M. Resano, J.M.S. Villegas, P.P. Manero, J.M. Sanchez, M.P. Bosch, A.E. Codins, M.S. Bruguera, L.R. Infante, A.P. Oyarzabal, R.N. Soldevila, D.C. Caiz, L.M. Bosch, E.C. Barbeta and J.R.G. Ronda 2010. Adverse reactions during transfusion of thawed haematopoietic progenitor cells from apheresis are closely related to the number of granulocyte cells in the leukapheresis product. Vox Sang. 99, 267-273.

22. Schlegel, P. G., M. Wölfl, J. Schick, B. Winkler and M. Eyrich 2009. Transient loss of consciousness in pediatric recipients of dimethylsulfoxide (DMSO)-cryopreserved peripheral blood stem cells independent of morphine co-medication. Haematologica. 94, 1473-1475.

23. Kersting, S. and L.F. Verdonck 2007. Stem cell transplantation nephropathy: A report of six cases. Biology of Blood and Marrow Transplantation. 13, 638-643.

24. Konuma, T., J. Ooi, S. Takahashi, A. Tomonari, N. Tsukada, T. Kobayashi, A. Sato, S. Kato, S. Kasahara, Y. Ebihara, T. Nagamura-Inoue, K. Tsuji, A. Tojo and S. Asano 2008. Cardiovascular toxicity of cryopreserved cord blood cell infusion. Bone Marrow Transplant. 41, 861-865.

25. Petropoulou, A. D., R. Bellochine, F. Norol, J. Marie and B. Rio 2007. Coronary artery spasm after infusion of cryopreserved cord blood cells. Bone Marrow Transplant. 40, 397-398.

26. Sahin, F., U.O. Turk, F. Yargucu, A. Donmez and S. Cagirgan 2006. Hypothermia during the infusion of cryopreserved autologous peripheral stem cell causes electrocardiographical changes: Report of two cases. Am. J. Hematol. 81, 627-630.

27. Ruiz-Delgado, G. J., C. Manc ás-Guerra, E.L. Tamez-G ómez, L.N. Rodr íguez-Romo, A. L ópez-Otero, A. Hern ández-Arizpe, D. G ómez-Almaguer and G.J. Ruiz-Arg üelles 2009. Dimethyl sulfoxide-induced toxicity in cord blood stem cell transplantation: Report of three cases and review of the literature. Acta Haematol. 122, 1-5.

28. Del Mastro, L., M. Venturini, C. Viscoli, M. Bergaglio, A. Signorini, C. Bighin, G. Bertell, C. Semino, G. Pietra, S. Bertoglio, M. Sertoli, A. Lambiase, R. Rosso and G. Melioli 2001. Intensified chemotherapy supported by DMSO-free peripheral blood progenitor cells in breast cancer patients. Annals of Oncology. 12, 505-508.

29. Zenh äusern R, Tobler A, Leoncini L, Hess OM and Ferrari P 2000. Fatal cardiac arrhythmia after infusion of dimethyl sulfoxide-cryopreserved hematopoietic stem cells in a patient with severe primary cardiac amyloidosis and end-stage renal failure. Ann. Hematol. 79, 523-526.

30. Mazur P 1977. The role of intracellular freezing in death of cells cooled at supraoptimal rates. Cryobiology. 14, 251-272.

31. Mazur, P., 1970. Cryobiology: The freezing of biological systems. Science. 168, 939-949.

32. Scholander, P. F., L. van Dam, J.W. Kanwisher, H.T. Hammel and M.S. Gordon 1957. Supercooling and osmoregulation in arctic fish. Journal of Cellular and Comparative Physiology. 49, 5-24.

33. DeVries AL and Wohlschlag DE 1969. Freezing resistance in some antarctic fishes. Science (New York, N.Y.). 163, 1073-5.

34. Caldwell AD, Bye PG and Briggs MH 1967. Side effects of dimethyl sulphoxide. Nature. 215.

35. David, N. A. 1972. The pharmacology of dimethyl Sulfoxide . Annual Review of Pharmacology. 12, 353-374.

36. WILLSON JE, BROWN DE and TIMMENS EK 1965. A TOXICOLOGIC STUDY OF DIMETHYL SULFOXIDE. Toxicol. Appl. Pharmacol. 7, 104-12.

37. KHARASCH, N. and B. THYAGARAJAN 1983. Structural basis for biological-activities of dimethylsulfoxide. Ann. N. Y. Acad. Sci. 411, 391-402.

38. Santos, N. C., J. Figueira-Coelho, J. Martins-Silva and C. Saldanha 2003. Multidisciplinary utilization of dimethyl sulfoxide: Pharmacological, cellular, and molecular aspects. Biochem. Pharmacol. 65, 1035-1041.

39. Cavas, M., D. Beltrán and J.F. Navarro 2005. Behavioural effects of dimethyl sulfoxide (DMSO): Changes in sleep architecture in rats. Toxicology Letters Toxicology Letters. 157, 221-232.

40. Qi W, Ding D and Salvi RJ 2008. Cytotoxic effects of dimethyl sulphoxide (DMSO) on cochlear organotypic cultures. Hear. Res. 236, 1-2.

41. LOVELOCK JE and BISHOP MW 1959. Prevention of freezing damage to living cells by dimethyl sulphoxide. Nature. 183, 1394-5.

42. Mazur P, 1984. Freezing of living cells: Mechanisms and implications. Am. J. Physiol. 247, 125-42.

43. Fowler, A. and M. Toner 2005. Cryo-injury and biopreservation. Ann. NY Acad. Sci. 1066, 119-135.

44. Aita, K., H. Irie, Y. Tanuma, S. Toida, Y. Okuma, S. Mori and J. Shiga 2005. Apoptosis in murine lymphoid organs following intraperitoneal administration of dimethyl sulfoxide (DMSO). Exp. Mol. Pathol. 79, 265-271.

45. Pal R., Bhonde R., Mamidi M.K. and Das A.K. 2012. Diverse effects of dimethyl sulfoxide (DMSO) on the differentiation potential of human embryonic stem cells. Arch.Toxicol.Archives of Toxicology. 86, 651-661.

46. Lin, C., C. Kalunta, F. Chen, T. Nguyen, J. Kaptein and P. Lad 1995. Dimethyl sulfoxide suppresses apoptosis in burkitt's lymphoma cells. Exp. Cell Res. 216, 403-410.

47. Ji, L., J. de Pablo and S. Palecek 2004. Cryopreservation of adherent human embryonic stem cells. Biotechnol. Bioeng. 88, 299-312.

48. Hegner, B., M. Weber, D. Dragun and E. Schulze-Lohoff 2005. Differential regulation of smooth muscle markers in human bone marrow-derived mesenchymal stem cells. J. Hypertens. 23, 1191-1202.

49. Zyuz'kov, G. N., L.A. Gur'yantseva, E.V. Simanina, V.V. Zhdanov, A.M. Dygai and E.D. Goldberg 2007. Effect of dimethylsulfoxide on the functions of mesenchymal and hemopoietic precursors. Bull. Exp. Biol. Med. 143, 535-538.

50. Ozdemir, E., K. Akgedik, S. Akdogan and E. Kansu 2008. The lollipop with strawberry aroma may be promising in reduction of infusion-related nausea and vomiting during the infusion of cryopreserved peripheral blood stem cells. Biology of Blood and Marrow Transplantation. 14, 1425-1428.

51. Kessinger A and Armitage JO 1991. The evolving role of autologous peripheral stem cell transplantation following high-dose therapy for malignancies. Blood. 77, 211-3.

52. Stroncek, D., S. Fautsch, L. Lasky, D. Hurd, N. Ramsay and J. McCullough 1991. Adverse reactions in patients transfused with cryopreserved marrow. Transfusion Transfusion. 31, 521-526.

53. Zambelli, A., G. Poggi, G. Da Prada, P. Pedrazzoli, A. Cuomo, D. Miotti, C. Perotti, P. Preti and G. Della Cuna 1998. Clinical toxicity of cryopreserved circulating progenitor cells infusion. Anticancer Res. 18, 4705-4708.

54. Windrum, P. and T.C.M. Morris 2003. Severe neurotoxicity because of dimethyl sulphoxide following peripheral blood stem cell transplantation. Bone Marrow Transplant. 31, 315.

55. Hanslick, J. L., K. Lau, K.K. Noguchi, J.W. Olney, C.F. Zorumski, S. Mennerick and N.B. Farber 2009. Dimethyl sulfoxide (DMSO) produces widespread apoptosis in the developing central nervous system. Neurobiol. Dis. 34, 1-10.

56. Authier N, Dupuis E, Kwasiborski A, Eschalier A and Coudoré F 2002. Behavioural assessment of dimethylsulfoxide neurotoxicity in rats. Toxicol. Lett. 132, 117-21.

57. Cavaletti G, Oggioni N, Sala F, Pezzoni G, Cavalletti E, Marmiroli P, Petruccioli MG, Frattola L and Tredici G 2000. Effect on the peripheral nervous system of systemically administered dimethylsulfoxide in the rat: A neurophysiological and pathological study. Toxicol. Lett. 118, 1-2.

58. Topacoglu H, Karcioglu O, Ozsarac M, Oray D, Niyazi Ozucelik D and Tuncok Y 2004. Massive intracranial hemorrhage associated with the ingestion of dimethyl sulfoxide. Vet. Hum. Toxicol. 46, 138-40.

59. Chaloupka JC, Huddle DC, Alderman J, Fink S, Hammond R and Vinters HV 1999. A reexamination of the angiotoxicity of superselective injection of DMSO in the swine rete embolization model. AJNR.American Journal of Neuroradiology. 20, 401-10.

60. Gao DY, Liu J, Liu C, McGann LE, Watson PF, Kleinhans FW, Mazur P, Critser ES and Critser JK 1995. Prevention of osmotic injury to human spermatozoa during addition and removal of glycerol. Hum. Reprod. 10, 1109-22.

61. Zhou, X., F. Gao, Z. Shu, J. Chung, S. Heimfeld and D. Gao 2010. Theoretical and experimental analyses of optimal experimental design for determination of hydraulic conductivity of cell membrane. Biopreserv. Biobank. 8, 147-152.

62. Martino, M., F. Morabito, G. Messina, G. Irrera, G. Pucci and P. Iacopino 1996. Fractionated infusions of cryopreserved stem cells may prevent DMSO-induced major cardiac complications in graft recipients. Haematologica. 81, 59-61.

63. GARAVENTA, A., F. PORTA, R. RONDELLI, G. DINI, G. MELONI, F. BONETTI, C. UDERZO, A. DEMANZINI, R. MINIERO, F. BRUTTI, P. COLLESELLI, S. BAGNULO, N. SANTORO and P. PAOLUCCI 1992. Early deaths in children after bmt. Bone Marrow Transplant. 10, 419-423.

64. THOME, S., J. CRAZE and C. MITCHELL 1994. Dimethylsulfoxide-induced serum hyperosmolality after cryopreserved stem-cell graft. Lancet. 344, 1431-1432.

65. Kurtzberg J, Laughlin M, Graham ML, Smith C, Olson JF, Halperin EC, Ciocci G, Carrier C, Stevens CE and Rubinstein P 1996. Placental blood as a source of hematopoietic stem cells for transplantation into unrelated recipients. N. Engl. J. Med. 335, 157-66.

66. Lee, S., S. Kim, H. Kim, E.J. Baek, H. Jin, J. Kim and H.O. Kim 2008. Post-thaw viable $CD34^{+}$ cell count is a valuable predictor of haematopoietic stem cell engraftment in autologous peripheral blood stem cell transplantation. Vox Sang. 94, 146-152.

67. Rodr ́guez, L., B. Velasco, J. Garc ́a and G.Á. Mart ́n-Henao 2005. Evaluation of an automated cell processing device to reduce the dimethyl sulfoxide from hematopoietic grafts after thawing. Transfusion. 45, 1391-1397.

68. Ferrucci, P. F., A. Martinoni, E. Cocorocchio, M. Civelli, S. Cinieri, D. Cardinale, F.A. Peccatori, G. Lamantia, A. Agazzi, C. Corsini, F. Tealdo, C. Fiorentini, C.M. Cipolla and G. Martinelli 2000. Evaluation of acute toxicities associated with autologous peripheral blood progenitor cell reinfusion in patients undergoing high-dose chemotherapy. Bone Marrow Transplant. 25, 173-177.

69. Shpall, E., C. LeMaistre, K. Holland, E. Ball, R. Jones, R. Saral, C. Jacobs, S. Heimfeld, R. Berenson and R. Champlin 1997. A prospective randomized trial of buffy coat versus CD34-selected autologous bone marrow support in high-risk breast cancer patients receiving high-dose chemotherapy. Blood. 90, 4313-4320.

70. Rowley, S., Z. Feng, L. Chen, L. Holmberg, S. Heimfeld, B. MacLeod and W. Bensinger 2003. A randomized phase III clinical trial of autologous blood stem cell transplantation comparing cryopreservation using dimethylsulfoxide vs dimethylsulfoxide with hydroxyethylstarch. Bone Marrow Transplant. 31, 1043-1051.

71. Ding, W., X. Zhou, S. Heimfeld, J. Reems and D. Gao 2010. A steady-state mass transfer model of removing CPAs from cryopreserved blood with hollow fiber modules. J. Biomech. Eng. 132, p.011002.

72. Ding, W., J. Yu, E. Woods, S. Heimfeld and D. Gao 2007. Simulation of removing permeable cryoprotective agents from cryopreserved blood with hollow fiber modules. J. Membr. Sci. 288, 85-93.

73. Glass, K. K. F., E.K. Longmire and A. Hubel 2008. Optimization of a microfluidic device for diffusion-based extraction of DMSO from a cell suspension. Int. J. Heat Mass Transfer. 51, 5749-5757.

74. Fleming KK, Longmire EK and Hubel A 2007. Numerical characterization of diffusion-based extraction in cell-laden flow through a microfluidic channel. J. Biomech. Eng. 129, 703-11.

75. Http://www.who.int/topics/hiv_aids/en/. *http://www.who.int/topics/hiv_aids/en/*.

76. McElrath, M. J. and B.F. Haynes 2010. Induction of immunity to human immunodeficiency virus type-1 by vaccination. Immunity. 33, 542-554.

77. Buchbinder, S. P., D.V. Mehrotra, A. Duerr, D.W. Fitzgerald, R. Mogg, D. Li, P.B. Gilbert, J.R. Lama, M. Marmor, C. del Rio, M.J. McElrath, D.R. Casimiro, K.M. Gottesdiener, J.A. Chodakewitz, L. Corey and M.N. Robertson 2008. Efficacy assessment of a cell-mediated immunity HIV-1 vaccine (the step study): A double-blind, randomised, placebo-controlled, test-of-concept trial. Lancet. 372, 1881-1893.

78. McElrath, M. J., S.C. De Rosa, Z. Moodie, S. Dubey, L. Kierstead, H. Janes, O.D. Defawe, D.K. Carter, J. Hural, R. Akondy, S.P. Buchbinder, M.N. Robertson, D.V. Mehrotra, S.G. Self, L. Corey, J.W. Shiver and D.R. Casimiro 2008. HIV-1 vaccine-induced immunity in the test-of-concept step study: A case-cohort analysis. Lancet. 372, 1894-1905.

79. Rerks-Ngarm, S., P. Pitisuttithum, S. Nitayaphan, J. Kaewkungwal, J. Chiu, R. Paris, N. Premsri, C. Namwat, M. de Souza, E. Adams, M. Benenson, S. Gurunathan, J.

Tartaglia, J.G. McNeil, D.P. Francis, D. Stablein, D.L. Birx, S. Chunsuttiwat, C. Khamboonruang, P. Thongcharoen, M.L. Robb, N.L. Michael, P. Kunasol and J.H. Kim 2009. Vaccination with ALVAC and AIDSVAX to prevent HIV-1 infection in thailand. New England Journal of Medicine. 361, 2209-2220.

80. Hladik, F. and M.J. McElrath 2008. Setting the stage: Host invasion by HIV. Nature Reviews Immunology. 8, 447-457.

81. Chen, H., J.J.P. Purtteman, S. Heimfeld, A. Folch and D. Gao 2007. Development of a microfluidic device for determination of cell osmotic behavior and membrane transport properties. Cryobiology. 55, 200-209.

82. Chen, H. 2009. Fundamental study of cell cryopreservation. PH.D thesis. University of Washington, Seattle.

83. Davson, H.,andJ. F. Danielli 1970. The permeability of natural membranes, Cambridge University Press, Cambridge, U.K.

84. McGann, L. E., M. Stevenson, K. Muldrew and N. Schachar 1988. Kinetics of osmotic water movement in chondrocytes isolated from articular cartilage and applications to cryopreservation. Journal of Orthopaedic Research. 6, 109-115.

85. Gao DY, McGrath JJ, Tao J, Benson CT, Critser ES and Critser JK 1994. Membrane transport properties of mammalian oocytes: A micropipette perfusion technique. J. Reprod. Fertil. 102, 385-392.

86. McGrath JJ 1985. A microscope diffusion chamber for the determination of the equilibrium and non-equilibrium osmotic response of individual cells. J. Microsc. 139, 249-263.

87. McGrath JJ 1997. Quantitative measurement of cell membrane transport: Technology and applications. Cryobiology. 34, 315-334.

88. Leibo SP 1980. Water permeability and its activation energy of fertilized and unfertilized mouse ova. J. Membr. Biol. 53, 179-188.

89. Kleinhans FW 1998. Membrane permeability modeling: Kedem-katchalsky vs a two-parameter formalism. Cryobiology. 37, 271-289.

90. Jacobs, M. H. 1933. The simultaneous measurement of cell permeability to water and to dissolved substances. Journal of Cellular and Comparative Physiology. 2, 427-444.

91. Shu ZQ, Kang XJ, Chen HH, Zhou XM, Purtteman J, Yadock D, Heimfeld S and Gao DY 2010. Development of a reliable low-cost controlled cooling rate instrument for the cryopreservation of hematopoietic stem cells. Cytotherapy. 12, 161-169.

92. HUNTER, J., A. BERNARD, B. FULLER, J. MCGRATH and R. SHAW 1992. Measurements of the membrane water permeability (lp) and its temperature-dependence (activation-energy) in human fresh and failed-to-fertilize oocytes and mouse oocyte. Cryobiology. 29, 240-249.

93. GAO, D., J. MCGRATH, J. TAO, C. BENSON, E. CRITSER and J. CRITSER 1994. Membrane-transport properties of mammalian oocytes - a micropipette perfusion technique. Journal of Reproduction and Fertility. 102, 385-392.

94. Gao DY, Benson CT, Liu C, McGrath JJ, Critser ES,Critser JK, 1996. Development of a novel microperfusion chamber for determination of cell membrane transport properties. Biophys. J. 71, 443-50.

95. Takamatsu, H., Y. Komori, S. Zawlodzka and M. Fujii 2004. Quantitative examination of a perfusion microscope for the study of osmotic response of cells. Journal of Biomechanical Engineering-Transactions of the ASME. 126, 402-409.

96. Chen, H., H. Shen, S. Heimfeld, K.K. Tran, J. Reems, A. Folch and D. Gao 2008. A microfluidic study of mouse dendritic cell membrane transport properties of water and cryoprotectants. International Journal of Heat and Mass Transfer. 51, 5687-5694.

97. Tseng, H., S. Sun, Z. Shu, W. Ding, J. Reems and D. Gao 2011. A microfluidic study of megakaryocytes membrane transport properties to water and dimethyl sulfoxide at suprazero and subzero temperatures. Biopreservation and Biobanking. 9, 355-362.

98. Devireddy, Ramachandra V., Raha, Debopam, Bischof,John C., 1998. Measurement of water transport during freezing in cell suspensions using a differential scanning calorimeter. Cryobiology. 36, 124-155.

99. Luo D, Han X, He L, Cui X, Cheng S, Lu C, Liu J and Gao D 2002. A modified differential scanning calorimetry for determination of cell volumetric change during the freezing process. Cryo Letters. 23, 229-236.

100. Han, X., D. Luo, X. Cui, S. Heimfeld and D. Gao 2007. A modified differential scanning calorimetry method for determining water transport properties in biological cells during the freezing process. Cell Preserv. Technol. 5, 25-32.

101. Mazur, P. 1963. Kinetics of water loss from cells at subzero temperatures and the likelihood of intracellular freezing. The Journal of General Physiology. 47, 347-369.

102. Toner, M., E.G. Cravalho and M. Karel 1990. Thermodynamics and kinetics of intracellular ice formation during freezing of biological cells. J. Appl. Phys. 67, 1582-1593.

103. Toner M, Cravalho EG,Karel M, 1993. Cellular response of mouse oocytes to freezing stress: Prediction of intracellular ice formation. J. Biomech. Eng. 115, 169-74.

104. Devireddy, R. and J. Bischof 1998. Measurement of water transport during freezing in mammalian liver tissue: Part II - the use of differential scanning calorimetry. J. Biomech. Eng. -Trans. ASME. 120, 559-569.

105. Cross-network PBMC processing SOP. *https://www.hanc.info/labs/Documents/HANC-LAB-0001_v4.0_2011-10-03_PBMC%20SOP.pdf*.

106. Devireddy, R., P. Barratt, K. Storey and J. Bischof 1999. Liver freezing response of the freeze-tolerant wood frog, rana sylvatica, in the presence and absence of glucose I. experimental measurements. Cryobiology. 38, 310-326.

107. Devireddy, R., P. Barratt, K. Storey and J. Bischof 1999. Liver freezing response of the freeze-tolerant wood frog, rana sylvatica, in the presence and absence of glucose II. mathematical modeling. Cryobiology. 38, 327-338.

108. Devireddy, R., D. Smith and J. Bischof 1999. Mass transfer during freezing in rat prostate tumor tissue. AIChE J. 45, 639-654.

109. Bischof, J. 2000. Quantitative measurement and prediction of biophysical response during freezing in tissues. Annu. Rev. Biomed. Eng. 2, 257-288.

110. Devireddy, R., D. Swanlund, T. Olin, W. Vincente, M. Troedsson, J. Bischof and K. Roberts 2002. Cryopreservation of equine sperm: Optimal cooling rates in the presence and absence of cryoprotective agents determined using differential scanning calorimetry. Biol. Reprod. 66, 222-231.

111. Devireddy, R., D. Swanlund, K. Roberts, J. Pryor and J. Bischof 2000. The effect of extracellular ice and cryoprotective agents on the water permeability parameters of human sperm plasma membrane during freezing. Human Reproduction. 15, 1125-1135.

112. ROWE, A., E. EYSTER and A. KELLNER 1968. Liquid nitrogen preservation of red blood cells for transfusion - a low glycerol-rapid freeze procedure. Cryobiology. 5, 119-&.

113. MERYMAN, H. and HORNBLOW.M 1972. Method for freezing and washing red blood-cells using a high glycerol concentration. Transfusion. 12, 145-&.

114. VALERI, C. 1975. Simplification of methods for adding and removing glycerol during freeze-preservation of human red blood-cells with high or low glycerol methods - biochemical modification prior to freezing. Transfusion. 15, 195-218.

115. MERYMAN, H. and M. HORNBLOWER 1977. Simplified procedure for deglycerolizing red blood-cells frozen in a high glycerol concentration. Transfusion. 17, 438-442.

116. Valeri, C., G. Ragno, L. Pivacek and E. O'Neill 2001. In vivo survival of apheresis RBCs, frozen with 40-percent (wt/vol) glycerol, deglycerolized in the ACP 215, and stored at 4 degrees C in AS-3 for up to 21 days. Transfusion. 41, 928-932.

117. Arnaud, F., E. Kapnik and H. Meryman 2003. Use of hollow fiber membrane filtration for the removal of DMSO from platelet concentrates. Platelets. 14, 131-137.

118. Castino, F. and S. Wickramasinghe 1996. Washing frozen red blood cell concentrates using hollow fibres. J. Membr. Sci. 110, 169-180.

119. Mata, C., E.K. Longmire, D.H. McKenna, K.K. Glass and A. Hubel 2008. Experimental study of diffusion-based extraction from a cell suspension. Microfluidics and Nanofluidics. 5, 529-540.

120. Rodriguez, L., C. Azqueta, S. Azzalin, J. Garcia and S. Querol 2004. Washing of cord blood grafts after thawing: High cell recovery using an automated and closed system. Vox Sang. 87, 165-172.

121. Perotti, C. G., C.D. Fante, G. Viarengo, P. Papa, L. Rocchi, P. Bergamaschi, L. Bellotti, A. Marchesi and L. Salvaneschi 2004. A new automated cell washer device for thawed cord blood units. Transfusion Transfusion. 44, 900-906.

122. RUBINSTEIN, P., L. DOBRILA, R. ROSENFIELD, J. ADAMSON, G. MIGLIACCIO, A. MIGLIACCIO, P. TAYLOR and C. STEVENS 1995. Processing and cryopreservation of placental umbilical-cord blood for unrelated bone-marrow reconstitution. Proc. Natl. Acad. Sci. U. S. A. 92, 10119-10122.

123. Decot, V., P. Houze, J.-. Stoltz and D. Bensoussan 2009. Quantification of residual DiMethylSulfoxide after washing cryopreserved stem cells and thawing tissue grafts. Biomed. Mater. Eng. 19, 293-300.

124. Houzé P, Dal Cortivo L, Anselme M, Bousquet B and Gourmel B 1999. Quantification of residual dimethyl sulfoxide in supernatants of haematopoietic stem cells by capillary zone electrophoresis. Journal of Chromatography.B, Biomedical Sciences and Applications. 728, 75-83.

125. Bauwens, D., P. Hantson, P. Laterre, L. Michaux, D. Latinne, M. De Tourtchaninoff, G. Cosnard and D. Hernalsteen 2005. Recurrent seizure and sustained encephalopathy associated with dimethylsulfoxide-preserved stem cell infusion. Leuk. Lymphoma. 46, 1671-1674.

126. Scerpa M.C., Daniele N., Landi F., Ciammetti C., Rossi C., Isacchi G., Zinno F., Caniglia M., Cometa A.M. and Locatelli F. 2011. Automated washing of human progenitor cells: Evaluation of apoptosis and cell necrosis. Transfus.Med.Transfusion Medicine. 21, 402-407.

127. Rowley, S. D., Z. Feng, D. Yadock, L. Holmberg, B. MacLeod and S. Heimfeld 1999. Post-thaw removal of DMSO does not completely abrogate infusional toxicity or the need for pre-infusion histamine blockade. Cytotherapy. 1, 439-446.

128. BEAUJEAN, F., O. HARTMANN, M. KUENTZ, C. LEFORESTIER, M. DIVINE and N. DUEDARI 1991. A simple, efficient washing procedure for cryopreserved human hematopoietic stem-cells prior to reinfusion. Bone Marrow Transplant. 8, 291-294.

129. Laroche, V., D.H. McKenna, G. Moroff, T. Schierman, D. Kadidlo and J. McCullough 2005. Cell loss and recovery in umbilical cord blood processing: A comparison of postthaw and postwash samples. Transfusion Transfusion. 45, 1909-1916.

130. WHO 2011. Global tuberculosis control 2011. http://www.who.int/tb/publications/global_report/2011/gtbr11_full.pdf.

131. Shu, Z., K.M. Weigel, S.D. Soelberg, A. Lakey, G.A. Cangelosi, K. Lee, J. Chung and D. Gao 2012. Cryopreservation of mycobacterium tuberculosis complex cells. J. Clin. Microbiol. 50, 3575-3580.

132. Bobadilla-del-Valle M, Ponce-de-Leon A, Kato-Maeda M, Hernandez-Cruz A, Calva-Mercado JJ, Chavez-Mazari B, Caballero-Rivera BA, Nolasco-Garcia JC and Sifuentes-Osornio J 2003. Comparison of sodium carbonate, cetyl-pyridinium chloride, and sodium borate for preservation of sputa for culture of *mycobacterium tuberculosis*. J. Clin. Microbiol. 41, 4487-4488.

133. Huang TS, Chen YS, Lee SSJ, Tu HZ and Liu YC 2005. Preservation of clinical isolates of *mycobacterium tuberculosis* complex directly from MGIT culture tubes. Ann. Clin. Lab. Sci. 35, 455-458.

134. Selvakumar N, Sudhamathi S, Duraipandian M, Frieden TR and Narayanan PR 2004. Reduced detection by ziehl-neelsen method of acid-fast bacilli in sputum samples preserved in cetylpyridinium chloride solution. International Journal of Tuberculosis and Lung Disease. 8, 248-252.

135. Kubica GP and Kim TH 1979. Preservation of mycobacteria at -70-degrees-C -- survival of unfrozen suspensions in transit. Tubercle. 60, 37-43.

136. Grover AA, Kim HK, Wiegesha EH and Smith DW 1967. Host-parasite relationships in experimental airborne tuberculosis .2. reproducible infection by means of an inoculum preserved at-70c. J. Bacteriol. 94, 832-835.

137. Kim TH and Kubica GP 1973. Preservation of mycobacteria - 100 percent viability of suspensions stored at -70 C. Appl. Microbiol. 25, 956-960.

138. Kim TH and Kubica GP 1972. Long-term preservation and storage of mycobacteria. Appl. Microbiol. 24, 311-317.

139. Kubica GP, Gontijofilho PP and Kim T 1977. Preservation of mycobacteria at 70-degrees-C persistence of key differential features. J. Clin. Microbiol. 6, 149-153.

140. Ahmad M, Srivastava BS and Agarwala SC 1978. Effect of incubation media on the recovery of *escherichia coli* K12 heated at 52 degrees C. J. Gen. Microbiol. 107, 37-44.

141. Wang SY, Hsu ML, Tzeng CH, Hsu HC and Ho CK 1998. The influence of cryopreservation on cytokine production by human T lymphocytes. Cryobiology. 37, 22-29.

142. Lavoie ET and Grasman KA 2005. Isolation, cryopreservation, and mitogenesis of peripheral blood lymphocytes from chickens (*gallus domesticus*) and wild herring gulls (*larus argentatus*). Arch. Environ. Contam. Toxicol. 48, 552-558.

143. Fujiwara S, Akiyama M, Yamakido M, Seyama T, Kobuke K, Hakoda M, Kyoizumi S and Jones SL 1986. Cryopreservation of human-lymphocytes for assessment of lymphocyte subsets and natural-killer cytotoxicity. J. Immunol. Methods. 90, 265-273.

144. Bloom BR 1994. Tuberculosis: pathogenesis, protection, and control. ASM Press, Washington, D.C.

145. Delta-Latta, P.2007.Mycobacteriology and antimycobacterial susceptibility testing; In Clinical microbiology procedures handbook, 2nd ed, Garcia, L., Isenberg, H., editors. ASM Press, Washington, DC. 7.1.2.1-7.1.2.9.

146. Zhou XM, Kang XJ, Shu ZQ, Chen HH, Ding WP, Du PG, Yadock D, Liu C, Chung J, Heimfeld S and Gao DY 2009. Cryopreservation of peripheral blood stem cells using a box-in-box cooling device. Biopreservation and Biobanking. 7, 107-114.

147. Zhou XM, Shu ZQ, Ding WP, Heimfeld S, Chung J, Du PG, Liu C and Gao DY 2011. Heat transfer analysis for the design and application of the passive cooling rate controlled device-box-in-box. Int. J. Heat Mass Transfer. 54, 2136-2143.

148. Nikaido H 1994. Prevention of drug access to bacterial targets - permeability barriers and active efflux. Science. 264, 382-388.

149. Nikaido H 2001. Preventing drug access to targets: Cell surface permeability barriers and active efflux in bacteria. Semin. Cell Dev. Biol. 12, 215-223.

150. Duthie SJ, Pirie L, Jenkinson AM and Narayanan S 2002. Cryopreserved versus freshly isolated lymphocytes in human biomonitoring: Endogenous and induced DNA damage, antioxidant status and repair capability. Mutagenesis. 17, 211-214.

151. Berney M, Hammes F, Bosshard F, Weilenmann HU and Egli T 2007. Assessment and interpretation of bacterial viability by using the LIVE/DEAD BacLight kit in combination with flow cytometry. Appl. Environ. Microbiol. 73, 3283-90.

152. Davey HM 2011. Life, death, and in-between: Meanings and methods in microbiology. Appl.Environ.Microbiol. 77, 5571-5576.

153. Stocks SM 2004. Mechanism and use of the commercially available viability stain, BacLight. Cytometry.Part A : The Journal of the International Society for Analytical Cytology. 61, 189-95.

154. Kim, J., W. Yeo, Z. Shu, S.D. Soelberg, S. Inoue, D. Kalyanasundaram, J. Ludwig, C.E. Furlong, J.J. Riley, K.M. Weigel, G.A. Cangelosi, K. Oh, K. Lee, D. Gao and J. Chung 2012. Immunosensor towards low-cost, rapid diagnosis of tuberculosis. Lab Chip. 12, 1437-1440.

155. CROWE, J., L. CROWE and D. CHAPMAN 1984. Preservation of membranes in anhydrobiotic organisms - the role of trehalose. Science. 223, 701-703.

156. LESLIE, S., E. ISRAELI, B. LIGHTHART, J. CROWE and L. CROWE 1995. Trehalose and sucrose protect both membranes and proteins in intact bacteria during drying. Appl. Environ. Microbiol. 61, 3592-3597.

157. Crowe LM, Reid DS,Crowe JH, 1996. Is trehalose special for preserving dry biomaterials? Biophys. J. 71, 2087-93.

158. Crowe, J. and L. Crowe 2000. Preservation of mammalian cells - learning nature's tricks. Nat. Biotechnol. 18, 145-146.

159. Crowe, J., L. Crowe, A. Oliver, N. Tsvetkova, W. Wolkers and F. Tablin 2001. The trehalose myth revisited: Introduction to a symposium on stabilization of cells in the dry state. Cryobiology. 43, 89-105.

160. Crowe JH, Tablin F, Wolkers WF, Gousset K, Tsvetkova NM,Ricker J, 2003. Stabilization of membranes in human platelets freeze-dried with trehalose. Chem. Phys. Lipids. 122, 1-2.

161. Crowe, J. H. and F. Tablin 2004. Stabilization of cells in the dry state by trehalose. In Vitro Cell. Dev. Biol. -Anim. 40, 11A-11A.

162. Török, Zsolt, Satpathy, Gyana R., Banerjee, Mitali, Bali, Rachna, Little, Erika, Novaes, Roberta, Ly, Hung Van, Dwyre, Denis M., Kheirolomoom, Azadeh, Tablin, Fern, Crowe, John H., Tsvetkova,Nelly M., 2005. Preservation of trehalose-loaded red blood cells by lyophilization. Cell Preservation Technology. 3, 96-111.

163. Crowe, J. H. 2007. Trehalose as a "chemical chaperone": Fact and fantasy. Adv. Exp. Med. Biol. 594, 143-158.

164. Sun, W. and P. Davidson 2001. Effect of dextran molecular weight on protein stabilization during freeze-drying and storage. CryoLetters. 22, 285-292.

165. Xu, W., Y. Chi, X. Wang and C. Chen 2012. Functional properties of spray-dried and freeze-dried egg white proteins glycated with dextran. J. Food Agric. Environ. 10, 173-177.